Regulation and function of Anoctamins, a new family of Ca^{2+} activated Cl^- channels

DISSERTATION ZUR ERLANGUNG DES DOKTORGRADES
DER NATURWISSENSCHAFTEN (DR.RER.NAT.)
DER FAKULTÄT FÜR BIOLOGIE UND VORKLINISCHE MEDIZIN
DER UNIVERSITÄT REGENSBURG

vorgelegt von

Yuemin Tian

aus Langfang, China

im Jahr 2012

Das Promotionsgesuch wurde eingereicht am:
12.10.2012

Die Arbeit wurde angeleitet von:
Prof. Dr. Karl Kunzelmann

Unterschrift:

Promotionsgesuch eingereicht am: 12. Oktober 2012

Die Arbeit wurde angeleitet von: Prof. Dr. Karl Kunzelmann

Prüfungsausschuss:

    Vorsitzender: Prof. Dr. Frank Schweda

    1.Gutachter: Prof. Dr. Karl Kunzelmann

    2.Gutachter: Prof. Dr. Richard Warth

    3.Prüfer: Prof. Dr. Gernot Längst

    Ersatzperson: Prof. Dr. Ralph Witzgall

SUMMARY

Anoctamins are a family of Ca^{2+} activated Cl^- channels (CaCCs) that are ubiquitously expressed in almost every cell type in our body. Anoctamins play an essential role in volume regulation, epithelial Cl^- secretion, neuronal excitability, and also nociception. Mutations in anoctamin proteins lead to various diseases including bone and muscle dystrophy, cerebellar ataxias, and blood coagulation defect. More importantly, up-regulation of anoctamins is highly linked to different types of cancers. This family of proteins were identified 2004 but their precise function is still under examination. In the following chapters I investigated how these channels are regulated, to get a better understanding of how they function as CaCC. I demonstrate that i) anoctamins are a family of CaCCs, ii) they produce volume-regulated chloride currents, iii) activation of Ano1 occurs in a calmodulin-dependent way, and iv) INO-4995 and other inositolphosphates control Ano1.

Anoctamins are a family of Ca^{2+} activated Cl^- channels

Ano1 and 2 are reported to be CaCCs, Ano6 operates as an essential component of the outwardly rectifying chloride channel (ORCC), while others were reported as intracellular proteins. It is therefore unclear whether anoctamins constitute a family of CaCCs, or reflect proteins with heterogeneous functions. Using whole cell patch clamping we demonstrate that Ano4-10 are able to produce transient Ca^{2+} activated Cl^- currents, when expressed in HEK293 cells. While some anoctamins (Ano1,2,4,6,7) were found to be well expressed in the plasma membrane, others (Ano8,9,10) show rather poor membrane expression and are mostly retained in the cytosol. The transient nature of the Cl^- currents produced by Ano1 may be due to deactivation occurring via a calmodulin-dependent kinase. The present results demonstrate that anoctamins are a family of CaCCs, which also induce permeability for cations. They are located in the plasma membrane or in intracellular compartments. Our results will support understanding of the physiological significance of anoctamins and their role in disease.

Anoctamin proteins produce volume-regulated chloride currents

All vertebrate cells can regulate their volume through activating chloride channels during regulatory volume decrease. Ano1 and other anoctamins function as CaCC. They play a role during cell swelling and are activated by an autocrine mechanism that involves ATP release

and binding to purinergic P2Y$_2$ receptors. A Ca^{2+} independent mechanism which engages extracellular-regulated protein kinases (ERK1/2) is also an important step during Ano1 activation induced by cell swelling. Swelling activated Cl$^-$ currents are abolished in the colonic epithelium and in salivary acinar cells in Ano1 knockout mice. Thus, amoctamin proteins constitute a crucial component of epithelial volume-regulated Cl$^-$ channels and may also have a function during cellular proliferation and apoptotic cell death.

Calmodulin-dependent activation of Ano1

Ano1 is activated upon an increase in intracellular Ca^{2+} concentration, but it is unclear whether Ca^{2+} binds directly to the channel or whether additional components are required. We demonstrate that Ano1 is strictly plasma membrane localized and requires cytoskeletal interactions to be fully activated. Despite the need for cytosolic ATP for full activation, phosphorylation by protein kinases is not required. In contrast, the Ca^{2+} binding protein calmodulin appears indispensable and interacts physically with Ano1. Openers of small- and intermediate-conductance Ca^{2+}-activated potassium channels known to interact with calmodulin also activated Ano1. These results reinforce the use of these compounds for activation of electrolyte secretion in diseases such as cystic fibrosis (CF).

Control of Ano1 by INO-4995 and other inositolphosphates

Earlier studies suggested CaCCs are regulated by membrane lipid inositol phosphates, and augmented by 1-O-octyl-2-O-butyryl-myo-inositol 3,4,5,6-tetrakisphosphate octakis (propionoxymethyl) ester (INO-4995). Here we examined whether Ano1 is a target of INO-4995, and if the channel is regulated by inositol phosphates. We found that INO-4995 directly activates Ano1 in Ano1 over expressing cells. The tetrakisphosphates Ins(3,4,5,6)P$_4$ or Ins(1,3,4,5)P$_4$ and enzymes controlling levels of InsP$_4$ or PIP$_2$ and PIP$_3$ had no effects on the magnitude or kinetics of Ano1 currents. In contrast in *Xenopus* oocytes, human airways and colonic epithelial cells, which endogenously express Ano1, Cl$^-$ currents were not acutely activated by INO-4995. However incubation with INO-4995 augmented Ano1-dependent currents activated by ionomycin or ATP in *Xenopus* oocytes and human airways epithelial cells, while intracellular Ca^{2+} signals were not affected. Our data indicate that Ano1 is the target for INO-4995, although the mode of action appears different for over-expressed and endogenous channels. INO-4995 may be useful for the treatment of CF lung disease.

ZUSAMMENFASSUNG

Anoctamine sind eine Familie von Ca^{2+} aktivierten Cl^- Kanälen (CaCCs), die ubiquitär in den meisten Zellen des Körpers exprimiert werden. Anoctamine spielen eine essentielle Rolle für die Volumenregulation, epitheliale Sekretion, neuronale Erregbarkeit und auch für die Nozizeption. Mutationen der Anoctamin-Proteine führen zu verschiedenen Erkrankungen wie Knochen- und Muskeldystrophie, zerebrale Ataxie und zu Defekten der Blutstillung. Darüber hinaus ist eine erhöhte Expression von Anoctaminen mit verschiedenen Krebsarten verbunden. Die Proteinfamilie wurde 2004 identifiziert, aber bis heute ist die exakte Funktion dieser Proteine unbekannt. In den folgenden Kapiteln untersuchten wir wie diese Kanäle reguliert werden, um ein besseres Verständnis über deren Funktion als CaCC zu bekommen: Anoctamine sind eine Familie von CaCCs, sie produzieren einen volumenregulierten Chloridstrom, Aktivierung von Ano1 ist von Calmodulin abhängig und schließlich kontrollieren INO-4995 und andere Inositolphosphate Ano1.

Anoctamine sind eine Familie von Ca^{2+} aktivierten Cl^- Kanälen

Ano1 und 2 sind als CaCCs beschrieben worden. Ano6 ist eine wichtige Komponente des auswärtsgleichgerichteten Chloridkanals (ORCC), während die anderen Anocatmine als intrazelluläre Proteine vorliegen. Es ist deswegen unklar, ob die Anoctamine eine Familie von CaCCs bilden, oder ob sie Proteine mit unterschiedlichen Funktionen darstellen. Mittels der *Patch*- Clamp- Technik in der *Ganzzell*-Konfiguration konnten wir zeigen, dass Ano4-10 in der Lage sind transiente Ca^{2+} aktivierte Cl^- Ströme zu produzieren, wenn sie in HEK293 Zellen exprimiert werden. Während manche Anoctamine (Ano1, 2, 4, 6, 7) in der Plasmamembran exprimiert werden, zeigen andere (Ano8, 9, 10) nur eine schwache Expression in der Plasmamembran und verbleiben eher zytosolisch. Die transiente Natur des Cl^- Stroms von Ano1 könnte durch eine Deaktivierung über eine Calmodulin- abhängige Kinase zustande kommen. Die vorliegenden Ergebnisse demonstrieren, dass Anoctamine eine Familie von Ca^{2+} aktivierten Cl^- Kanälen sind, die auch für Kationen permeabel sind. Sie sind sowohl in der Plasmamembran als auch im Zytosol lokalisiert. Unsere Ergebnisse werden das Verständnis über die physiologische Bedeutung der Anoctamine bei der Entstehung von Krankheiten vertiefen.

Anoctamin Proteine erzeugen einen volumen-regulierten Chlorid Strom

Alle vertebralen Zellen können ihr Volumen durch die Aktivierung eines Chlorid Kanals während der regulatorischen Volumenabnahme regulieren. Ano1 und andere Anoctamine sind funktionell CaCCs. Sie spielen eine Rolle während des Zellschwellens und werden über einen

autokrinen Mechanismus, über ATP Freisetzung und Aktivierung von purinergen $P2Y_2$ Rezeptoren aktiviert. Ein Ca^{2+} unabhängiger Mechanismus, an dem extrazellulär-regulierte Protein Kinasen (ERK1/2) beteiligt sind, ist ein zusätzlicher wichtiger Schritt für die Aktivierung von Ano1 durch Zellschwellung. Durch Schwellung aktivierte Cl^- Ströme sind reduziert in Epithelzellen des Kolons und Azinuszellen der Speicheldrüse von Ano1 defizienten Mäusen. Darum sind Anoctamin Proteine eine kritische Komponente von epithelialen volumen-regulierten Cl^- Kanälen und haben deswegen auch eine Funktion während der Zellteilung und der Apoptose.

Calmodulin- abhängige Aktivierung von Ano1

Ano1 wird während des Anstiegs der intrazellulären Ca^{2+} Konzentration aktiviert, aber es ist unklar ob Ca^{2+} direkt am Kanal wirkt oder ob zusätzliche Komponenten gebraucht werden. Wir konnten zeigen, dass Ano1 grundsätzlich in der Plasmamembran lokalisiert ist und zytoskeletale Interaktionen für die vollständige Aktivierung benötigt. Zytosolisches ATP ist für die vollständige Aktivierung notwendig, eine Phosphorylierung durch Kinasen jedoch nicht. Dagegen ist das Ca^{2+}-bindende Protein Calmodulin unabdingbar für die Aktivierung und interagiert physikalisch mit Ano1. Öffner von Ca^{2+} aktivierten Kalium Kanälen mit kleinen und mittleren Leitfähigkeiten, die mit Calmodulin interagieren, aktivieren auch Ano1. Diese Ergebnisse bekräftigen die Verwendung von diesen Verbindungen für die Aktivierung einer Elektrolytsekretion in Krankheiten wie Mukoviszidose.

Kontrolle von Ano1 durch INO-4995 und anderen Inositolphosphaten

Frühere Studien deuteten an, dass CaCCs über das Membranlipid Inositolphosphat reguliert wird und die Aktivität über 1-O-octyl-2-O-butyryl-myo-inositol 3,4,5,6-tetrakisphosphate octakis (propionoxymethyl) ester (INO-4995) verstärkt werden kann. Wir untersuchten deswegen, ob Ano1 ein Angriffsziel für INO-4995 ist und ob Ano1 durch Inositolphosphate reguliert wird. Wir fanden, dass INO-4995 in Ano1 überexprimierten Zellen direkt Ano1 aktiviert. Tetrakisphosphat Ins(3,4,5,6)P_4 oder Ins(1,3,4,5)P_4 und Enzyme, die den Gehalt von InsP_4 oder PIP_2 und PIP_3 regulieren, hatten keinen Effekt auf die Größe oder Kinetik des Ano1 Stroms. Dagegen wurde der endogene Cl^- Strom in *Xenopus* Oozyten, humanen Luftwegs- und Kolonepithelzellen nicht akut von INO-4995 aktiviert. Allerdings wurde der Ano1-abhängige Strom, aktiviert durch Ionomycin oder ATP, nach Inkubation mit INO-4995 in *Xenopus* Oozyten und humanen Luftwegsepithelzellen verstärkt, während der intrazelluläre Ca^{2+} Signalweg nicht beeinflusst wurde. Unsere Daten zeigen, dass Ano1 ein Angriffsziel für INO-4995 ist, obwohl die Art der Aktivierung in über-exprimierten oder endogenen Kanälen unterschiedlich ist. Ino-4995 könnte für die Behandlung der Mukoviszidose von Nutzen sein.

CONTENTS

CHAPTER 1

Introduction

Ion channels are pore-forming proteins that help establish and control the voltage gradient across the plasma membrane of cells by allowing the flow of ions down their electrochemical gradient. Gated ion channels consist of one or more subunits with amphipathic α helical membrane-spanning segment. Ion channels have four functional components. 1) Gating of the ion channel; these membrane proteins have several conformations that can result in an open or closed channel; 2) ion channel sensors: which can detect different signals, for example: (a) membrane potential changes; (b) second messenger, which can be sensed at the cytoplasmic side of the plasma membrane; (c) ligands, which bind to the extracellular side of these membrane proteins; 3) the selectivity filter through which ions with positive or negative charge or only one class of ions can go through; 4) the pore, when the channel opens, the selectively permeable ions can get through freely down their chemical gradient. As mentioned above, the ion channels can be classified by the particular ions that are conducted by the channel pore, so subsequently I will refer to them as sodium, potassium, calcium, water, and chloride channels.

Sodium channels are ion channels, which can primarily conduct sodium ions through a cell's plasma membrane. Na^+ is the most abundant cation in extracellular fluid in our body. Since extracellular Na^+ concentration is much higher than the intracellular one, equilibrium potential for Na^+ is always positive, so when sodium channel is open, Na^+ will move down its chemical gradient and get into the cell, inducing membrane voltage depolarization. For example, diffusion of Na^+ through epithelial sodium channels (ENaC) leads to absorption of salt and water. ENaC is expressed in many epithelial tissues; among them are endometrial epithelial cells. Through ENaC activation and membrane voltage depolarization, voltage gated calcium channels are activated to induce prostaglandin E2 (PGE2) production, a key step for embryo implantation (139).

Potassium channels are the most widely distributed type of ion channels, ubiquitously expressed in virtually all living organisms. The equilibrium potential for K^+ is strongly negative and usually plays a role in generating cell resting membrane potential, so K^+ is either at equilibrium or tends to move out of the cell, nevertheless inwardly rectifying K^+ channels are responsible for K^+ influx into the cell. Other kinds of K^+ channels play a key role in excitable cells, where these channels help terminate action potentials.

Calcium channels are ion channels, which display selective permeability to calcium ions. The equilibrium potential for Ca^{2+} is always positive, so Ca^{2+} tends to flow into the cell. When Ca^{2+} channels are open, Ca^{2+} rapidly enters the cell down a steep electrochemical gradient. This inward movement of Ca^{2+} is a very important signal, because Ca^{2+} is a common second messenger with downstream effects on many cellular processes.

Water channels are membrane proteins that form channels that are just large enough to allow water molecules to pass through. The first identified water channel was aquaporin 1 (AQP1), a 28-kDa protein. AQP1 belongs to a large family of aquaporins that have representatives in organisms as diverse as bacteria, plants and animals (2). In mammals the various aquaporin isoforms have different tissue distributions, different mechanisms of regulation, and varying abilities to transport small neutral molecules other than water. In the lipid bilayer, AQP1 exists as tetramers. Each monomer consists of six membrane-spanning helices as well as two shorter helices that dip into the plane of the membrane (147). These structures form a permeation pathway for the single-file diffusion of water. Since most of the other channels are permeable for different cations, Cl^- channel is the most important anion channel for balancing cation movement and to move Cl^- either into or out of the cell. I will thus focus on Cl^- channels.

Chloride channels

Cl^- channels are ubiquitously expressed and found in all eukaryotic cells, plant cells, protozoa, bacteria and yeast. In contrast to cation channels, they generally have a role in nonexcitable cells such as epithelial cells, where they participate in electrolyte secretion. Chloride ion

channel research has been neglected for many years. It is now appreciated that these channels play important functional roles in diverse processes, such as blood pressure regulation, cell cycle and apoptosis, muscle tone, volume regulation, synaptic transmission and even cellular excitability (121). Cl⁻ channels form pores in the plasma membrane and in intracellular membranes and are permeable to various anions, such as iodide, bromide, but also for nitrates, phosphates and even negatively charged amino acids. We refer mostly to these anion channels as Cl⁻ channels, because Cl⁻ is the most abundant anion in all organisms. From the functional point of view, Cl⁻ channels have been classified according to their gating mechanisms, which may depend on changes in the cell volume, transmembrane voltage, on a protein kinase/nucleotide mediated mechanism, an increase in intracellular Ca^{2+} concentration, or binding of a ligand. They also participate in many housekeeping processes, for example volume regulation, pH regulation in organelles, electro genesis and control of synaptic activity. The Cl⁻ channels are important for transepithelial transport and the control of water flow, and because their selectivity is not strict, they often provide permeation pathways for a large variety of anions.

CFTR and others Cl⁻ channels

The most extensively examined Cl⁻ channel is the cystic fibrosis transmembrane conductance regulator (CFTR). Mutations of this channel cause the most common fatal genetic disorder among the Caucasian population. Cystic fibrosis (CF) is an autosomal recessive disorder that results in an abundance of thick airway mucus, pancreatic insufficiency, obstruction of the bile ducts, high sweat chloride, intestinal blockage, nasal polyps and chronic sinusitis (28). CFTR is a cAMP dependent Cl⁻ channel that is expressed in the apical membrane of epithelial cells (151). In the airways, where CF patients show the most serious defect, CFTR and CaCCs have intensive cross talk (Fig. 1) (98). It was reported that purinergic receptors such as $P2Y_2$ or $P2Y_6$ couple to both second messengers: cAMP and Ca^{2+} (49). Intracellular Ca^{2+} affects the activity of enzymes that control intracellular cAMP levels such as adenylate cyclase and phosphodiesterase (119). On the other hand, cAMP affects proteins that control intracellular

Ca^{2+} levels for example the endoplasmic reticulum (ER) Ca^{2+} ATPase SERCA or IP_3 receptors (18). Intracellular Cl^- via the Cl^- channel Best1 affects Ca^{2+} transport across the ER-membrane and Ca^{2+} influx via ORAI and TRP channels, because Cl^- serves as a counter ion for Ca^{2+} (10). Recently we proposed that CFTR translocates a proton receptor to the plasma membrane of *Xenopus* oocytes and allows for extracellular protons to activate CaCCs (89). CFTR and Ano1/6 may interact directly or through scaffold proteins such as NHERF1 or other PDZ-domain proteins. Finally, other novel messengers like the IP_3-receptor binding protein IRBIT may link IP_3/Ca^{2+} signaling to CFTR (194).
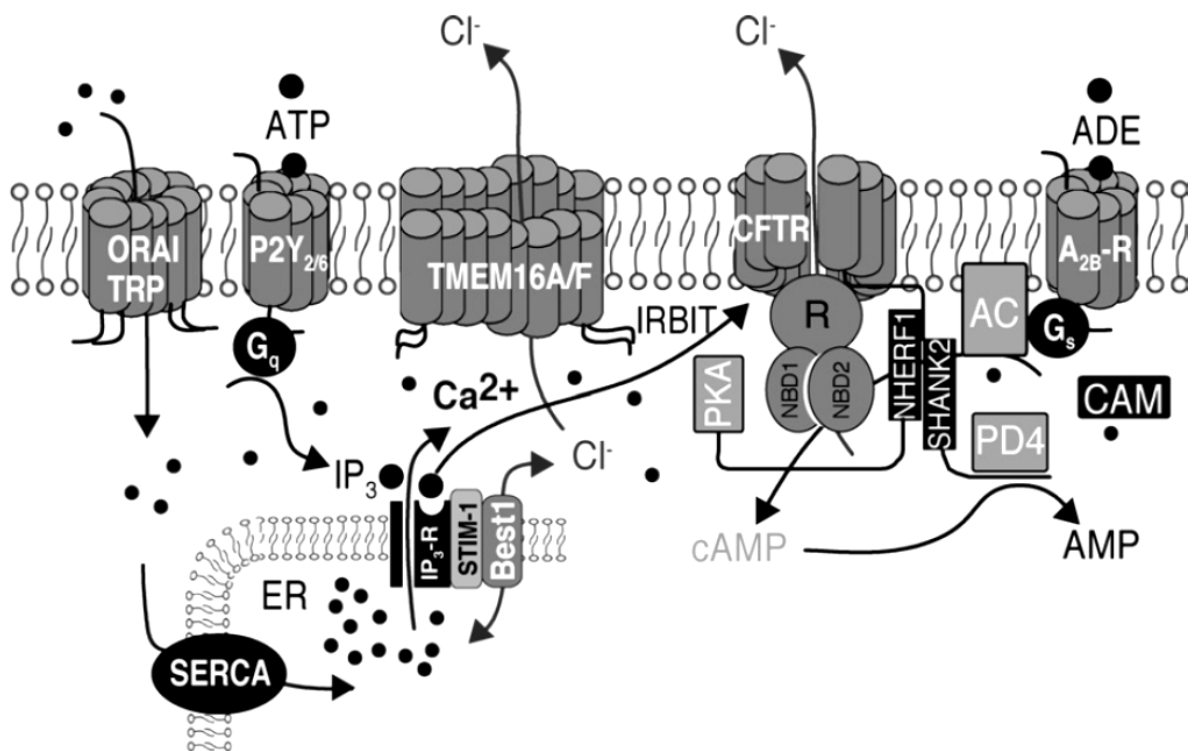
Fig. 1: Ca^{2+}-dependent Cl^- secretion may occur at several levels. (i) Purinergic receptors such as $P2Y_2/P2Y_6$ increase both intracellular cAMP and Ca^{2+}. (ii) Intracellular Ca^{2+} affects the activity of enzymes that control intracellular cAMP (adenylate cyclase, AC; phosphodiesterase, PD). (iii) Intracellular cAMP affects proteins that control intracellular Ca^{2+} levels (SERCA). (iv) Intracellular Cl^- concentration affects Ca^{2+} transport over the ER-membrane (via the Cl^- channel Best1) and Ca^{2+} influx (via ORAI/TRP). (v) CFTR and TMEM16A/F may interact directly or through scaffold proteins (NHERF1 and other PDZ-domain proteins). (vi) CFTR translocates Gq-coupled receptors to the plasma membrane

that allow for Ca^{2+} increase and activation of TMEM16A. (vii) Novel messengers like IRBIT link IP_3/Ca^{2+} signaling to CFTR.

Another very well studied and understood family of Cl^- channel is the ClC chloride channels family, which is a family of voltage dependent Cl^- channels. Mammalian tissues contain nine different genes that encode for ClC channels (79). The volume regulated anion channel (VRAC) is ubiquitously expressed in animal cells and is involved in cell volume regulation, cell division, apoptosis, transport processes, metabolism and the regulation of electrical excitability (45; 146). Although biophysical properties had been extensively discussed, its molecular identity has not yet been identified. Until recently this was also the case for calcium activated Chloride channels (CaCCs). For a long time its molecular identity was unknown. From here, I will focus on CaCCs, because these are the Cl^- channels I work most intensively on during my thesis.

Calcium activated chloride channels

Ca^{2+} activated Cl^- channels are abundant proteins and are present in many different cell types, although with slight differences regarding their biophysical properties and pharmacology (51; 63). CaCCs play various roles in cell physiology including epithelial secretion (166), sensory transduction and adaptation (158), regulation of smooth muscle contraction (103), control of neuronal and cardiac excitability (39), and also nociception (105). Prior to 2008, the proteins responsible for CaCCs were unknown; indeed, several other proteins were proposed as molecular candidates. These proteins included ClC-3 (73), ClCAs (107), and the bestrophins (11).

ClC-3 belongs to voltage-gated chloride channel superfamily and may be responsible for the volume-regulated outwardly rectifying Cl^- current (40). Although reported as Ca^{2+} activated Cl^- channels, there is serious doubt that ClCAs are even ion channels at all. It has been suggested that they are more likely accessory proteins of ion channels (126). In contrast bestrophin-1 is expressed in the retinal pigment epithelium and certain mutations in

bestrophin-1 cause degeneration of the retina and blindness (95). Bestrophin-2 is expressed in goblet cells of the colon and may play a role in bicarbonate secretion (199). Although bestrophins are indeed CaCCs, their expression and functional roles are more restricted.

Only recently it has been reported simultaneously by three independent groups that TMEM16a and b, which are also named anoctamin 1 (Ano1) and anoctamin 2 (Ano2), belong to a family of ten members of unidentified proteins with 8 membrane spanning domains. These proteins have been reported as the true molecular identities of CaCCs (19; 149; 197). One might speculate that the other members of the anoctamin family also function as CaCCs and contribute to calcium activated chloride current in different tissues. If they are, this is an exciting finding since these proteins have previously attracted significant interest in other research fields, particularly cancer and developmental biology.

There is hardly any tissue in which CaCCs does not have at least a modulatory role, and consequently anoctamins are expressed in all of these tissues (97). The character of Cl^- currents generated by Ano1 fit very well to endogenous CaCC currents. Obviously, silencing of Ano1 in different cells abolishes CaCC currents and mice in which knockdown of Ano1 produces defects in calcium dependent Cl^- secretion in a number of tissues, which support the concept of Ano1 forming an essential component of CaCC (124; 137; 169).

The physiological role of Ano1

Ano1 is widely expressed in epithelia including salivary gland, pancreas, gut, mammary glands and the airways (97). Ano1 also performs important functions in nonepithelial tissues, namely its pacemaker activity in the gut and regulation of vascular and airway smooth muscle tone (26; 120). Ano1 can also mediate nociceptive signals. It is expressed in small dorsal root ganglion neurons and triggered by bradykinin (105), which is a very potent inflammatory and pain inducing substance.

The structure of Ano1
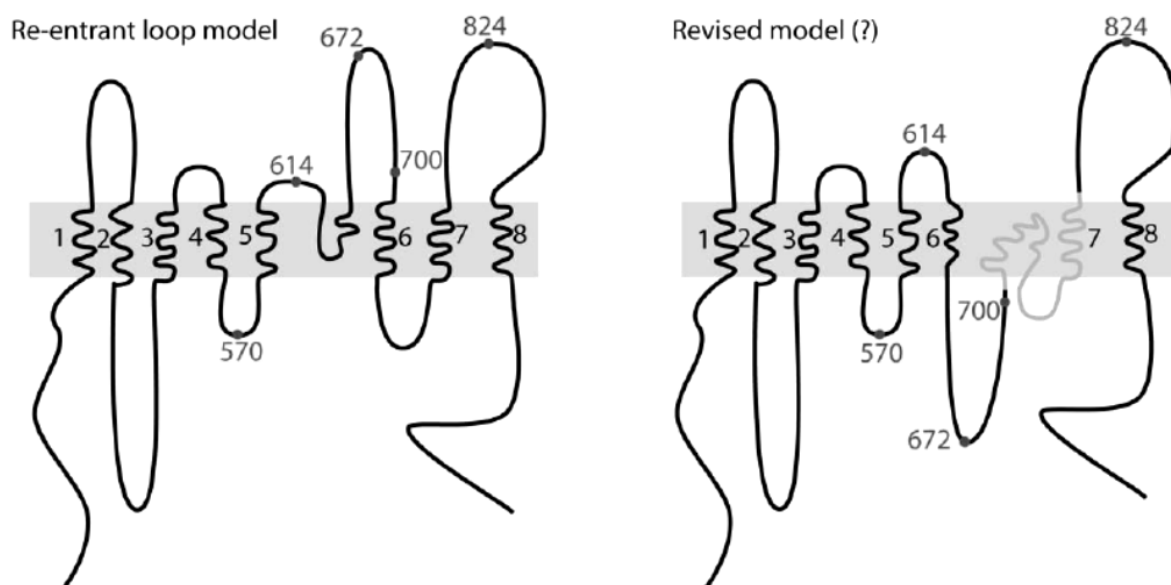
Fig. 2: Topological Models of mAno1. The locations of HA tags are indicated with gray numbers. Left, Re-entrant loop model. Right, revised model. The topology of the sequence depicted in gray remains in question.

The tertiary structure of Ano1 contains eight predicted transmembrane helices, intracellular NH2- and COOH ends and a pore, formed by the 5th and 6th transmembrane helices together with a p-loop dipping back into the membrane (Fig. 2 left). However, in 2012 the research team led by Criss Hartzell proposed an alternative model for Ano1. Their data contradict the popular re-entrant loop model by showing that the putative extracellular loop 4 (amino acids 650-706) is oriented intracellularly and may contain a Ca^{2+} binding site (Fig. 2 right) (198). In this new model, there is no putative pore forming domain and the authors also did not find the selectivity filter, so the true structure of Ano1 still needs to be determined. It is also indicated that Ano1 does not exist as a single protein, but as obligate homodimer (47; 153). As the quaternary structure of Ano1 is not altered by changes in cytosolic Ca^{2+}, dimerization appears to be permanent.

Different splicing of Ano1

Human Ano1 primary transcript undergoes alternative splicing. Three alternative exons: 6b, 13, and 15, corresponding to segments b, c, and d, respectively, which are differently spliced in human organs. Alternative splicing of Ano1 gene has an impact on ion channel properties (52). For example, skipping of exon-6b may increase Ca^{2+} sensitivity, while skipping of exon 13 abolishes the characteristic time-dependent activation observed for CaCCs.

Gating of Ano1

Ano1 is gated by both voltage and Ca^{2+}, but unlike voltage-gated channels that have amphipathic transmembrane helices with charged amino acids that serve to sense voltage, or EF hand to bind to Ca^{2+}, Ano1 has no such sequences. Deletion of the alternatively-spliced segment (ΔEAVK) alters both voltage-dependent gating and Ca^{2+} sensitivity (191). One candidate for the Ca^{2+} binding site is a stretch of five glutamic acids located in the first intracellular loop because of its resemblance to the "Ca^{2+} bowl" of the large-conductance K^+ channel (191). Another candidate for Ca^{2+} sensors are E702 and E705, and mutation of these glutamates residues dramatically altered Ca^{2+} sensitivity (198). Except for the Ca^{2+} binding site, calmodulin (CAM) is also a good candidate that could serve as an accessory subunit for Ca^{2+} dependent Ano1 activation. CAM is a calcium-binding messenger protein that is activated by binding of Ca^{2+} and then modifies its interactions with various target proteins. We reported that CAM binds to a 22-amino acid region that overlaps with the b segment in the N-terminus called CAM-BD1 and is essential for Ano1 activation (169).

Ano1 and cancer

Ano1 has also attracted the interest of cancer biologists because the gene is amplified in head, and neck squamous cell carcinomas, parathyroid tumors, breast, pancreatic and gastric cancer and its expression level may correlate with cell proliferation (84). Gastrointestinal stromal tumor (GIST) is the most common kind of mesenchymal tumor found in the gastrointestinal tract. Ano1 is highly upregulated in these tumors (46). Although Ano1 may not be the cause of the tumor, its function may support tumor progression.

Other anoctamins

Members of the anoctamin family are found throughout the eukaryotes, including mammals, flies, worms, plants, protozoa and also yeast. However, the anoctamins seem to be best represented in higher vertebrates. Mammals have 10 genes encoding anoctamin family members, whereas invertebrates and plants have distinctly fewer. C. elegans, for example, has only two Anoctamin genes and Drosophila has six paralogues (64). The phylogenetic tree (Fig. 3) (197) shows how different members of anoctamins are constructed through evolution.

Ano2 is the closest relative of Ano1 in the phylogenetic tree (Fig. 3), and it displays similar electrophysiological properties when compared to Ano1. In olfactory sensory neurons, odorants binding to G-protein coupled olfactory receptors open cyclic nucleotide gated channels by elevating cAMP (65). Ca^{2+} influx through the cyclic nucleotide gated channels then activates CaCCs that depolarize the receptor potential. Ano2 localized in the cilia and dendritic knobs of olfactory sensory neurons is the best candidate for the pore-forming subunit of CaCCs in olfactory sensory neurons (158). Ano2 is also highly expressed in photoreceptor synaptic terminals and may serve to regulate synaptic output in these cells (160). Ano3 was a silent member within the anoctamin family, until this year when it was reported through association analyses that the Ano3 locus is associated with eczema in families ascertained through asthma (38), and with Alzheimer's disease (AD) (17). So it is interesting to check whether Ano3 is also a CaCC and how is it related to these diseases. Ano4 until now has no functional correlate, but according to our data, it is also a CaCC, which can be activated through both purinergic receptor and directly by increasing intracellular Ca^{2+}, it will be discussed in chapter 2.

Ano5, also named GDD1, is highly expressed in cardiac and skeletal muscle as well as bone, and is greatly up-regulated during myocyte differentiation (116; 174). Autosomal dominant mutations in a conserved cysteine-356 in the first extracellular loop of Ano5 lead to abnormal bone mineralization and bone fragility called gnathodiphyseal dysplasia (GDD) (175). The

importance of Ano5 in skeletal muscle physiology is further enhanced by the recent finding that mutations in Ano5 produce several recessive muscular dystrophies (15; 66; 108). The phenotypes resulting from Ano5 mutations are related to dysferlinopathies. In particular a deficiency in dysferlin causes defective skeletal muscle membrane repair (9). It has been suggested that chloride currents are important in membrane repair (50) and Ano5 may be the chloride channel involved in this process. The role of Ano5 in muscle membrane repair is still speculative, but we have already determined Ano5 function as a CaCC and it needs un-physiological high Ca^{2+} to be activated. It is helpful to elucidate its role in musculoskeletal pathologies.
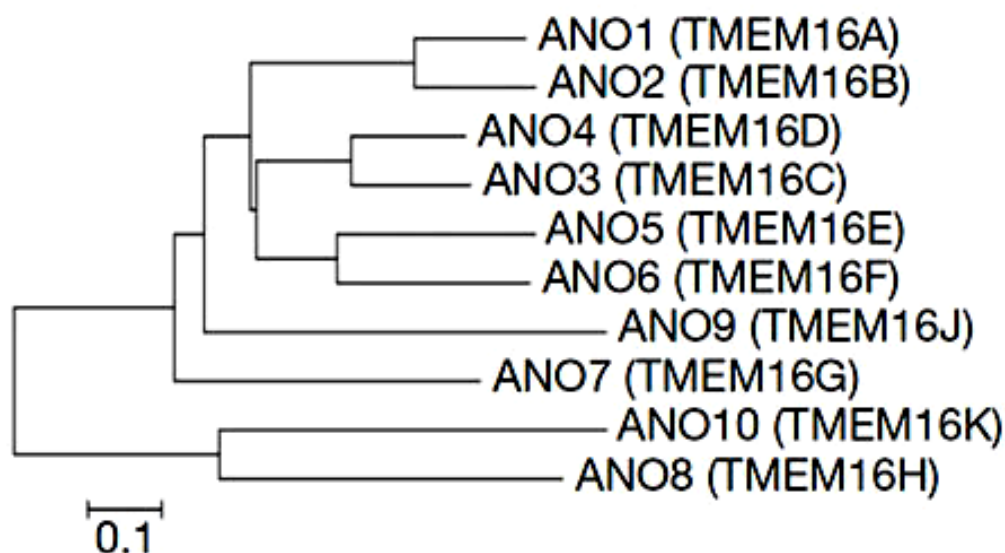
Fig. 3: Phylogenetic tree depicting the anoctamin family in humans. Scale bar, 0.1 nucleotide substitutions per site**.**

Ano6 is ubiquitously expressed and has been reported to function as a phospholipid scramblase. Ano6 mutant patients have defect in phospholipid scrambling activity, which leads to a defect in blood coagulation, called Scott syndrome (163). Our group has reported that Ano6 is a crucial component of outwardly rectifying chloride channels (ORCC), which can be activated during membrane depolarization or apoptosis (110). Since Ano6 belongs to the anoctamin family, the Ca^{2+} dependence scramblase activity suggests it could be activated

by Ca^{2+} and function as an CaCC. According to our data, Ano6 can also be activated by Ca^{2+} ionophore ionomycin in over-expressed HEK293 cells, the current showed outward rectification and also cation permeability, which fits with a recent finding that Ano6 is a non-selective cation channel (195). Taken together, Ano6 is not only a scramblase, but also an outwardly rectifying CaCC with cation permeability (110).

Ano7 (NGEP), which is highly expressed in the prostate, was discovered by analysis of expressed sequence tag databases (29). Ano7 is expressed on the apical and lateral membranes of normal prostate, and the enhanced expression is closely linked to prostate cancer (13). Ano7 has two isoforms generated by a differential splicing event. The short variant is derived from 4 exons and encodes a 20-kDa intracellular, possibly a nuclear protein. The long form is derived from 18 exons and encodes a 95-kDa protein that is predicted to contain 8 transmembrane domains (30).

Ano8 is also broadly expressed although at lower levels (97). We have found there is a Cl^- current attached to it, which can be activated by Ca^{2+} in Ano8 over-expressed HEK 293 cells, but compared to classical CaCCs the current activation is delayed, and with relatively small amplitude.

Ano9 is encoded by 23 exons and is also named TP53I5 (tumor protein P53 inducible protein 5). It is located at human chromosome locus, 11p15.5, and expressed in human colorectal, lung and breast cancer (86). Ano9 was also reported by our group to inhibit Ano1 current in a co-expression model (148). The function of Ano9 and its relationship with cancer still needs to be investigated.

Ano10 mutations have been linked to autosomal- recessive cerebellar ataxias associated with moderate gait ataxia, down-beat nystagmus and dysarthric speech (182). Affected individuals display severe cerebellar atrophy. We have detected that Ano10 also functions as a CaCC, with some permeability for cations. It is possible that our findings can be helpful to investigate the association between Ano10 function and cerebellar ataxias.

Intention and outline of the present thesis

Anoctamins have been identified a few years ago. They provide a new view for the function of CaCCs. Although these important proteins are expressed ubiquitously, for most of them the functions have not been clarified in detail. In this thesis I aimed in elucidate regulation and various functions of Ano1 and also other anoctamins, to introduce new knowledge which will help to increase our understanding of this family of chloride channels.

In Chapter 2 we provide evidence that the entire family of anoctamins form CaCCs. This will be very helpful to understand why patients with different anoctamin mutations have their pathological symptoms. Volume regulation, which is always accompanied by elevation of intracellular Ca^{2+}, is a fundamental process for the survival of every living cell and organism. CaCCs are involved in this process. We focused on endogenous anoctamins in HEK293 cells and found that all of them contribute to cell volume regulation. We have also found that Ano1 knock-out mice have abolished volume regulated chloride currents. These results will be discussed in Chapter 3. Ano 1 functions as CaCC, but does not contain a typical Ca^{2+} binding domain. Prior to my work, the Ca^{2+} regulatory site was still elusive. We have found that calmodulin is the key accessory protein for this channel activation. In chapter 4 we have investigated what role calmodulin plays in activation of Ano1 and why ATP is necessary for full channel activation.

In Chapter 5, we ask whether Ano1 is inhibited by inositol 3,4,5,6-tetrakisphosphate (82; 32; 20), which is a downstream product of $InsP_3$ and suggested to inhibit CaCCs. But this is not the case in the Ano1 overexpressing system. Nevertheless, the membrane permeable compound 1-O-octyl-2-O-butyryl-myo-inositol 3,4,5,6-tetrakisphosphate octakis (propion-oxymethyl) ester (INO-4995) can activate the channel acutely, and through repeated incubation it can enhance membrane expression in HT_{29} cells.

CHAPTER 2

Anoctamins are a family of Ca^{2+} activated Cl$^-$ channels

Abstract

Anoctamin 1 (Ano1; TMEM16A) and anoctamin 2 (Ano2; TMEM16B) are novel Cl$^-$ channels transiently activated by increase in intracellular Ca^{2+}. These channels are essential for epithelial Cl$^-$ secretion, smooth muscle peristalsis and olfactory signal transduction, and are central to several inherited diseases and certain types of cancer. Surprisingly, another member of this protein-family, Ano6, operates as a Ca^{2+} activated phospholipid scramblase, while others were reported as intracellular proteins. It is therefore unclear whether anoctamins constitute a family of Ca^{2+} activated Cl$^-$ channels, or reflect proteins with heterogeneous functions. Using whole cell patch clamping we demonstrate that Ano 4 – 10 are all able to produce transient Ca^{2+} activated Cl$^-$ currents, when expressed in HEK293 cells. While some anoctamins (Ano1,2,4,6,7) were found to be well expressed in the plasma membrane, others (Ano8,9,10) show rather poor membrane expression and were mostly retained in the cytosol. The transient nature of the Cl$^-$ currents was demonstrated to be independent of intracellular Ca^{2+} levels. We show that inactivation of Ano1 currents occurs in the continuous presence of elevated Ca^{2+} concentrations, possibly by calmodulin-dependent kinase. The present results demonstrate that anoctamins are a family of Ca^{2+} activated Cl$^-$ channels, which also induce permeability for cations. They may operate as Cl$^-$ channels located in the plasma membrane or in intracellular compartments. These results will support our understanding of the physiological significance of anoctamins and their role in disease.

Introduction

Ca^{2+} activated Cl^- currents (CaCC) are abundant and are present in nearly every cell type, where they fulfill very different functions (63). It is now well accepted that TMEM16A (anoctamin 1, Ano1) forms the plasma membrane localized Ca^{2+} activated Cl^- channel (19; 149; 197). Voltage-and calcium-dependent gating of Ano1 has been examined in detail, and is linked to the first intracellular loop (191). Ano1 is essential for Cl^- secretion in a number of epithelial tissues (124; 137), for smooth muscle contraction (109; 168), the function of nociceptive neurons and smooth muscle pacemaker cells (72; 77; 105). Ano2, the closest relative of Ano1, has been shown to form a CaCC in olfactory receptors (14; 142).

The family of anoctamins consists of 10 different proteins, but only Ano 1, Ano2, and Ano6 have been examined in more detail (14; 51; 92). For Ano6 a dual role as Fas ligand activated Cl^- channel and phospholipid scramblase has been described (110; 163). However, whether Ano3-10 also produces Ca^{2+} activated Cl^- currents similar to Ano1 and Ano2, is currently unclear. A recent report claimed that Ano3-7 are intracellular proteins (42), although we demonstrated earlier that most anoctamins overexpressed in HEK293 cells can be detected in the cell membrane (148).

Anoctamins do not show any obvious homology to other ion channels. Ano 1 contains 8 predicted transmembrane helices, intracellular NH2-and COOH ends and a pore, formed by the 5th and 6th transmembrane helices, containing a p-loop dipping back into the membrane (197). The other anoctamins (2-10) show a high degree of structural similarity, which is particularly obvious for the putative pore region (92). Apart from some indirect evidence showing enhanced ATP-induced halide permeability in Ano6 and Ano7 expressing cells (148), it is not clear whether other anoctamins also produce Ca^{2+} activated Cl^- currents. We demonstrated earlier that Ano6 produces an outwardly rectifying chloride channel, which is activated during stimulation of Fas receptors upon induction of apoptosis (110). Notably, at high intracellular Ca^{2+} concentrations as induced by Ca^{2+} ionophores, Ano6 was reported to operate as a membrane phospholipid scramblase (163). In contrast to Ano1 and Ano2, Ano6 Cl^- currents were not activated by physiological Ca^{2+} concentrations (110). As demonstrated

in the present report, high intracellular Ca^{2+} levels are required to activate Ano6. Although plasma membrane-expression of some anoctamins is very poor, the present experiments also demonstrate for the first time that essentially all anoctamins are able to produce Cl^- currents when activated by an increase in $[Ca^{2+}]_i$. We speculate that anoctamins may operate as plasma membrane or intracellular Cl^- channels.

Materials and Methods

Cell culture, cDNAs, siRNAs and transfection

HEK 293 and HT_{29} cells were grown in DMEM and DMEM-F12 separately (GIBCO, Karlsruhe, Germany) supplemented with 10% fetal bovine serum at 37°C in a humidified atmosphere with 5% CO_2. Cells were placed on fibronectin-and collagen-coated 18 cm diameter cover slips and co-transfected with cDNA encoding either hTMEM16A, D, E, F, G, H, J, K, or empty pcDNA3.1 vector (mock) along with $P2Y_2$ receptor and CD8. Expression of TMEM16A, F, H, J was suppressed each by two independent sets of RNAi. Duplexes of 25nucleotide of RNAi were designed and synthesized by Invitrogen (Paisley, UK) and Ambion (Darmstadt, Germany). RNAi was transfected using Lipofectamin 2000 (1 µg/µl) and cells were examined 48 h or 72 h after transfection. Transfections were carried out using lipofectamine 2000 (Invitrogen) according to the manufactures protocol. Successful knockdown of anoctamins was demonstrated by real time RT-PCR (93).

Patch Clamping

2-3 days after transfection of His-tagged anoctamins or siRNA, respectively, overexpressing HEK293 or siRNA-transfected HT_{29} cells were identified by incubating the cells 1-2 min with Dynabeads CD8 (Invitrogen). His-tagging of anoctamins did not interfere with its properties as a Cl^- channel. Cover slips were mounted on the stage of an inverted microscope (IM35, Zeiss) and kept at 37 °C. The bath was perfused continuously with ringer solution (mM: NaCl 145, KH_2PO_4 0.4, K_2HPO_4 1.6, d-glucose 5, $MgCl_2$ 1, Ca-gluconate 1.3, pH 7.4) or NMDG solution (NMDG 145, HCl 130, KH_2PO_4 0.4, K_2HPO_4 1.6, d-glucose 5, $MgCl_2$ 1,

Ca-gluconate 1.3, pH 7.4) at the rate of 5 ml/min. For fast whole cell patch clamping pipettes were filled with intracellular like solution containing (mM: KCl 30, potassium gluconate 95, NaH$_2$PO$_4$ 1.2, Na$_2$HPO$_4$ 4.8, EGTA 1, calcium gluconate 0.758, MgCl$_2$ 1.034, D-glucose 5, ATP 3, pH was 7.2) or CsCl solution containing (mM: CsCl 130, NaH$_2$PO$_4$ 1.2, Na$_2$HPO$_4$ 4.8, EGTA 1, calcium gluconate 0.758, MgCl$_2$ 1.034, D-glucose 5, ATP 3, pH was 7.2) and had an input resistance of 2 – 4 MΩ. In other experiments K^{+} in the pipette filling solution was replaced by NMDG^{+}. For all solutions Ca^{2+} concentrations were adjusted to 10^{-7} (pipette) and 1.3 mM (bath). Experiments were conducted as described earlier (124). During experiments cells were current clamped and membrane voltages were measured. In intervals cells were voltage clamped to ± 50 mV in steps of 10 mV for 1 s. The applied clamp voltages were corrected for liquid junction potentials. Because current voltage relationships were linear (except for Ano6), membrane conductances were usually calculated according to Ohm's law. For some experiments, patch pipettes (P6060S; New England Biolabs, Germany) were loaded with pre-activated calmodulin-dependent kinase II (5000 U/ml). In these experiments, CAMKII was given sufficient time (40 min) to enter the cell before stimulation with ionomycin, and the cell was current clamped during this time.

Measurement of intracellular Ca^{2+} concentration

For single cell fluorescence measurements HEK293 cells were grown on glass covers slips, mounted in a cell chamber and perfused with ringer solution at 8 ml/min at 37˚C. Cell fluorescence measurements was measured continuously on an inverted microscope Axiovert S100 (Zeiss, Germany) with a Flua 20x/0.75 objective (Zeiss, Germany) and a high speed polychromator system (VisiChrome, Visitron Systems, Germany). Cells were loaded with 2 μM Fura-2, AM (Molecular Probes) in ringer solution or Opti-MEM (GIBCO) under experimental conditions with 0.2% pluronic (Molecular Probes) for 1h at 37°C. Fura-2 was excited at 340/380 nm, and the emission was recorded between 470 and 550 nm using a CCD-camera (CoolSnap HQ, Visitron Systems, Germany). Control of experiment, imaging acquisition, and data analysis were done with the software package Meta-Fluor (Universal imaging, USA) and Origin (OriginLab Corporation, USA). For calibration of intracellular

Ca^{2+} concentration were perfused with ringer solution and Ca^{2+} free ringer with 1 µM ionomycin, 10 µM monensin and 5 µM nigericin.

Iodide Quenching

Quenching of the intracellular fluorescence generated by the iodide- sensitive enhanced yellow fluorescent protein (YFP) was used to measure anion conductance. YFP fluorescence was excited at 490 nm using a semi-automatic Novostar plate reader (BMG-Labtech, Offenburg, Germany). I⁻ influx was induced by replacing 20 mM extracellular Cl⁻ by I⁻. Background fluorescence was subtracted and auto-fluorescence was negligible. Changes in fluorescence induced by I⁻ are expressed as initial rates of fluorescence decrease (arbitrary units/sec).

Immunocytochemistry

Transfected HEK293 cells were grown on glass cover slips and fixed for 10 min with 4% (w/v) paraformaldehyde at room temperature. Cells were incubated for 5 minutes with 0.1% SDS in PBS. After washing, cells were permeabilized and blocked with 2% (w/v PBS) BSA and 0.04% (v/v PBS) Triton X-100 for 1 h and incubated overnight with primary anti His AB (1:500, Qiagen, Hilden, Germany) and anti ß-catenin (1:500, Sigma, Taufkirchen, Germany) at 37°C. Binding of the primary antibody was visualised by incubation with a secondary donkey anti mouse antibodies conjugated with AlexaFluor^(R) 546 (1:400, Molecular Probes, Invitrogen). Nuclei were stained with Hoe33342 (0.1 µg/ml PBS, Aplichem, Darmstadt, Germany). ß-catenin was visualized using an Alexa 488-labeled secondary antibody. Cells were mounted on glass slides with fluorescent mounting medium (DAKO Cytomation, Hamburg, Germany) and examined with an ApoTome Axiovert 200M fluorescence microscope (Zeiss, Göttingen, Germany).

Results and Discussion

Activation of Ano1,4,5,6,7,8,9 and 10 by ATP-induced increase in intracellular Ca^{2+}
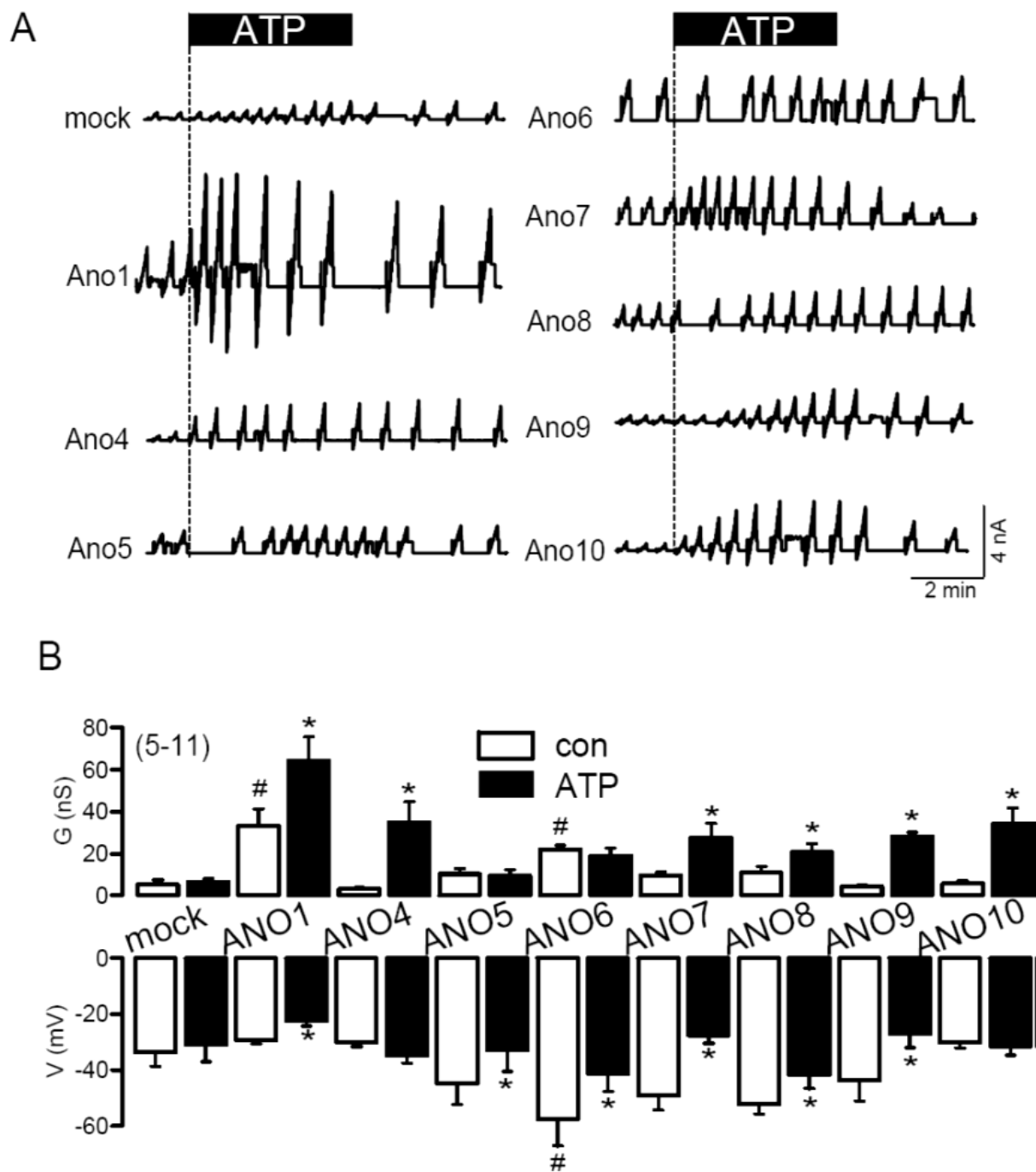
Fig. 1: Activation of anoctamins by ATP. (A) Continuous recordings of whole cell currents measured in HEK293 cells expressing different human anoctamins and activation by 10 μM ATP. In intervals cells were voltage clamped from -50 to + 50 mV in steps of 10 mV. (B) Summary of the calculated peak conductances and membrane voltages of transiently activated anoctamins. Mean ± SEM (number of cells). # different to mock; p < 0.05; ANOVA. *

significant activation; $p < 0.05$; paired t-test.

Previous studies have demonstrated that Ano1 can be activated by stimulation of G-protein coupled receptors, such as purinergic P2Y$_2$ receptors, which increase $[Ca^{2+}]_i$ (197). Because Ano2 has also been demonstrated to operate as a Ca^{2+} activated Cl$^-$ channel (14; 142), we asked whether other anoctamins are also able to produce Ca^{2+} activated Cl$^-$ currents. To that end we coexpressed different anoctamins together with P2Y$_2$ receptors in HEK293 cells, which were stimulated by 10 µM ATP, in the presence of a cytosol-like pipette filling solution and extracellular Ringer solution (c.f. Methods). We observed that overexpressed Ano1 and Ano6 produce significant whole cell Cl$^-$ currents, even in the absence of ATP-stimulation (97). In cells expressing Ano1, 4, 7, 8, 9, and 10, whole cell currents of variable magnitudes were activated by ATP (Fig. 1). Current activation by ATP was fast (below 1 s) for Ano1, but was delayed for the other anoctamins. It is currently unclear whether this is due to a reduced sensitivity towards intracellular Ca^{2+}, since intracellular Ca^{2+} levels are increased equally fast in all cells by either ATP or ionomycin, when assessed by Fura-2 (Fig. 2). Increase of $[Ca^{2+}]_i$ may not only activate the Cl$^-$ channel, but may also trigger inhibition of anoctamins via CAMKII, which may actually counteract further activation.
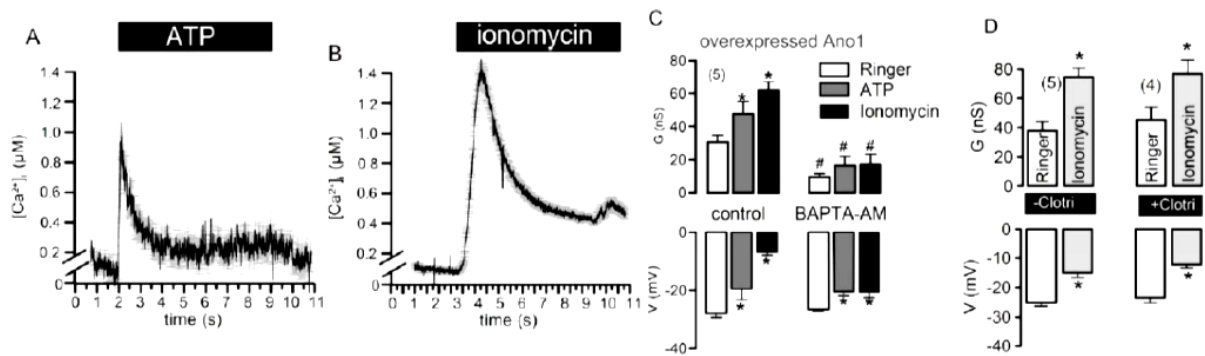
Fig. 2: Ca^{2+} dependence of anoctamins. (A, B) Time course for (A) ATP-induced (10 µM; summary of 30 experiments) and (B) ionomycin-induced (1 µM; summary of 16 experiments) increase in $[Ca^{2+}]_i$ in HEK293 cells, as detected by ratiometric Fura-2 fluorescence. (C) Summary of baseline (control) and activated whole cell conductances obtained in Ano1 expressing HEK293 cells under control conditions and after pre-incubation with 25 µM BAPTA-AM. (D) Summary of ionomycin activated whole cell conductance in the presence or absence of 10 µM clotrimazole, an inhibitor of Ca^{2+} activated K$^+$ channels (number of experiments). # different control; $p < 0.05$; ANOVA. * significant activation; $p < 0.05$; paired

t-test.

CAMKII inhibition was suggested in a recent study (169) and is also demonstrated in the present paper for both, Ano1 and Ano6. For all anoctamins except of Ano4, membrane voltages were depolarized through stimulation of purinergic receptors and increase of $[Ca^{2+}]_i$, which is expected upon increase of a Cl$^-$ conductance along with cation influx through store operated Ca^{2+} channels (Fig. 1B). Surprisingly, expression of Ano6 hyperpolarized the membrane voltage of non-stimulated cells, which is probably due to its partial permeability for K$^+$ ions as further described below. We wondered whether largely enhanced baseline Cl$^-$ currents in Ano1-expressing cells are due to activation of by the baseline Ca^{2+} concentration of 100 nM (Fig. 2A). In fact, 30 min pre-incubation with the Ca^{2+} chelator BAPTA-AM (25 µM) abolished this baseline Cl$^-$ conductance (Fig. 2C). We hypothesize that an inhibitory factor or additional protein is missing that keeps overexpressed channels closed under control conditions. As described below, this unknown protein could be another anoctamin, like Ano9, which may be able to heterooligomerize with Ano1 (Fig. 6G). Moreover, since expression of anoctamins also induced a cation permeability (c.f. below), we exclude a possible contribution of endogenous Ca^{2+} activated SK4 K$^+$ channels: Activation of whole cell currents in Ano1 expressing HEK293 cells by ionomycin was identical in the absence or presence of 10 µM of the SK4 inhibitor clotrimazole (Fig. 2D). No message (RT-PCR) was detected for either SK4 or the large conductance Ca^{2+} activated (BK) K$^+$ channel in HEK293 cells (data not shown).

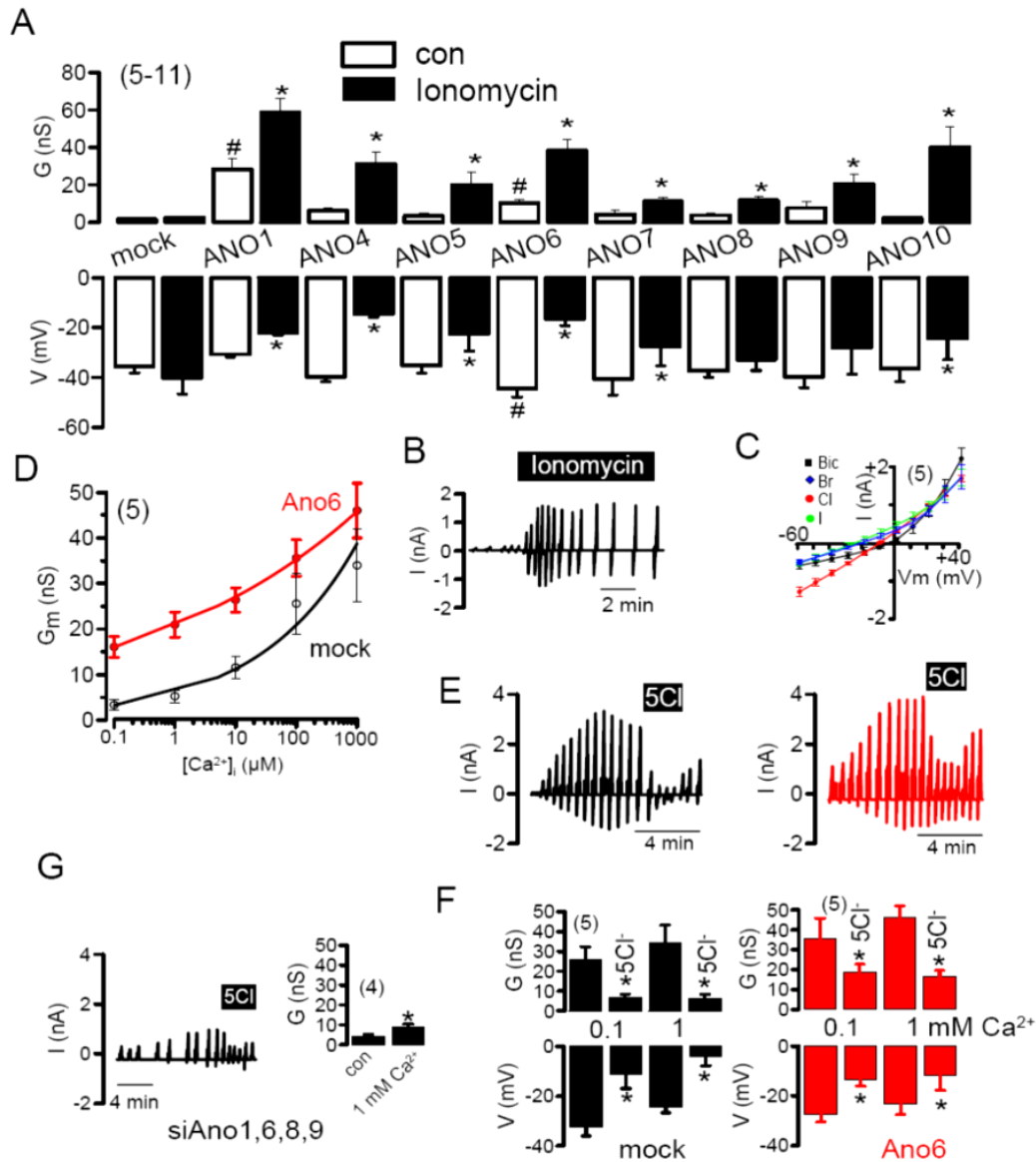*Activation of anoctamins by Ca^{2+} ionophore*

Stimulation by 10 µM ATP raised intracellular Ca^{2+} levels to about 1 µM, which is mainly due to release of Ca^{2+} from intracellular ER stores (Fig. 2A) (10). This Ca^{2+}-increase may not be sufficient to activate every member of the anoctamin family. We therefore stimulated the cells with the Ca^{2+} ionophore ionomycin (1 µM), which raised $[Ca^{2+}]_i$ in a more sustained manner to levels well above 1 µM (Fig. 2B). In fact whole cell currents could be activated in cells expressing Ano5 or Ano6, when stimulated by ionomycin, suggesting that these channels require higher and maybe more sustained Ca^{2+} levels to be activated (Fig. 3A). Close

to the plasma membrane ionomycin raises [Ca^{2+}]$_i$ probably to much higher levels than suggested by Fura-2 measurements. We examined the Ca^{2+} dependence of Ano6 by varying cytosolic (patch pipette) Ca^{2+} concentrations and detected substantial activation of Cl$^-$ currents only at concentrations as high as 10 µM or larger (Fig. 3D). Moreover Ano6, shows little inactivation during continuous stimulation with 1 µM ionomycin (Fig. 3B). Anion selectivity was similar for Ano1, 4, 6, and 10, and was I$^-$ > Br$^-$ > Cl$^-$ > HCO$_3^-$, suggesting a low field strength anion selectivity. HCO$_3^-$ was conducted surprisingly well by Ano6 (Fig. 3C). It is therefore entirely possible that Ano6 serves as a channel for bicarbonate secretion in airways and other epithelial tissues.

Notably, at very high [Ca^{2+}]$_i$ of 0.1 and 1 mM, whole cell Cl$^-$ currents were also activated in mock transfected cells, which express Ano6 endogenously (Fig. 3D, E). Replacement of extracellular Cl$^-$ by gluconate strongly inhibited whole cell currents and depolarized membrane voltages, indicating activation of whole cell Cl$^-$ currents at high [Ca^{2+}]$_i$ in both mock transfected and Ano6 overexpressing cells (Fig. 3D-F). We speculate that endogenous anoctamins may be activated only at very high [Ca^{2+}]$_i$ (3). Indeed when endogenous Ano6 (together with Ano1, 8 and 9) were knocked-down simultaneously by siRNA, we found reduced baseline currents: Current activated by 1 mM [Ca^{2+}] in the patch pipette filling solution were largely attenuated (Fig. 3G). Because of the lack of suitable antibodies we assessed knockdown of anoctamins by real time RT-PCR. Expression levels (relative to ß-actin) were very different for the endogenous anoctamins, with anoctamin 6 being the most abundant anoctamin (n = 3 for all): Ano1 1.4 x 10^{-6} (downregulation by 52 %); Ano6 3.1 x 10^{-4} (downregulation by 82 %); Ano8 1.3 x 10^{-4} (downregulation by 42 %); Ano9 2.0 x 10^{-8} (downregulation by 76 %). Thus Ano6 and maybe Ano8 have probably the largest impact on endogenous Ca^{2+} activated Cl$^-$ conductance. It remains currently unclear why endogenous anoctamins require such high [Ca^{2+}]$_i$ to be activated.

In more than 20 cell lines and in oocytes we examined endogenous expression of anoctamins. Ano6 and Ano8 were always expressed most abundantly (92). Thus, there is no "empty" system without background expression of endogenous anoctamins. However, given the low

Fig. 3: Activation of anoctamins by ionomycin. (A) Summary of the calculated ionomycin (1 µM) activated peak conductances and measured (currents clamp) membrane voltages of HEK293 cells expressing anoctamins. (B) Whole cell currents activated by ionomycin in Ano6-expressing cells. (C) Mean current/voltage relationships for Ano6 whole cell currents, with different anions (Cl⁻, I⁻, Br⁻, bicarbonate) present in the bath solution. (D) Concentrations response curve for the Ca²⁺ activation of whole cell conductance in Ano6 overexpressing and mock transfected HEK293 cells. (E) Continuous original recordings of the whole cell conductance (left: mock; black; right: Ano6; red) activated by 1 mM Ca²⁺ in the patch pipette solution, and effects of removal of extracellular Cl⁻ (5Cl⁻). In intervals cells were voltage clamped from -50 to + 50 mV in steps of 10 mV. (F) Summaries of the calculated whole cell conductances and measured membrane voltages in the presence of 0.1 and 1 mM Ca²⁺, before and after removal of extracellular Cl⁻ (5Cl⁻). (G) Original current recording and summary of the effects of 1 mM Ca²⁺ on HEK293 cells treated with siRNA for Ano1,6,8, and 9. Mean ± SEM (number of cells). # different to mock; $p < 0.05$; ANOVA. * significant activation or effect of 5 Cl; $p < 0.05$; paired t-test.

levels for endogenous anoctamins compared to overexpressed proteins (about 1000 times higher according to real time RT-PCR analysis), possible heterooligomerization of endogenous and overexpressed proteins does not appear to be a major problem in the present study.

*Contribution of nonselective currents and gating by cations*
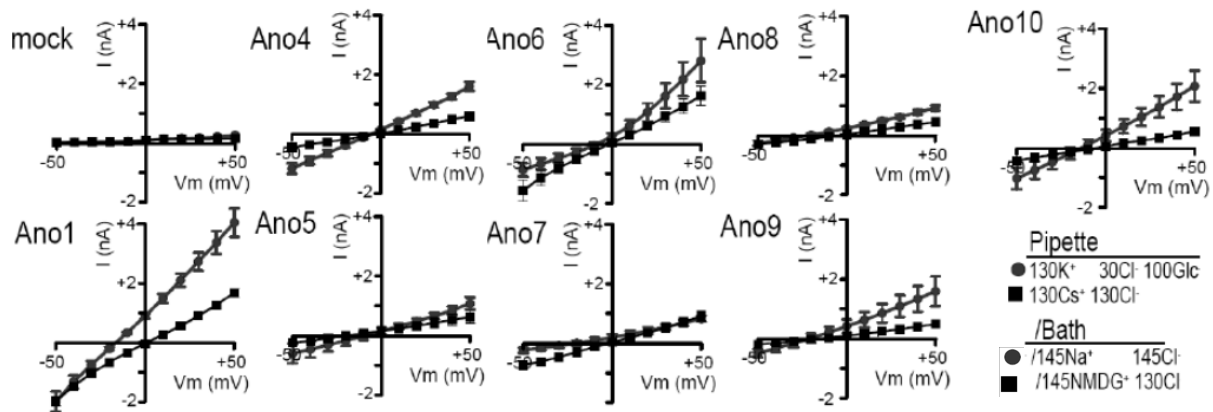
Fig. 4: Cation dependence of anoctamin currents. Summary I/V curves of whole cell currents activated by ionomycin (1 µM) in anoctamin-expressing HEK293 cells. Currents were measured in the presence of a cytosolic like solution in the patch pipette and a bath (gray circles), or with Cs^+/Cl^- in the patch pipette and $NMDG^+/Cl^-$ in the bath (black squares).

Cl^- currents activated by ionomycin or high intracellular (pipette) Ca^{2+} concentrations demonstrated rather linear current/voltage relationships (Fig. 4). We compared currents activated by ionomycin in the presence of extra-and intracellular cations (cytosol-like pipette filling solution and bath Ringer solution), with currents detected in the absence of extra-and intracellular cations (patch pipette 132 mM CsCl, bath 132 mM NMDGCl) (c.f. Methods). In general, replacing intracellular K^+ by Cs^+ and extracellular Na^+ by impermeable $NMDG^+$ markedly reduced whole cell currents produced by some anoctamins (Fig.4). We further examined possible cation permeability of anoctamins by replacing intracellular K^+ and extracellular Na^+ by $NMDG^+$ separately (Fig. 5). Indeed we found that removal of intracellular K^+ depolarized Vm and reduced outward currents, while removal of bath Na^+ hyperpolarized Vm and reduced inward (and outward) currents (Fig. 5). Particularly in Ano6 expressing cells permeability for K^+ ions was detected. Indirect evidence for cation

conductance of anoctamins has already been provided earlier (97; 96). Moreover, anoctamins are also permeable for Ca^{2+}, as reported for Ano6 (195). Taken together these results suggest that anoctamins are either poorly selective for anions or lead to parallel activation of a cation conductance.
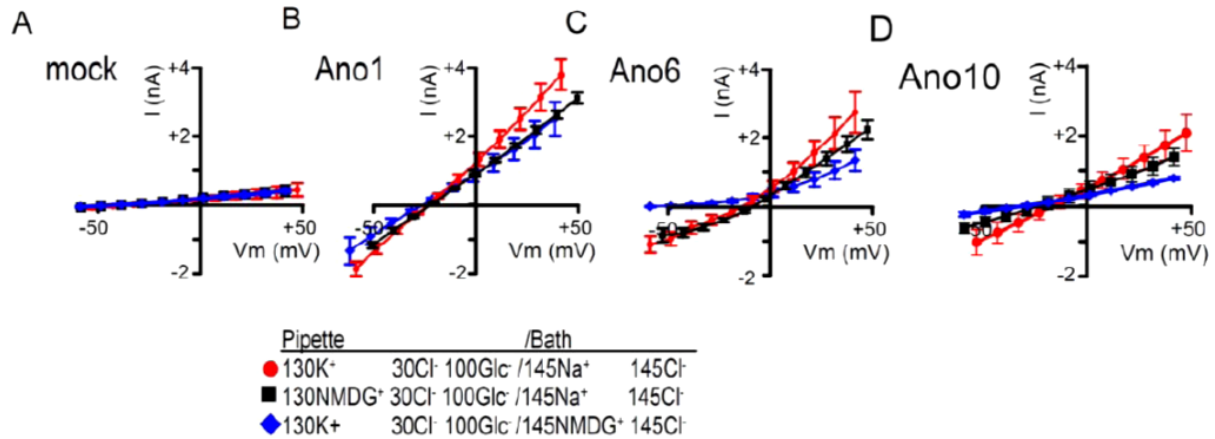
Fig. 5: Ano1, Ano6, and Ano10 induce permeability for cations. Summary I/V curves of whole cell currents obtained in Ano1 (B), Ano6 (C), and Ano10 (D) overexpressing HEK293 cells or mock transfected (A) cells. Effects of replacement of intracellular K+ by NMDG (black squares) and replacement of extracellular Na+ by NMDG+ (blue diamonds).

Inactivation of anoctamins

Increase in intracellular Ca^{2+} activates anoctamins only transiently. On the other hand, overexpression of Ano1 in HEK293 and other cell types leads to channels that are partially active even under baseline Ca^{2+} concentrations of 100 nM (Fig. 1,2) (97). We observed that during transient activation/deactivation of Ano1 whole cell Cl^- currents declined even below the initial high current levels, This was observed during continuous stimulation by ATP (10 μM) or ionomycin (1 μM), or when 1 μM Ca^{2+} was provided through the patch pipette filling solution (1 μM) (Fig. 6A). This suggests that increase in $[Ca^{2+}]_i$ initially activates the channel but then triggers inactivation by a Ca^{2+} dependent process. Spontaneous current-inactivation was not due to a loss of ATP or calmodulin, since we also observed inactivation when both components (3 mM ATP, 2 μM calmodulin) were present in the patch pipette. Because Ca^{2+}/calmodulin dependent kinase II (CAMKII) inhibits overexpressed Ano1 currents (169), we hypothesized that an increase of Ca^{2+} may activate CAMKII, which in turn inhibits Ano1.

In fact, in the presence of the CAMKII-blocker KN62 (5 µM), inactivation of the channel was significantly attenuated (Fig. 6B). Similar to Ano1, also Ano6 contains 4 putative CAMKII phosphorylation sites in the N-terminus (Supplemental Fig S2). Thus inhibition of CAMKII by 10 µM KN62 also increased activation of Ano6 by 1 µM ionomycin (ΔG_{Iono} = 29.6 ± 3.6 (w/o KN62) vs. 43.3 ± 4.5 nS (w/ KN62); n = 5).

Moreover, when patch pipettes were loaded with pre-activated CAMKII (5000 U/ml), activation of whole cell currents in Ano1-overexpressing cells was significantly reduced (Fig. 6C). Thus CAMKII inhibits overexpressed Ano1, which is reminiscent to inhibition of CaCC by CAMKII in smooth muscle cells (60). Along this line, a splice variant of Ano1 (ac-Ano1) had been reported to have a higher Ca^{2+} sensitivity than the splice form abc-Ano1 (52), which we used in our experiments. As reported by Ferrera et al, we also found that the channel is activated at [Ca^{2+}]$_i$ below 100 nM (Fig. 6D). However, we also found that ac-Ano1 currents inactivated at lower Ca^{2+}concentrations than the splice form abc-Ano1 (Fig. 6D). We tried to further localize the molecular site within Ano1 that is in charge for its only transient activation. Since activation of Ano6 produces more sustained currents (110), we generated a chimeric protein in which the N-terminus of Ano1 was replaced by that of Ano6 (Ano1N6). Notably whole cell currents generated by the chimeric Ano1N6 channel were no longer transient, but generated a rather sustained current when activated by 1 µM ionomycin (Fig. 6E, F). This suggests that the N-terminus controls both activation and inactivation of anoctamins. Notably, potential binding sites for calmodulin have been found in the N-terminus of Ano1, along with a number of putative phosphorylation sites, including those for CAMKII (92).

Overexpressed anoctamins behaves differently

The data presented above indicate that Ano6, 8, and 9, when overexpressed in HEK293 cells, produce Cl$^-$ currents upon increase in intracellular Ca^{2+} by ionomycin. However, although all three paralogs are expressed endogenously in HEK293 cells, no currents are activated in mock transfected cells (Fig. 3A) (3). However, when increasing [Ca^{2+}]$_i$ to very high levels ($\geq$ 10 µM), endogenous anoctamins were activated (Fig. 3B, E). This may be due to a lack of

sufficient membrane expression of endogenous anoctamins. Endogenous anoctamins are
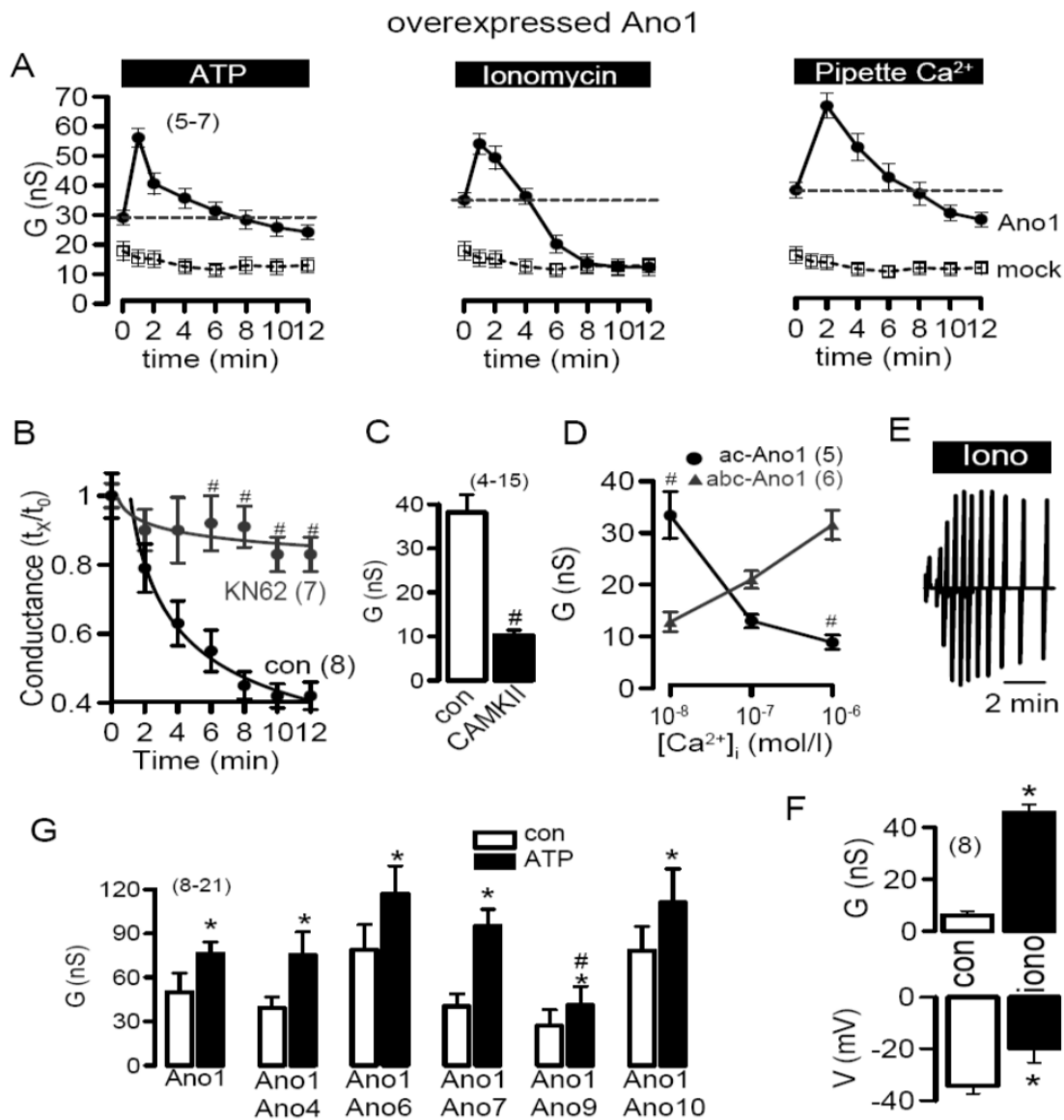
Fig. 6: Increase in $[Ca^{2+}]_i$ activates and subsequently inhibits anoctamins. (A) Activation and time dependent decay of Ano1 whole cell currents in HEK293 cells, when activated by ATP (10 µM), ionomycin (1 µM), and 1 µM Ca^{2+} in the patch pipette solution. (B) Time dependent decay of whole cell currents activated by 1 µM Ca^{2+} (patch pipette) in the absence or after pre-incubation with the inhibitor of CAMKII, KN62 (25 µM/2 hrs). (C) Activation of Ano1-whole cell currents by ionomycin and effect of active CAMKII (5000 U/ml; 40 min) on current activation. (D) Ca^{2+} dependent activation of the splice forms ac-Ano1 and abc-Ano1. (E) Sustained whole cell conductances activated by 1 µM ionomycin in HEK293 cells expressing the chimeric protein Ano1N6 in which the N-terminus of Ano1 has been replaced by that of Ano6. (F) Summary of the effect of ionomycin (1 µM) on whole cell conductance and membrane voltage in Ano1N6 expressing HEK293 cells. (G) Summary of whole cell conductances measured in HEK293 cells coexpressing different anoctamins. Mean ± SEM

(number of cells). # different to con or Ano1, respectively; $p < 0.05$; ANOVA. * significant activation; $p < 0.05$; paired t-test.

expressed at much lower levels than overexpressed proteins and may be inhibited by endogenous accessory proteins, such as CAMKII. Alternatively, specific Ca^{2+} release and/or influx pathways need to be triggered to activate these endogenous anoctamins. The overall linear structures appear similar in all anoctamins (Supplemental Fig. S1) and an analysis of putative functional domains revealed a number of similar motifs and putative phosphorylation sites in all ten anoctamins (Supplemental Fig. S2). Notably, Ano1 exists as a stable dimer (47; 153), and may even form heterooligomeric proteins with other anoctamins (148). In the present study we therefore coexpressed different anoctamins and found that only coexpression of Ano9 inhibited Ano1-currents activated by ATP, suggesting a specific interaction of different anoctamin paralogs (Fig. 6G).

The present results suggest that endogenous and overexpressed anoctamins behave differently. We found earlier that calmodulin and 1-EBIO, a calmodulin-dependent activator of K$^+$ channels, activate overexpressed Ano1 (169). In the present study we made use of a well established technique to assess endogenous Ca^{2+} activated Cl$^-$ currents in HT$_{29}$ cells stably expressing I$^-$-sensitive yellow fluorescent protein (YFP). Cellular YFP-fluorescence is quenched by iodide influx from the bath solution, (181) (Fig. 7A-C). Stimulation of purinergic receptors by ATP, dose dependently activated I$^-$ influx and YFP quenching, indicating activation of a Ca^{2+} dependent Cl$^-$ conductance (Fig. 7A, B). ATP activated Cl$^-$ conductance was blocked by typical Ano1-inhibitors (Fig. 7C). Moreover, siRNA-knockdown of Ano1 inhibited ATP-induced whole cell currents in HT$_{29}$ cells in another study (53). We examined the effects of 1-EBIO on Ca^{2+} dependent Cl$^-$ conductance in HT$_{29}$ cells. However, even at a concentration of 1 mM 1-EBIO was unable to directly activate a Cl$^-$ conductance (data not shown). It only slightly and dose dependently augmented ATP (1 μM) -activated Cl$^-$ conductance (Fig. 7D). A number of 1-EBIO-related compounds (DCEBIO, riluzole, CBIQ, NS8593, CYPPA, NS309, NS4591) were examined in a dose dependent manner. However, for none of them we found activation of a Cl$^-$ conductance and receptor-mediated activation by ATP was not augmented (data not shown).We further performed experiments in a human

airway epithelial cell line expressing the most common mutant form of CFTR, F508del-CFTR (CFBE/F508del-CFTR). We found: i) that ATP (10 µM) activated a whole cell Cl$^-$ conductance of 3.5 ± 0.4 nS (n = 5), while direct application of 1-EBIO (100 µM) did not. ii)
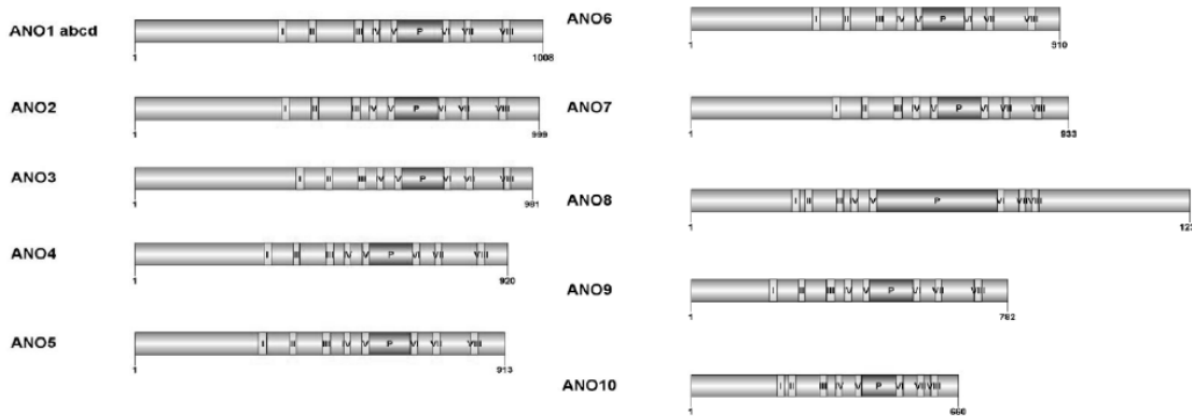
Supplemental Fig. S1: Structure prediction of anoctamins

Motif	ANO1	ANO2	ANO3	ANO4	ANO5	ANO6	ANO7	ANO8	ANO9	ANO10
N-glycosylation[1]	yes (5)	yes (4)	yes (4)	yes (3)	yes (5)	yes (6)	yes (1)	yes (1)	yes (4)	no
Coiled-Coils[1]	yes (3)	yes (3)	yes (1)	yes (1)	yes (2)	yes (3)	no	yes (4)	yes (1)	yes (2)
SH3 binding motif[3]	yes	yes	yes	yes	yes	yes	yes	yes	yes	yes
WW binding motif[3]	yes	yes	yes	yes	yes	yes	yes	yes	yes	yes
PDZ binding motif[3]	GGVL	HTNV	no	no	KSTL	no	no	no	STDV	no
EF-Hand[4]	no	no	no	no	no	no	no	no	no	no
Calmodulin binding site[5]	yes (3)	yes (2)	no	yes (2)	yes (1)	yes (1)	yes (2)	no	yes (1)	yes (1)
N-Terminus										
cAMP- and cGMP-dep. PK[1]	yes (4)	yes (2)	yes (1)	no	yes (1)	yes (4)	yes (1)	no	no	no
Protein kinase C[1]	yes (5)	yes (6)	yes (4)	yes (3)	yes (3)	yes (2)	yes (4)	yes (2)	yes (3)	yes (3)
Casein kinase II[1]	yes (2)	yes (6)	yes (5)	yes (6)	yes (5)	yes (5)	yes (4)	yes (8)	yes (4)	yes (2)
N-myristoylation site[1]	yes (3)	yes (7)	yes (4)	yes (4)	yes (1)	yes (2)	yes (5)	yes (4)	yes (2)	no
Amidation site[1]	yes (2)	no	yes (1)	no	yes (1)	no	no	yes (2)	no	no
Calmodulin-dependent Kinase II[2]	yes (5)	yes (4)	yes (13)	yes (4)	yes (5)	yes (4)	yes (7)	yes (1)	no	yes (1)
Tyrosine kinase[1]	no	no	no	no	yes (1)	no	no	no	no	yes (1)
ATP/GTP-binding site motif[1]	no	no	no	no	no	no	no	no	no	yes (2)
C-Terminus										
cAMP- and cGMP-dep. PK[1]	no	no	yes (1)	no	no	no	no	yes (1)	no	no
Protein kinase C[1]	no	no	no	no	yes (1)	yes (2)	no	yes (8)	yes (2)	yes (1)
Casein kinase II[1]	yes (1)	no	no	no	no	no	yes (1)	yes (5)		yes (1)
N-myristoylation site[1]	no	yes (3)	no	no	yes (1)	no	yes (2)	yes (9)	yes (2)	no
Calmodulin-dependent Kinase II[2]	no	no	no	no	no	yes (1)	yes (1)	yes (7)	no	no
Tyrosine kinase[1]	no	no	no	no	no	no	no	no	yes (1)	no

Supplemental Fig. S2: Anoctamin Motif Scan. Anoctamins were analyzed using the following resources: [1]Combet C., Blanchet C., Geourjon C. and Deléage G., NPS@: Network Protein Sequence Analysis, TIBS 25:147-150, 2000. [2]H.D. Huang, T.Y. Lee, S.W. Tseng and J.T. Horng. KinasePhos: a web tool for identifying protein kinase-specific phosphorylation sites, Nucleic Acids Research, 33: W226-229, 2005.[3]Brannetti B, Helmer-Citterich M. iSPOT: A web tool to infer the interaction specificity of families of protein modules. Nucleic Acids Res. 31: 3709-11, 2003.[4]Sigrist CJA, Cerutti L, de Castro E, Langendijk-Genevaux PS, Bulliard V, Bairoch A, Hulo N. PROSITE, a protein domain database for functional characterization and annotation, Nucleic Acids Res. 38: 161-6 (2010) [5]CALMODULIN TARGET DATABASE, http://calcium.uhnres.utoronto.ca/ctdb/ctdb/home.html.
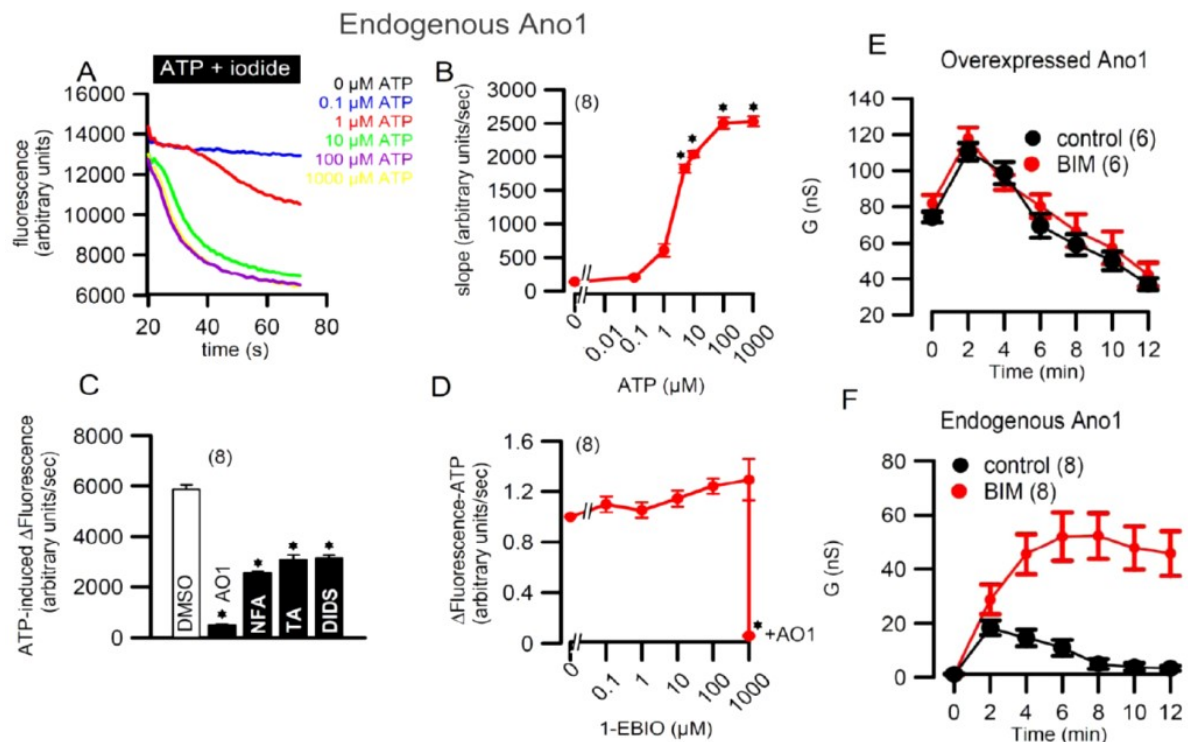
Fig. 7: Ca^{2+} activated halide permeability in HT_{29} cells expressing endogenous Ano1. (A) Application of different concentrations of ATP leads to influx of extracellular I^- (20 mM) and concentration dependent quenching of fluorescence in HT_{29} cells, stably expressing YFP. (B) Concentration response curve for ATP-induced YFP-fluorescence-quenching, indicating concentration-dependent activation of a Ca^{2+} activated Cl^- conductance by ATP. (C) Summary of the inhibition of ATP-induced fluorescence-quenching in HT_{29} cells by typical inhibitors of Ano1 (AO1 20 µM; NFA 10 µM; tannic acid TA 20 µM; DIDS 100 µM). (D) Incubation with 1-EBIO enhanced ATP-induced I^- uptake and quenching of YFP-fluorescence in a dose dependent manner. The Ca^{2+} activated Cl^- conductance was inhibited at the end of the experiment by AO1 (20 µM). Cells were measured in the presence of clotrimazole (10 µM) to inhibit a possible contribution by the Ca^{2+} dependent K^+ channel SK4. (E) Inhibition of protein kinase C by pre-incubation with bisindolylmaleimide 1 (BIM; 0.1 µM/2 hrs) did not affect activation and time course for inactivation of Ano1 overexpressed in HEK293 cells. (F) Inhibition of PKC by BIM augmented endogenous Ano1 currents in HT_{29} cells. Mean ± SEM (number of cells). * difference to control; $p < 0.05$; paired t-test.

activation of the whole cell Cl$^-$conductance through ATP-stimulation was slightly augmented by 0.7 ± 0.08 nS (n = 5) in the presence of 1-EBIO.

Taken together these results demonstrate i) that endogenous Ano1 behaves differently than overexpressed Ano1, and ii) that 1-EBIO is probably not useful to directly activate Ca^{2+} activated Cl$^-$ secretion in airways of CF patients.

Finally, we detected differential regulation by protein kinase C of Ano1 overexpressed in HEK293 cells and endogenous Ano1 in HT$_{29}$ cells: While inhibition of protein kinase C by preincubation with bisindolylmaleimide 1 (BIM; 0.1 μM/2 hrs) did not affect activation (by 1μM ionomycin) of overexpressed Ano1 (Fig. 7E) (169), it augmented endogenous Ano1-currents in HT$_{29}$ cells (Fig. 7F). Thus properties and regulation of overexpressed anoctamins may not fully reflect those of native channels.

Most anoctamins are plasma membrane localized

A recent report did not find membrane expression or Ca^{2+} activated Cl$^-$ currents for Ano3-7 (42). This is in contrast to our earlier results which demonstrate plasma membrane expression for Ano1, 2, 5, 6, 7, and 9 when overexpressed in HEK293 and FRT cells (148). Moreover, it was shown recently that Ano6 is an essential component of outwardly rectifying Cl$^-$ channels (ORCC) and, at the same time, operates as a membrane localized phospholipid scramblase (110; 163). Moreover, also Ano5 and Ano7 were detected in the plasma membrane in earlier studies (29; 116). We re-examined plasma membrane expression of overexpressed anoctamins in HEK293 cells and, again, found clear membrane expression for Ano1,4,5,6 and 7 and a weak membrane staining for Ano8, 9, and 10 (Fig. 8). We produced additonal YFP- fusion proteins for Ano6, Ano8 and Ano9. Life cell imaging of YFP-fluorescence suggested (partial) membrane expression for Ano6, 8, and 9 (Supplemental Fig. S3). For Ano10 we managed to introduce a FLAG-tag into the 3rd extracellular domain and labeled non-permeabilized cells. The results show a spotted membrane expression of Ano10 (Supplemental Fig. S3). Thus the present data fully confirm those obtained in earlier studies (148).

Nevertheless overexpressed Ano8, 9, and 10 show poor membrane expression. Since endogenous anoctamins are expressed at much lower levels, these anoctamins may not even accumulate at significant numbers in the plasma membrane of native cells. It is therefore entirely possible that Ano8, 9, and 10 have an intracellular rather than plasma membrane function. Currently available commercial antibodies are mostly of insufficient quality to stain endogenous anoctamins. Noteworthy, in contrast to Duran et al, we expressed only human anoctamins and acutely activated anoctamins, by either receptor stimulation or by ionomycin.
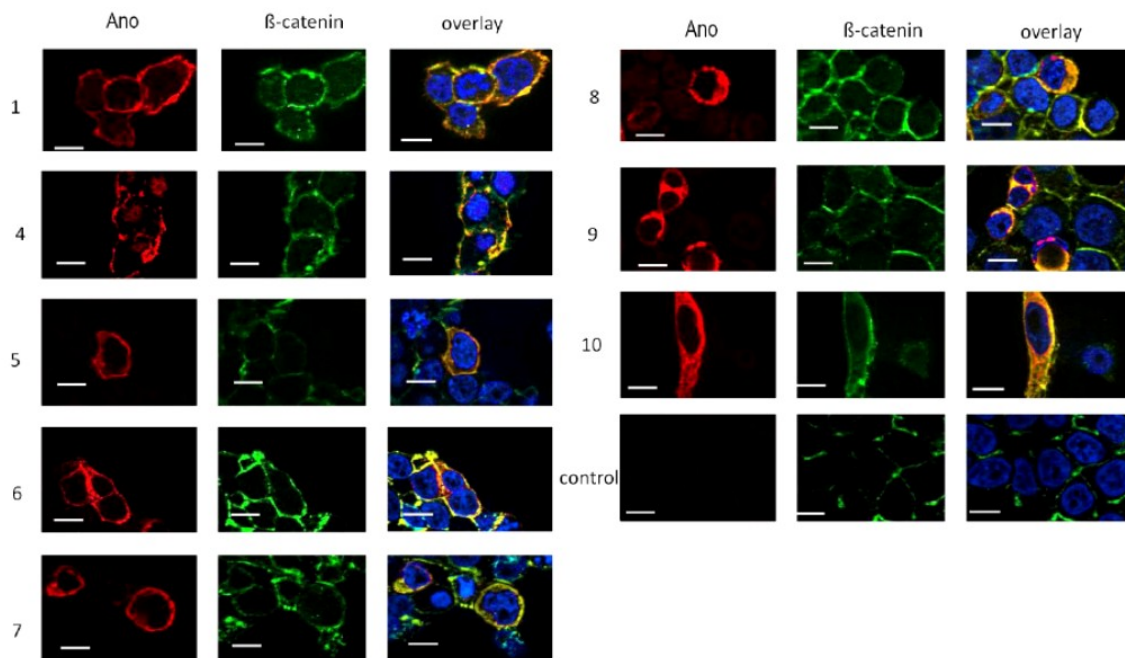
Fig. 8: Plasma membrane localization of anoctamins. Immunocytochemistry of human anoctamins (red) overexpressed in HEK293 cells, and co-staining of ß-catenin. Nuclei are shown in blue (DAPI staining). Bars indicate 20 µm.
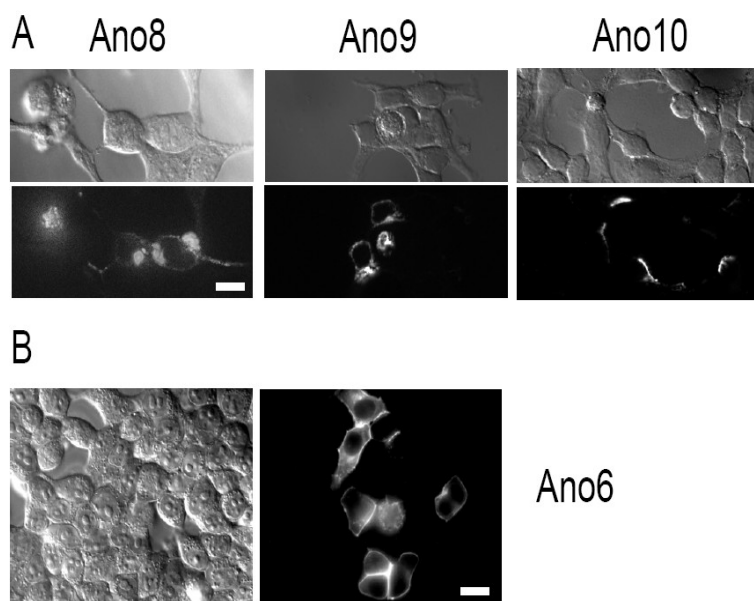
Supplemental Fig. S3: (A) Immunocy- tochemistry of hAno8, hAno9, and hAno10 as expressed in HEK293 cells. Ano8 and Ano9 were visualized using YFP fusion proteins (live staining). Ano10 contained a FLAG-tag in the predicted 3rd extracellular loop, and was labeled using a FLAG-antibody (non-per- meabilized cells) Bar = 10μm. **(B)** YFP-Ano6 expressed in HEK293 cells. Live imaging of YFP fluorescence. Bar = 20μm.

Since activation of most anoctamins was found to be transient, it is possible to overlook these currents, particularly if they are small, as those found for Ano5, 7, 8 and 9 (Fig. 1, 2). In summary, our present results suggest that anoctamins form a family of Ca^{2+} activated Cl$^-$ channels, which may have their function in the plasma membrane or in intracellular compartments. In addition to their property as Ca^{2+} activated Cl$^-$ channels, anoctamins may either have some permeability for cations, or their expression activates independent cation channels. These results may help to understand the physiological function of anoctamins and their role in disease.

Acknowledgments

CHAPTER 3

TMEM16 proteins produce volume regulated chloride currents that are reduced in mice lacking TMEM16A

Abstract

All vertebrate cells regulate their cell volume by activating chloride channels of unknown molecular identity, thereby activating regulatory volume decrease (RVD). We show that the Ca^{2+} activated Cl^- channel TMEM16A together with other TMEM16 proteins are activated by cell swelling through an autocrine mechanism that involves ATP release and binding to purinergic $P2Y_2$-receptors. TMEM16A channels are activated by ATP through increase in intracellular Ca^{2+} and by a Ca^{2+}- independent mechanism engaging extracellular regulated protein kinases (Erk1/2). The ability of epithelial cells to activate a Cl^- conductance upon cell swelling, and to decrease their cell volume (RVD) was dependent on TMEM16 proteins. Activation of $I_{Cl,swell}$ was reduced in the colonic epithelium and in salivary acinar cells from mice lacking expression of TMEM16A. Thus TMEM16 proteins appear to be a crucial component of epithelial volume-regulated Cl^- channels and may also have a function during proliferation and apoptotic cell death.

Key words: swelling activated Cl^- channels, TMEM16A, RVD, regulatory volume decrease

Introduction

Regulation of cell volume is fundamental to all cells, particularly during cell growth and division. External hypotonicity leads to cell swelling and subsequent activation of volume regulated chloride and potassium channels, to release intracellular ions and to re-shrink the cells, a process termed regulatory volume decrease (RVD) (162). Volume regulated chloride currents ($I_{Cl,swell}$) have dual functions during cell proliferation as well as apoptotic volume decrease (AVD), preceding apoptotic cell death (123). While $I_{Cl,swell}$ is activated in swollen cells to induce RVD, AVD takes place under normotonic conditions to shrink cells (100; 101). Early work suggested intracellular Ca^{2+} as an important mediator for activation of $I_{Cl,swell}$ and volume-regulated K^+ channels (70), while subsequent studies found an only permissive role of Ca^{2+} for activation of $I_{Cl,swell}$ (129; 162). In addition a plethora of factors and signaling pathways have been implicated in the activation of $I_{Cl,swell}$, making cell volume regulation an extremely complex process (69; 100; 162). These factors include intracellular ATP, the cytoskeleton, phospholipase A2-dependent pathways and protein kinases such as extracellular regulated kinase Erk1/2 (69; 162). Previous approaches in identifying swelling activated Cl^- channels have been unsuccessful or have produced controversial data. Thus none of the previous candidates such as pI_{Cln}, the multidrug resistance protein, or ClC-3 are generally accepted to operate as volume regulated Cl^- channels (56; 80). Notably, the cystic fibrosis transmembrane conductance regulator (CFTR) had been shown in earlier studies to influence $I_{Cl,swell}$ and volume regulation (177; 178; 180). The variable properties of $I_{Cl,swell}$ suggest that several gene products may affect $I_{Cl,swell}$ in different cell types.

The TMEM16 transmembrane protein family consists of 10 different proteins with numerous splice variants that contain 8-9 transmembrane domains and have predicted intracellular N- and C-terminal tails (85). TMEM16A (also called ANO1) is required for normal development of the murine trachea (135) and is associated with different types of tumors, dysplasia and nonsyndromic hearing impairment (21; 85). TMEM16A has been identified as a subunit of Ca^{2+} activated Cl^- channels that are expressed in epithelial and non-epithelial tissues (19; 149; 197). Interestingly, members of the TMEM16 family have been suggested to play a role in osmotolerance in *Saccharomyces cerevisiae* (165). Here we show that TMEM16 proteins also

contribute to $I_{Cl,swell}$ and regulatory volume decrease.

Material and Methods

Cell culture, cDNAs, and transfection

Cell lines from human embryonic kidney (HEK293), human colon carcinoma (HT$_{29}$), and human cystic fibrosis pancreatic epithelial (CFPAC) cells were cultured as described previously (90). cDNA for mouse TMEM16B was purchased from ImaGenes GmbH (Berlin, Germany, Clone name: IRAVp968H1167D). cDNA for human TMEM16A were cloned into pcDNA3.1 V5-His (Invitrogen, Karlsruhe, Germany) from total RNA of 16HBE-14o cells (bronchial epithelium; kindly provided by Prof. D. Gruenert, CPMRI, San Francisco, USA) by RT-PCR using the primer 5´- AAAAGCGGCCGCGGCCACGATGAGGGTC -3´ and 5´- AAATCTAGAAACAGGACGCCCCCGTGGTA-3´. All cDNAs were verified by sequencing. 16HBE-14o cells express a TMEM16A isoform containing the exons a, b and c, according to Caputo, A. et. al. (19). Plasmids were transfected into HEK293 cells using standard methods (lipofectamine, Invitrogen, Karlsruhe, Germany). All experiments were performed 48 hours after the transfection.

Western blotting

Protein was isolated from transfected HEK293 cells in a lysis buffer containing 50 mM Tris-HCl 150mM NaCl, 50mM Tris, 100mM DTT, 1% NP-40, 0,5 % Deoxycholate sodium, and 1% protease inhibitor cocktail (Sigma, Germany) and was separated by 7 % SDS-PAGE. For Western blot analysis, proteins separated by SDS-PAGE were transferred to a PVDF membrane (GE Healthcare Europe GmbH, Munich, Germany) using semi dry transfer unit (BioRad, Munich, Germany). Membranes were incubated with primary antibodies (dilution from 1:2000 to 1:5000) overnight at 4°C. Proteins were visualized using a suitable (HRP) conjugated secondary antibody (dilution 1:30000) and ECL Detection Kit (GE Healthcare, Munich, Germany). Protein bands were detected on a FujiFilm LAS-3000.

Patch clamp

Cells were grown on cover slips which were mounted in a perfused bath on the stage of an inverted microscope (IM35, Zeiss) and kept at 37 °C. Cells and acini isolated from mouse glands were allowed to settle onto poly-L-lysine coated cover slips. The bath was perfused continuously with Ringer solution at about 10 ml/min. For activation of volume dependent Cl$^-$ currents, isotonic Ringer bath solution (mM: NaCl 145, KH$_2$PO$_4$ 0.4, K$_2$HPO$_4$ 1.6, d-glucose 6, MgCl$_2$ 1, Ca-gluconate 1.3, pH 7.4) was changed to isotonic control solution in which 50 mmol/l NaCl was replaced by 100 mmol/l mannitol. Subsequently, mannitol (50, 75 and 100 mmol/l) was removed to produce extracellular hypotonicity of -50, -75, and -100 mosmol/l, i.e. 17%, 25% and 33% hypotonicity.   Patch-clamp experiments were performed in the fast whole-cell configuration. Patch pipettes had an input resistance of 2–4 MΩ, when filled with an intracellular like "physiological" solution containing (mM) KCl 30, K-gluconate 95, NaH$_2$PO$_4$ 1.2, Na$_2$HPO$_4$ 4.8, EGTA 1, Ca-gluconate 0.758, MgCl$_2$ 1.034, D-glucose 5, ATP 3, pH was 7.2, the Ca^{2+} activity was 0.1 μM. We choose this solution since it enabled normal swelling/shrinkage behavior and allowed for direct comparison of results from patch clamping and volume measurements. The access conductance was measured continuously and was 30 – 140 nS. Currents (voltage clamp) and voltages (current clamp) were recorded using a patch-clamp amplifier (EPC 7, List Medical Electronics, Darmstadt, Germany), the LIH1600 interface and PULSE software (HEKA, Lambrecht, Germany) as well as Chart software (AD-Instruments, Spechbach, Germany). Data were stored continuously on a computer hard disc and were analyzed using PULSE software. In regular intervals, membrane voltages (V$_c$) were clamped in steps of 10 mV from -50 to +50 mV relative to resting potential. Membrane conductance G$_m$ was calculated from the measured current (I) and V$_c$ values according to Ohm law**.**

Animals and Ussing chamber experiments

Generation of a null allele of Tmem16a and TMEM16A knockout animals has been described previously (135). Pups (1-4 days) were sacrificed with Isofluran (Baxter, Germany). The pancreas and submandibular glands were removed and epithelial cells were dispersed in a PBS buffer composed of Collagenase VIII (Sigma, Taufkirchen, Germany). Tracheas were

dissected, opened longitudinally on the opposite side of the cartilage free zone and were transferred immediately into an ice cold buffer solution. Stripped colon was put into ice cold Ringer bath solution (mM: NaCl 145, KH_2PO_4 0.4, K_2HPO_4 1.6, d-glucose 6, $MgCl_2$ 1, Ca-gluconate 1.3, pH 7.4) containing amiloride (10 μM) and indomethacin (10 μM). For activation of volume dependent Cl^- currents, isotonic Ringer bath solution (mM: NaCl 145, KH_2PO_4 0.4, K_2HPO_4 1.6, d-glucose 6, $MgCl_2$ 1, Ca-gluconate 1.3, pH 7.4) was changed to isotonic control solution in which 50 mmol/l NaCl was replaced by 100 mmol/l mannitol. Subsequently, mannitol was removed to produce extracellular hypotonicity of - 100 mosmol/liter, i.e. 33% hypotonicity. Tissues were mounted into a micro-perfused Ussing chamber with a circular aperture of 0.785 mm^2. Luminal and basolateral sides of the epithelium were perfused continuously at a rate of 5 ml/min. Bath solutions were heated to 37 °C, using a water jacket. Experiments were carried out under open circuit conditions. Data were collected continuously using PowerLab (AD-Instruments, Australia). Values for transepithelial voltages (V_{te}) were referred to the serosal side of the epithelium. Transepithelial resistance (R_{te}) was determined by applying short (1s) current pulses ($\Delta I = 0.5$ μA). R_{te} and equivalent short circuit currents (I_{SC}) were calculated according to Ohm's law ($R_{te} = \Delta Vte/\Delta I$, $I_{SC} = V_{te}/R_{te}$).

RT-PCR, cDNA, siRNA, RealTime PCR

TMEM16A was cloned from airway epithelial cells (16HBE14o-), corresponding to isoform abc (19). TMEM16A-K610A, TMEM16A-S967A, and TMEM16A-S970A were produced by PCR-based side directed mutagenesis. Expression of mRNAs encoding all 10 human TMEM16-proteins were examined in HEK293, HT_{29} and CFPAC cells by standard RT-PCR using real time and additional primers: (name, accession number: sense, antisense): hTMEM16C, NM_031418.2: 5'-TCAGAGCAGAAGGCTTGATG-3', 5'-AAACATGATAT-CGGGGCTTG-3', hTMEM16D, NM_178826.2: 5'-TGACTGGGATTTGATAGACTGG-3', 5'- GCTTCAAACTGGGGTCGTAT-3', hTMEM16GL, NM_001001891.3: 5'-GCTCTGTGG-TGATCGTGGT-3', 5'-GGCACGGTACAGGATGATAGA-3', hTMEM16GS, NM_00100 1666.3: 5'-GGCTCTTACGGGAGCACAG-3', 5'-CAAACGAGGACGAAGTCGAT-3' and

hTMEM16K, NM_018075.3: 5'-CAGGGTCTTCAAACGTCCAT-3', 5'-TCATCGTTTCAA-AAGCCAACT-3'. Expression of TMEM16A, TMEM16F, TMEM16H, and TMEM16J were suppressed by two independent sets of siRNA. Duplexes of 25-nucleotide of siRNA were designed and synthesized by Invitrogen (Paisley, UK) and Santa Cruz (Heidelberg, Germany). siRNA was transfected using Lipofectamin (1 µg/µl) and cells were examined 48 h or 72 h after transfection. Suppression of expression of TMEM16A, TMEM16F, TMEM16H, and TMEM16J was verified by real time PCR. Total RNA was isolated from HEK293 or HT$_{29}$ cells using NucleoSpin RNA II columns (Macherey-Nagel, Düren, Germany). Total RNA (2 µg) was reverse-transcribed using random primer and RT (M-MLV Reverse Transcriptase, Promega, Mannheim, Germany). The oligonucleotide primers were designed for real-time PCR as folowing (name, accession number: sense and antisense primer): hTMEM16A, NM_018043.4: 5'-CCTCACGGGCTTTGAAGAG-3', 5'-CTCCAAGACTCTGGCTTCGT-3', hTMEM16B, NM_020373.1: 5'-TGGATGTGCAACAATTGAAGA-3', 5'-GCATTCTGCTG-GTCACACAT-3', hTMEM16E, NM_213599.1: 5'-TGGAAACATTAAAGAAGCCATTTA-3', 5'-GAGTTTGTCCGAGCTTTTCG-5', hTMEM16F, NM_001025356.1: 5'-AGGAATGTTTT-GCTACAAATGGA-3', 5'-GTCCAAGGTTTTCCAACACG-3' hTMEM16H, NM_020959.1: 5'-GGAGGACCAGCCAATCATC-3', 5'-TGCTCGTGGACAGGGAAC-3', hTMEM16J, NM_001012302.2: 5'-CAAACCCCAGCTGGAACTC-3', 5'-GGATCCGGAGGCTCTCTT-3', ß-actin, NM_001101: 5'-CAACGGCTCCGGCATGTG-3', 5'-CTTGCTCTGGGCCTCGTC-3'. Real-time PCR was performed in a Light Cycler (Roche), using the Quanti Tect SYBR Green PCR Kit (Qiagen, Hilden, Germany). Each reaction contained 2 µl Master Mix (including *Taq* polymerase, DNTPs, SYBR green buffer), 1 pM of each primer sence and anti-sense, 2.5 mM MgCl$_2$, and 2 µl cDNA. After activation of the Taq polymerase for 10 min at 94° cDNA was amplified by 15 s at 94°C, 10 s at 55°C, and 20 s at 72°C, for 50 cycles. The amplification was followed by a melting curve analysis to control of the PCR products. Analysis of the data was performed using Light Cycler software 3.5.3. Standard curves for TMEMs mRNA and ß-actin mRNA were produced by using cDNA of transfected HEK cells at different dilutions. The ratio of the amount of TMEM to ß-actin mRNA was calculated for each sample and analysis was performed in triplicates.

Analysis of cell volume and FACS

For cell volume measurements, HEK293 cells were loaded with 2 µg calcein-AM (Molecular Probes) and 0.025% Pluronic in standard bath solution (Ringer) for 30–60 min at 37°C. Analysis was done at excitation wavelength of 500 nm and emission wavelength of 520-550 nm. Cell swelling and RVD were observed for 10-15 min after applying hypotonic bath solution. To produce extracellular hypotonicity, isotonic Ringer bath solution (mM: NaCl 145, KH_2PO_4 0.4, K_2HPO_4 1.6, d-glucose 6, $MgCl_2$ 1, Ca-gluconate 1.3, pH 7.4) was changed to isotonic control solution in which 50 mmol/l NaCl was replaced by 100 mmol/l mannitol. Subsequently, mannitol was removed to reduce extracellular hypotonicity by 100 mosmol/liter (33% hypotonicity). Experiments were performed 48h after transfection of HEK293 cells with cDNAs encoding $P2Y_2$ and hTMEM16A and 72h after transfection with siRNA targeting TMEM16 family members or scrambled. All the compounds were dissolved in the bath solutions and their effect on cell swelling was analyzed after 5-10 min incubation. Cell volume of HEK293 cells was also assessed by flow cytometry (Prof. Mathias Mack, University Hospital Regensburg) before (t = 0) and 30 sec (t = 0.5 min) and 5 min (t = 5 min) after swelling which was induced by reduction of the solution osmolarity to 1/3. In flow cytometry experiments, HEK293 cells were resuspended in PBS and the average volume of 30000 cells per condition was determined.

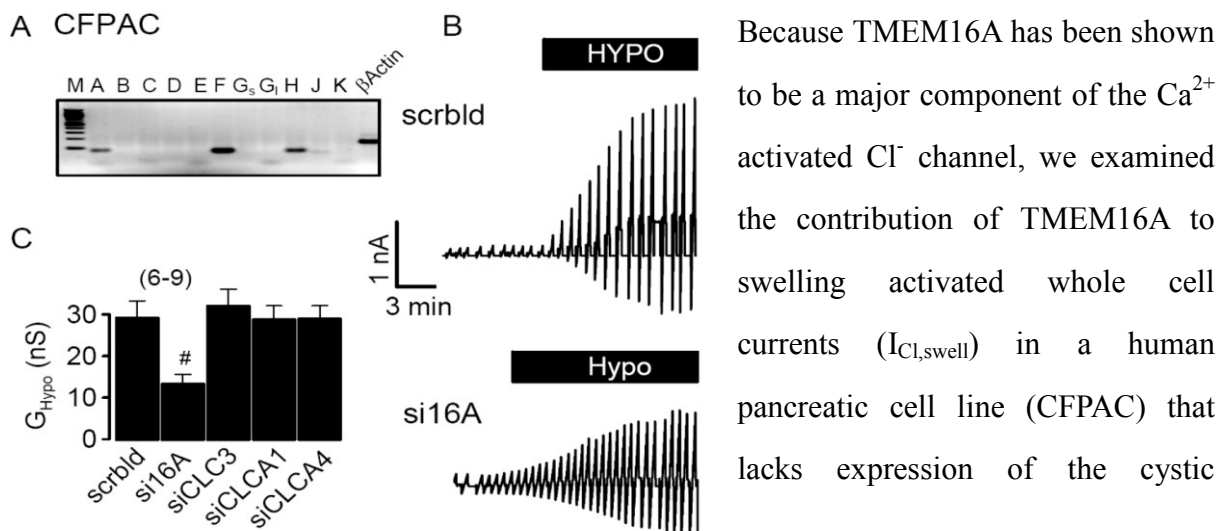*Materials and statistical analysis*

All compounds (ionomycin, carbachol, ATP, tamoxifen, 4,4'-diisothio-cyanostilbene-2, 2'-disulfonic acid (DIDS), suramin, 1,2-bis(2-aminophenoxyl)ethane-N,N,N',N'-tetraacetic acid-AM, U0126, staurosporine, $CFTR_{inh-172}$, apyrase, MTSET, cyclopiazonic acid) were of highest available grade of purity and were from Sigma (Taufkirchen, Germany) or Merck (Darmstadt, Germany). The anti-hTMEM16A was a generous gift from Prof. van de Rijn (Dept. of Pathology, Stanford University, USA).   All cell culture reagents were from GIBCO/Invitrogen (Karlsruhe, Germany). For activation of volume dependent Cl⁻ currents, isotonic Ringer bath solution (mM: NaCl 145, KH_2PO_4 0.4, K_2HPO_4 1.6, d-glucose 6, $MgCl_2$ 1, Ca-gluconate 1.3, pH 7.4) was changed to isotonic control solution in which 50 mmol/l

NaCl was replaced by 100 mmol/l mannitol. Subsequently, mannitol (50, 75 and 100 mmol/l) was removed to produce extracellular hypotonicity of -50, -75, and -100 mosmol/l, i.e. 17%, 25% and 33% hypotonicity. Regulatory volume decrease (RVD) due to swelling activation of ion channels is an initial event which was assessed by analysis of the initial volume decrease. RVD indicates initial rate of regulatory volume decrease or initial RVD rate, RVDi(%) = (Vmax-Vmin)/(Vmax-Vo) x 100% (4). Initial rate of RVD in hepatocytes is controlled by extracellular ATP (125). Student's t-test (for paired or unpaired samples as appropriate) and analysis of variance (ANOVA) was used for statistical analysis. P<0.05 was accepted as significant.

Results and Discussion

Suppression of $I_{Cl,swell}$ by siRNA-TMEM16A in three different cell lines

Because TMEM16A has been shown to be a major component of the Ca^{2+} activated Cl^- channel, we examined the contribution of TMEM16A to swelling activated whole cell currents ($I_{Cl,swell}$) in a human pancreatic cell line (CFPAC) that lacks expression of the cystic
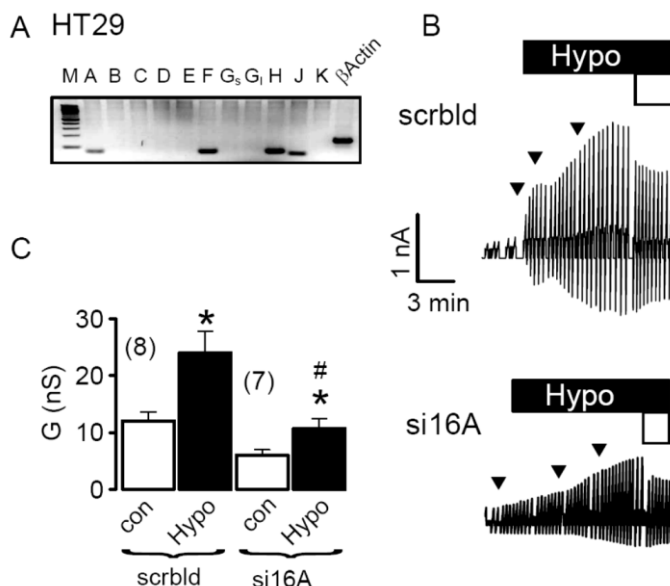
Fig. 1: Activation of $I_{Cl,swell}$ in CFPAC cells requires TMEM16A channels. (A) RT-PCR analysis indicates expression of TMEM16A, TMEM16F, and TMEM16H in CFPAC cells. M = marker, A-K = TMEM16A-K. Gs, Gl; short and long splice variants. (B) Original recordings of whole cell currents in CFPAC cells activated by hypotonic bath solution (33%). Cells were voltage clamped in intervals from -50 to +50 mV. Treatment with siRNA for TMEM16A (si16A) reduced the swelling activated whole cell current, when compared to cells treated with scrambled (scrbld) RNA. (C) Summary of swelling activated whole cell conductances (G_{Hypo}) measured in CFPAC cells treated with scrambled RNA or after RNAi-knockdown of TMEM16A, CLC-3, and CLCA-proteins. Mean ± SEM, (n) = number of cells measured. # significant inhibition of $I_{Cl,swell}$ by RNAi-knockdown of TMEM16A when compared to treatment with scrambled (scrbld) RNA (unpaired t-test).

fibrosis transmembrane conductance regulator (CFTR) Cl$^-$ channel (90). CFPAC cells express TMEM16A, F, and H and show pronounced activation of whole cell Cl$^-$ currents when exposed to hypotonic bath solution (90) (Fig. 1A, B). Activation of whole cell currents was suppressed by siRNA for TMEM16A, but not by siRNA knockdown of CLC3, ClCA1, and CLCA4, which are also expressed in CFPAC cells (Fig. 1C). This result was confirmed in HT$_{29}$, which also expresses TMEM16A, F, H, J. (Fig. 2A).

$I_{Cl,swell}$ was activated upon exposure to increasing extracellular hypotonicity (17%, 25%, and 33%; arrows) (Fig. 2B). Partial removal of Cl$^-$ from the extracellular bath solution (white bars;

Fig. 2: Activation of $I_{Cl,swell}$ in HT$_{29}$ cells requires TMEM16A channels. (A) RT-PCR analysis indicates expression of TMEM16A, TMEM16F, TMEM16H, and TMEM16J in HT$_{29}$ cells. M = marker, A-K = TMEM16A-K. Gs, Gl; short and long splice variants. (B) Original recordings of whole cell currents in HT$_{29}$ cells, activated by a gradual increase of extracellular hypotonicity (17%, 25%, and 33%; arrows). Cells were voltage clamped in intervals from -50 to +50 mV. Partial replacement of extracellular Cl$^-$ by gluconate (open bar; 30 mM Cl$^-$) inhibited whole cell outward currents. Treatment with siRNA for TMEM16A (si16A) reduced the swelling activated whole cell current, when compared to cells treated with scrambled (scrbld) RNA. (C) Summary of whole cell conductances measured in HT$_{29}$ cells under control conditions (open bars; normotonic bath solution) and after exposure to 33% hypotonicity (black bars). Mean ± SEM, (n) = number of cells measured. *significant increase in whole cell conductance (paired t-test). # significant inhibition of $I_{Cl,swell}$ by RNAi-knockdown of TMEM16A, when compared to treatment with scrambled (scrbld) RNA (unpaired t-test).

30 mM Cl$^-$) reduced $I_{Cl,swell}$ and depolarized Vm by 9.1 ± 0.8 mV (n = 7), indicating activation of a Cl$^-$ conductance by hypotonic bath solution. Importantly, activation of $I_{Cl,swell}$ was reduced by siRNA-TMEM16A (Fig. 2B, C). Finally, the role of TMEM16A for $I_{Cl,swell}$ was examined in HEK293 cells, which also express endogenous TMEM16-proteins (Fig. 3A). Equal to HT$_{29}$ and CFPAC cells, $I_{Cl,swell}$ was activated upon exposure to hypotonic bath

solution (Fig. 3B). Partial removal of Cl$^-$ from the ex tracellular bath solution reduced $I_{Cl,swell}$ and depolarized Vm by 8.2 ± 0.9 mV (n = 7). Most importantly, $I_{Cl,swell}$ was inhibited by siRNA-TMEM16A (Fig. 3B, C).
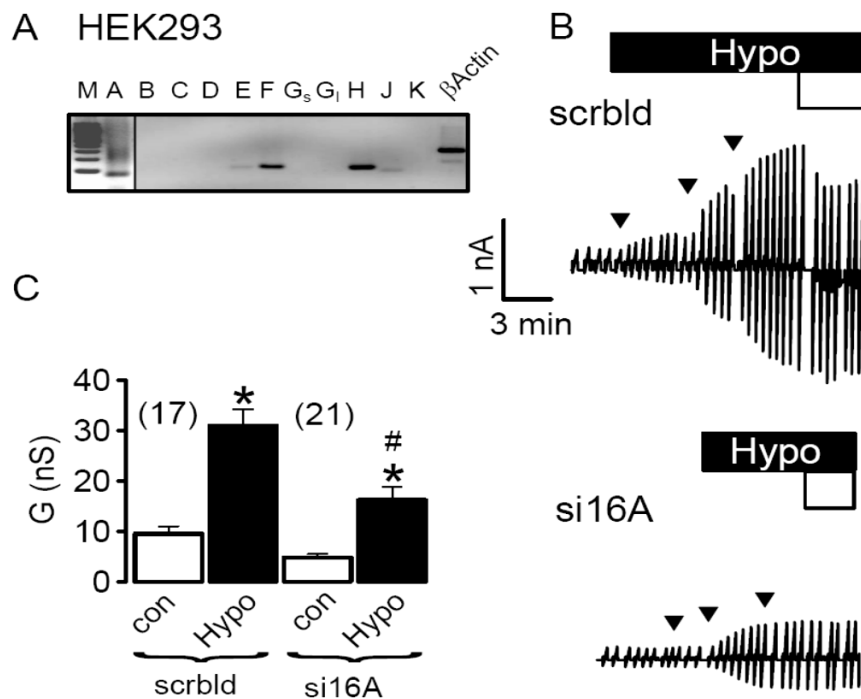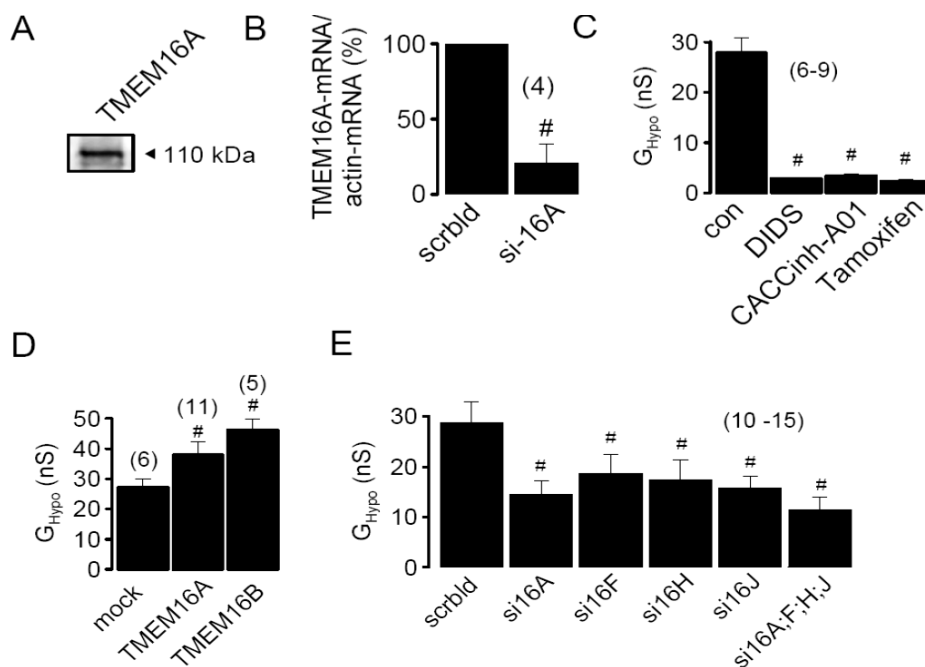

Fig. 3: Activation of ICl,swell in HEK293 cells requires TMEM16A channels. (A) RT-PCR analysis indicates expression of TMEM16A, TMEM16F, and TMEM16H, in HEK293 cells. PCR product of TMEM16A becomes only visible when cDNA input was doubled. M = marker, A-K = TMEM16A-K. Gs, Gl; short and long splice variants. (B) Original recordings of whole cell currents in HEK293 cells, activated by a gradual increase of extracellular hypotonicity (17%, 25%, and 33%; arrows). Cells were voltage clamped in intervals from -50 to +50 mV. Partial replacement of extracellular Cl- by gluconate (open bar; 30 mM Cl-) inhibited whole cell outward currents. Treatment with siRNA for TMEM16A (si16A) reduced the swelling activated whole cell current, when compared to cells treated with scrambled (scrbld) RNA. (C) Summary of whole cell conductances measured in HEK293 cells under control conditions (open bars; normotonic bath solution) and after exposure to 33% hypotonicity (black bars). Mean ± SEM, (n) = number of cells measured. *significant increase in whole cell conductance (paired t-test). # significant inhibition of ICl,swell by RNAi-knockdown of TMEM16A, when compared to treatment with scrambled (scrbld) RNA (unpaired t-test).

Members of the TMEM16-family participate in $I_{Cl,swell}$

HEK293 cells which express low but detectable amounts of TMEM16A (Fig. 3A, 4A), were incubated with two different batches of siRNA and knockdown of TMEM16A was verified by

real time RT-PCR (Fig. 4B). Activation of whole cell conductance by hypotonic bath solution (G_{Hypo}) was potently inhibited by the inhibitor of TMEM16A-currents, DIDS (100 µM) (197), the specific inhibitor of Ca^{2+} activated Cl^- currents CACCinh-A01 (31) and tamoxifen (100 µM) (Fig. 4C).
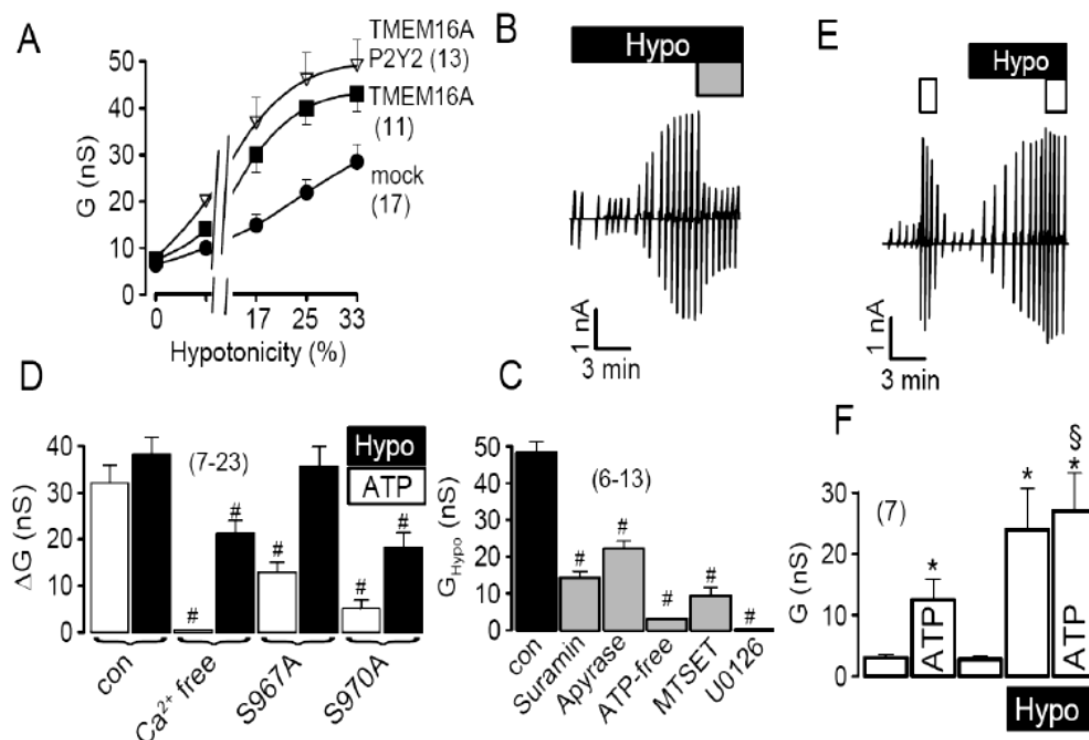

Fig. 4: Activation of $I_{Cl,swell}$ in HEK293 cells depends on the presence of TMEM16 channels. (A) Western blot analysis indicates expression of endogenous TMEM16A in HEK293 cells (B) Realtime PCR analysis of expression of TMEM16A in HEK293 cells treated with scrambled siRNA (scrbld) and TMEM16A-siRNA (si16A). (C) Inhibition of swelling activated whole cell conductances (G_{Hypo}) in HEK293 cells by DIDS (100 µM), CaCCinh-A01 (10 µM), and tamoxifen (100 µM). (D) Summary of G_{Hypo} in HEK293 cells expressing empty plasmid (mock), TMEM16A, or TMEM16B. (E) Summary of swelling induced whole cell conductances in cells treated with siRNA for various TMEM16 proteins. Mean ± SEM, (n) = number of cells measured. # significant difference when compared to control cells (mock, scrbld, absence of inhibitors) (unpaired t-test).

We further confirmed the role of TMEM16 proteins for swelling activated Cl^- currents by overexpression of exogenous TMEM16A or TMEM16B, another Ca^{2+} activated Cl^- channel and member of the TMEM16 family (132). Overexpression of both TMEM16-proteins augmented swelling activated Cl^- currents in HEK293 cells (Fig. 4D). This suggests that several TMEM16-proteins may contribute to swelling activated Cl^- currents. We therefore knocked down endogenous TMEM16F, H and J individually or simultaneously, each by two

different batches of siRNA, which in each case significantly reduced $I_{Cl,swell}$ (Fig. 4E). Since knockdown of each TMEM16 protein caused a non-additive reduction in $I_{Cl,swell}$, this may suggest that TMEM16 proteins heterooligomerize to form swelling activated Cl^- channels. In preliminary studies we found that endogenous volume activated Cl^- channels in HEK293 cells were potently suppressed by expression of K610A-TMEM16A, a TMEM16A-mutant that produced very little Cl^- conductance (unpublished data).

Role of purinergic signaling for activation of TMEM16A by cell swelling

Coexpression of G-protein coupled receptors has been shown to increase Ca^{2+} activated Cl^- currents produced by TMEM16A (197). Although P2Y$_2$ receptors are expressed endogenously in HEK293 cells, additional expression of exogenous purinergic P2Y$_2$ receptors further increased swelling activated whole cell currents in HEK293 cells (Fig. 5A).

Fig. 5: Role of purinergic signaling for activation of TMEM16A in HEK293 cells by cell swelling. (A) Activation of whole cell conductance by increased extracellular hypotonicity in cells expressing empty plasmid (mock), TMEM16A, or TMEM16A together with P2Y$_2$-receptors. (B) Swelling activation of whole cell currents in a HEK293 cell and inhibition of the current by suramin (100 μM; grey bar). (C) Inhibition of the swelling activated whole cell conductance by suramin (100 μM), apyrase (3 U/ml), and ATP-free

pipette solution, the cystein reagent MTSET (2.5 mM) and the inhibitor of extracellular regulated kinase (Erk1/2) U0126 (25 µM). (D) Summary of swelling activated (Hypo) and ATP induced whole cell conductances in TMEM16A expressing HEK293 cells, under control conditions and after removal of Ca^{2+} from both pipette and bath solution. Both ATP and swelling induced whole cell conductances were reduced under Ca^{2+} free conditions and when two Erk1/2 consensus sides in TMEM16A were mutated. (E) Activation of whole cell currents by ATP (open bar; 10 µM), before and after swelling activation whole cell currents (Hypo). (F) Summary of whole cell conductances in the absence and presence of ATP hypotonic bath solution. Mean ± SEM, (n) = number of cells measured. *significant ATP-effect (paired t-test). # significant difference when compared to control (unpaired t-test). §significant difference when compared to the absence of hypotonic bath solution (unpaired t-test).

Intracellular ATP and swelling induced ATP-release from cells has been identified as an important factor for RVD (54). Moreover, it has been shown that ATP binds to purinergic $P2Y_2$-receptors and activates TMEM16A (197). We found that blockage of $P2Y_2$ receptors with 100 µM suramin largely reduced swelling activated whole cell currents (Fig. 5B, C), confirming the role of $P2Y_2$-signaling for $I_{Cl,swell}$. Since ATP release is obviously a critical factor for activation of $I_{Cl,swell}$, we exposed the cells to hypotonic bath solution in the presence of the ATP-hydrolyzing enzyme apyrase, or removed ATP from the pipette filling solution, which both significantly reduced $I_{Cl,swell}$ (Fig. 5C). Moreover, TMEM16A has been shown to be inhibited by the sulfhydryl-reagent MTSET, which reacts with three cysteine residues in the putative pore forming loop of TMEM16A (197). MTSET also blocked swelling activated whole cell currents in HEK293 cells. Remarkably, the Erk1/2-inhibitor U0126 completely inhibited $I_{Cl,swell}$ thus clearly implying a role of this kinase for activation of TMEM16-channels (Fig. 5C). Notably, also ATP, i.e. Ca^{2+} activated whole cell currents were reduced by U0126 (data not shown).

We further examined the contribution of Ca^{2+} and Erk1/2 for activation of $I_{Cl,swell}$ and Ca^{2+} dependent activation of TMEM16A by ATP, using Ca^{2+} free solution (in patch pipette and bath) and by mutating two potential C-terminal Erk1/2 consensus sides (S967, S970) in TMEM16A. We found that eliminating Ca^{2+} abolished activation of TMEM16A by ATP and inhibited $I_{Cl,swell}$ (Fig. 5D). Mutating ser 967 to alanine inhibited ATP-activated currents, while mutating ser 970 to alanine inhibited both, ATP-activated Cl^- currents (TMEM16A) and

$I_{Cl,swell}$ (Fig. 5D). Thus both swelling activation and ATP-dependent activation of TMEM16A use Ca^{2+} and Erk1/2 as intracellular messengers. While $I_{Cl,swell}$ requires Erk1/2 for activation, Ca^{2+} has only a permissive function (25; 179). ATP release by swollen cells may activate Erk1/2 at very low local extracellular ATP concentrations, and may thereby induce swelling activated Cl⁻ conductance, as reported earlier (179).

To further demonstrate that ATP and cell swelling target the same Cl⁻ channel, we applied ATP before and after exposure to hypotonic bath solution (paired experiments). We observed that after activation of $I_{Cl,swell}$, ATP induced (Ca^{2+} dependent) whole cell currents were largely reduced (Fig. 5E, F). Similar non-additive effects of ATP and cell swelling on whole cell Cl⁻ conductance were observed in HT_{29} cells (data not shown).

TMEM16 proteins are essential for RVD in HEK293 cells

To further confirm the role of TMEM16-channels for $I_{Cl,swell}$ and regulatory volume decrease (RVD) we loaded HEK293 cells with the fluorescence dye calcein (1). Hypotonic bath solution induced cell swelling and decreased calcein fluorescence which was followed by a 98 % recovery after 20 min, indicating RVD (Fig. 6A).
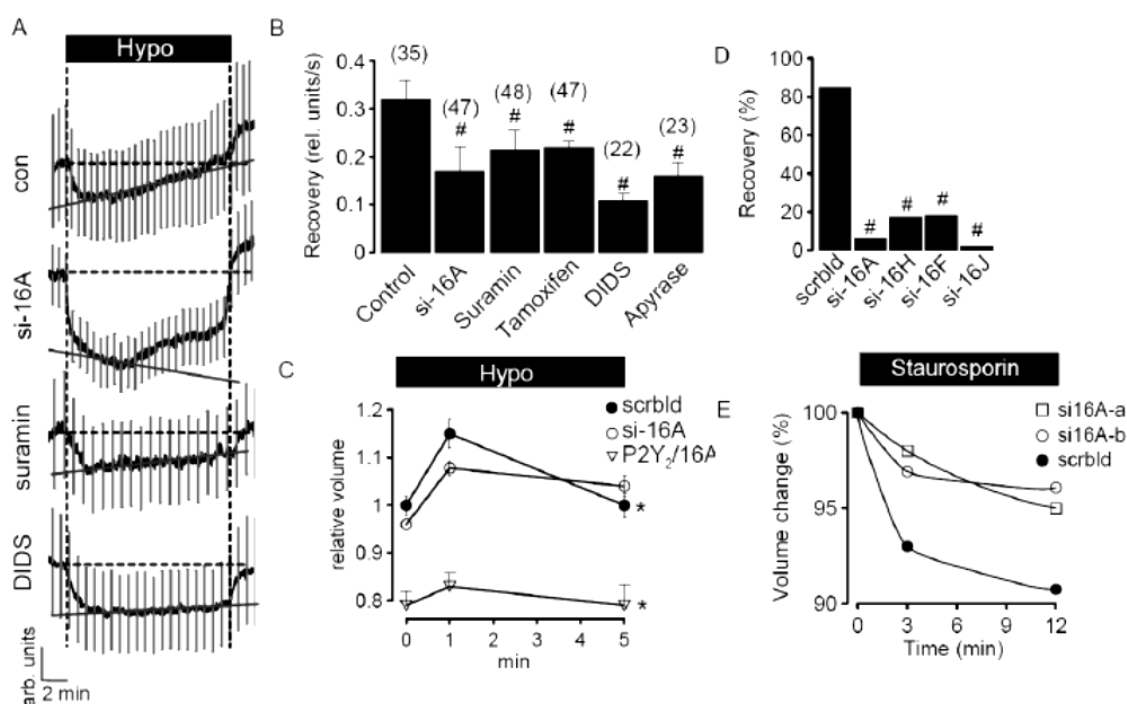
Fig. 6: TMEM16 proteins are essential for RVD in HEK293 cells. (A) Swelling (Hypo) induced changes in calcein fluorescence in control HEK293 cells and cells treated with siRNA for TMEM16A or suramin (100 µM) or DIDS (100 µM). Mean curve ± SEM (n = 10). (B) Summary of the rate of fluorescence recovery per second, indicating recovery of the cell volume from hypotonic swelling. Treatment with siRNA for TMEM16A or exposure to various inhibitors of $I_{Cl,swell}$ inhibited recovery of the cell volume, i.e. RVD. (C) Hypotonic cell swelling and recovery from cell swelling of cells treated with i) scrambled RNA, ii) TMEM16A-RNAi or iii) coexpressing P2Y$_2$-receptors/TMEM16A, as determined by FACS analysis of 30.000 cells per experiment. Experiments were performed in triplicates. (D) Summary of volume, i.e. fluorescence recovery after hypotonic cell swelling of HEK293 cells treated with siRNA for the different TMEM16-proteins, as determined by FACS analysis of 30.000 cells per experiment. (E) Apoptotic cell shrinkage induced by staurosporin (2 µM) under normotonic conditions in cells treated with two different batches of siRNA for TMEM16A (si16A-a, si16A-b), or when treated with scrambled RNA (FACS analysis of 30.000 cells). Mean ± SEM, (n) = number of cells measured. *significant recovery from cell swelling of cells treated with scrambled siRNA (paired t-test). # significant difference when compared to control (unpaired t-test).

Recovery from swelling was reduced in cells treated with siRNA-TMEM16A (42 % after 20 min). Similarly inhibition of P2Y$_2$-receptors by suramin, or application of the Cl$^-$ channel blockers tamoxifen and DIDS, or apyrase, all significantly reduced RVD (Fig. 6A, B).

These results obtained in single cell measurements were confirmed by FACS-analysis of a larger number of cells. HEK293 cells treated with scrambled siRNA increased their cell volume, which returned to control values within 5 min of exposure to hypotonic bath solution (Fig. 6C). In contrast, cells treated with siRNA for TMEM16A did not return to their initial volume, demonstrating reduced RVD. Notably, overexpression of P2Y$_2$-receptors together with TMEM16A reduced the cell volume of HEK293 cells under control conditions. Overexpression of P2Y$_2$ receptors probably sensitizes HEK293 cells towards extracellular ATP, thus P2Y$_2$/TMEM16A expressing cells activate Cl$^-$ channels more rapidly and therefore tend to reduce their cell volume. Moreover, their large RVD-capacity counteracts any tendency to swell and therefore the cells show only a small increase in cell volume when exposed to hypotonic bath solution (Fig. 6C). We determined the rate of recovery from cell swelling and found that not only TMEM16A but also the other TMEM16 proteins expressed in HEK293 cells contribute to RVD, as demonstrated by siRNA-knockdown of the individual TMEM16 proteins (Fig. 6D).

It has been reported earlier that cell shrinkage due to opening of ion channels not only occurs during hypotonic swelling, but also in normotonic solution, when cells go into apoptotic cells death (102; 123). Apoptotic volume decrease (AVD) is an initial step during apoptosis, which can be induced by compounds such as staurosporin (102). When we exposed HEK293 cells to staurosporin we observed a decrease in cell volume, indicating AVD (Fig. 6E). In contrast, knockdown of TMEM16A with two independent siRNAs significantly reduced AVD, suggesting that TMEM16A is important for both cell volume regulation (RVD) and apoptotic cell death (AVD).

Impaired $I_{Cl,swell}$ in epithelial tissues of mice lacking TMEM16

TMEM16A is expressed at high levels in the submandibular gland and to lower degree in hepatocytes (135; 149); (Unigene-database). We examined activation of $I_{Cl,swell}$ in freshly isolated acinar cells from submandibular glands and in hepatocytes of 1-4 day old wt (+/+) mouse pups and compared the results with those obtained in cells from mice lacking expression of TMEM16A (-/-). Exposure to hypotonic solution of submandibular acinar cells from +/+ animals activated a whole cell current that was essentially absent in cells from -/- animals (Fig. 7A, C).
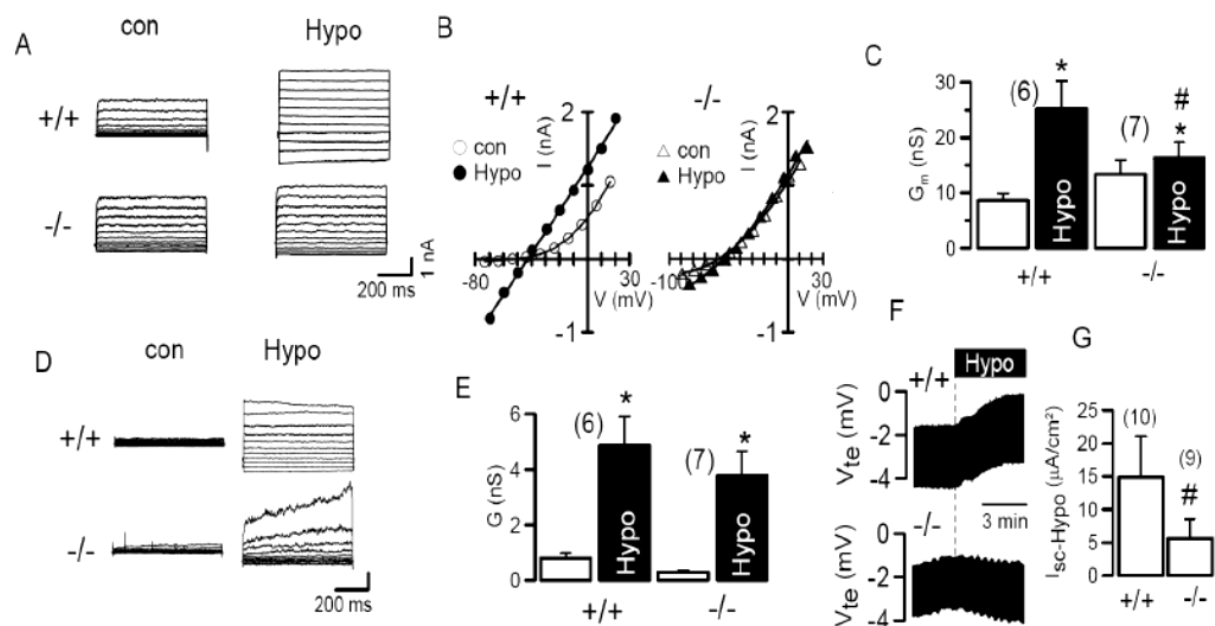
Fig. 7: Impaired $I_{Cl,swell}$ in epithelial tissues of mice lacking TMEM16-/-. (A,B) Whole cell

currents and corresponding i/v curves obtained in submandibular acinar cells of TMEM16A-knockout mice (-/-) and wild type litter mates (+/+) before and after exposure to hypotonic (33%) bath solution. (C) Summary of the whole cell conductances induced by hypotonic bath solution in wt and knockout animals. (D, E) Whole cell currents and corresponding whole cell conductances obtained in hepatocytes of TMEM16A-knockout mice (-/-) and wild type litter mates (+/+), before and after exposure to hypotonic bath solution. (F) Recording of the change in transepithelial voltage (V_{te}) induced by hypotonic bath solution (25%) in wt (+/+) and knockout (-/-) animals. (G) Summary of the ion transport, i.e. the short circuit currents induced by hypotonic bath solution in wt (+/+) animals and knockout (-/-) littermates. Mean ± SEM, (n) = number of cells measured. *significant increase in whole cell conductance (paired t-test). # significant difference when compared to wt (+/+) (unpaired t-test).

Thus the volume activated whole cell conductance was almost abolished in submandibular gland cells from -/- mice (Fig. 7C). In hepatocytes $I_{Cl,swell}$ was of similar magnitude in both cells from +/+ and -/- animals, however, currents activated in -/- cells showed a different time dependence, suggesting some contribution of TMEM16A to $I_{Cl,swell}$ also in hepatocytes (99).

Volume activated Cl⁻ currents have also been identified previously in the basolateral membrane of colonic epithelial cells (37). Opening of basolateral Cl⁻ channels due to exposure to hypotonic bath solution reduced the lumen negative transepithelial voltage (V_{te}) in the distal colonic epithelium (Fig. 7F). In contrast the distal colon from TMEM16A-/- animals showed little changes when exposed to hypotonic solution, and thus swelling induced short circuit currents were significantly reduced in the TMEM16A-/- colon (Fig. 7F, G). Taken together the data clearly indicate that TMEM16A channels contribute to volume regulated Cl⁻ currents in native mouse epithelial cells. The present results suggest that volume regulated Cl⁻ channels may be composed of different members of the TMEM16-family, probably in a tissue specific manner, thus giving rise to variable properties of $I_{Cl,swell}$ in different cell types and tissues (56). As these channels also control apoptotic cell shrinkage, they may affect cell survival, which could explain the role of these proteins in tumor development (85).

Acknowledgments

CHAPTER 4

Calmodulin-dependent activation of the epithelial calcium-dependent chloride channel

TMEM16A

Abstract

TMEM16A (anoctamin 1, Ano1), a member of a family of 10 homologous proteins has been shown to form an essential component of Ca^{2+} activated Cl^- channels. TMEM16A null mice exhibit severe defects in epithelial transport along with tracheomalacia and death within one month after birth. Despite its outstanding physiological significance, the mechanisms for activation of TMEM16A remain obscure. TMEM16A is activated upon increase in intracellular Ca^{2+}, but it is unclear whether Ca^{2+} binds directly to the channel or whether additional components are required. We demonstrate that TMEM16A is strictly membrane localized and requires cytoskeletal interactions to be fully activated. Despite the need for cytosolic ATP for full activation, phosphorylation by protein kinases is not required. In contrast, the Ca^{2+} binding protein calmodulin appears indispensable and interacts physically with TMEM16A. Openers of small and intermediate conductance Ca^{2+} activated potassium channels like 1-EBIO, DCEBIO or riluzole known to interact with calmodulin, also activated TMEM16A. These results reinforce the use of these compounds for activation of electrolyte secretion in diseases such as cystic fibrosis.

Key words: Ca^{2+} activated Cl^- channels, TMEM16A, Anoctamin 1, Ano1, Ca^{2+}, Calmodulin, exocytosis, SK4, 1-EBIO, patch clamp, cystic fibrosis

Own experimental contribution: All patch clamping experiments performed in whole cells, Westen blot, immunoprecipitation, and parts Ussing chamber experiments.

Own written contribution: Methods, Results, Parts of Introduction and Discussion.

Other contributions: Designed experiments and analyzed data.

Introduction

Broadly expressed Ca^{2+} activated Cl^- channels (CaCC) are of fundamental importance in many tissues, as they control electrolyte secretion, neuronal excitability, and smooth muscle contraction. CaCC have been identified as TMEM16A (19; 149; 197). TMEM16A (anoctamin 1, ANO1) belongs to a family of 10 TMEM16-proteins (TMEM16A-K, ANO1-10). TMEM16A has eight putative transmembrane domains (TMD) and a p-loop between TMD 5 and 6. Along with multiple splice variants, several isoforms are coexpressed in a tissue specific manner, which provide a Ca^{2+} activated Cl^- conductance of distinct biophysical and pharmacological features (52; 92). It has been shown that alternative splicing of TMEM16A changes voltage dependence and Ca^{2+} sensitivity (52). Moreover, membrane expression, time dependence and amplitude of the current, Ca^{2+} dependence as well as sensitivity towards inhibitors vary among TMEM16 proteins. Preliminary data suggest that these proteins can exist as heterooligomeric complexes (148).

TMEM16A shows common characteristics of the native CaCCs, present in a large number of tissues and cell types (19; 44; 63; 149; 197). We and others demonstrated the fundamental importance of TMEM16A for Ca^{2+} dependent Cl^- secretion in a number of epithelial tissues (124; 137; 138). TMEM16A is essential for Ca^{2+} dependent Cl^- currents in airways, large intestine, salivary gland, pancreatic gland and hepatocytes (124; 137; 138). Severe transport defects were detected in epithelial tissues of TMEM16A knockout mice, leading to reduced saliva production and attenuated mucociliary clearance of the airways (104; 124; 137). Thus TMEM16A is essential for proper development and hydration of the airways (135). Knockout animals die early because of instable airways and because they cannot digest and absorb food. The outstanding physiological significance of TMEM16A is further supported by its role in pacemaker cells, where it controls smooth muscle contraction, and by its contribution to generation of acute nociceptive signals (59; 72; 77; 105; 197). Moreover, TMEM16A does also participate in fundamental cellar mechanisms such as regulation of the cell volume, and it interferes with E. coli alpha-hemolysin-induced shrinkage of erythrocytes and subsequent hemolysis (3; 155).

Although it is clear that TMEM16A produces Cl^- currents upon increase in , it is not known whether binds directly to the channel. A string of negatively charged glutamic acid residues in the first intracellular loop could form a Ca^{2+} binding pocket, but its role for Ca^{2+} binding remains currently unclear (57). The available data do not explain the mechanism for activation of TMEM16A by Ca^{2+} and whether phosphorylation or membrane trafficking are required. Here we elucidate the mechanisms for activation of TMEM16A and found that both ATP and calmodulin are required. The present results suggest a regulation of TMEM16A similar to Ca^{2+}-activated K^+ (SK) channels. Also, both types of channels share pharmacological properties (78). Understanding the regulation of TMEM16A will allow the development of novel classes of pharmaceutical compounds, such as benzimidazolinones. Because both Ca^{2+} dependent K^+ and Cl^- channels are expressed in human airways, in contrast to adult human colon which does not express Ca^{2+} activated Cl^- channels, benzimidazolinones are promising tools to reinstall Cl^- secretion in airways in cystic fibrosis (CF).

Materials and Methods

Cell culture, cDNAs, and transfection

HEK293 and Calu-3 cells were grown in DMEM (Gibco, Karlsruhe, Germany) supplemented with 10% fetal bovine serum at 37°C in a humidified atmosphere with 5% CO_2. Cells were plated on fibronectin- and collagen-coated cover slips and co-transfected with cDNA encoding either mTMEM16A, hTMEM16A, hSK4, or empty pcDNA3.1 vector (mock) along with $P2Y_2$ receptor and CD8. Transfections were carried out using lipofectamine 2000 (Invitrogen, Karlsruhe, Germany) according to the manufactures protocol.

Patch Clamping

At 2 or 3 days after transfection, transfected cells were identified by incubating the cells 1-2 min with Dynabeads CD8 (Invitrogen). Coverslips were mounted on the stage of an inverted microscope (IM35, Carl Zeiss, Jena, Germany) and kept at 37 °C. The bath was perfused continuously with Ringer at the rate of 5 ml/min. For fast whole cell patch clamping

pipettes were filled with intracellular like "physiological" solution containing (mM) KCl 30, potassium gluconate 95, NaH_2PO_4 1.2, Na_2HPO_4 4.8, EGTA 1, calcium gluconate 0.758, $MgCl_2$ 1.034, D-glucose 5, ATP 3 (pH 7.2), with an input resistance of 2–4 MΩ. Experiments were conducted as described earlier (124).

Ussing chamber experiments

After isolation, mouse tracheas were put immediately into ice cold buffer solution. Tracheas were opened longitudinally and mounted into a perfused micro Ussing chamber with a circular aperture and a diameter of 0.95 mm. Luminal and basolateral sides of the epithelium were perfused continuously at a rate of 5 ml/min with solution containing (mM) NaCl 145, KH_2PO_4 0.4, K_2HPO_4 1.6, D-glucose 5, $MgCl_2$ 1, HEPES 5, and Ca gluconate 1.3, pH 7.4, that was heated to 37°C. Experiments were carried out under open-circuit conditions. Values for transepithelial voltages (Vte) were referred to the serosal side of the epithelium. Transepithelial resistance (Rte) was determined by applying short (1 s) current pulses (ΔI = 0.5 µA) and after subtracting the resistance of the empty chamber using Ohm's law.

ReAsH labeling and electron microscopy

HEK293 or COS-7 cells were transiently transfected using DEAE dextran/chloroquine (Ausubel et al., 1996). Three days later cells were incubated for 1 hour at 37°C with 450 nM ReAsH (resorufin arsenical hairpin binding reagent; Invitrogen), 12.5 µM 1, 2-ethanedithiol (EDT; Fluka, Buchs, Switzerland); the cells were washed twice briefly with 500 nM 2, 3-dimercapto-1-propanol (BAL; Fluka), incubated in 500 nM BAL for 20 minutes at 37°C, washed again three times with HBSS and fixed with 2% glutaraldehyde overnight. Cells were blocked for 30 minutes in 50 mM glycine, 10 mM KCN, 20 mM aminotriazole, 0.001% H_2O_2 and were washed with new buffer containing 1 mg/ml of diaminobenzidine. Photoconversion was performed by exposing the cells at 4°C to a 585 nm light source. Finally the cells were washed again and embedded in Durcupan (Fluka). Thin sections (50-nm) were analyzed in a Zeiss EM 902 transmission electron microscope equipped with a cooled CCD digital camera (TRS, Moorenweis, Germany).

Western blotting, immunoprecipitation

Protein was isolated from transfected HEK293 cells in lysis buffer containing 50 mM Tris-HCl, 150 mM NaCl, 100 mM DTT, 0.2% Triton X-100, 5U/ml of benzonase and 1% protease inhibitor cocktail (Sigma-Aldrich, Taufkirchen, Germany). Prior to the addition of 1–5 μg of the primary antibody, protein lysates were precleared with protein A agarose beads (Pierce, Rockford, IL, USA). Incubation with primary antibodies was performed 3 h at 4°C, and the protein–antibody complex was immobilized by the addition of 25 μl of protein A agarose beads for 1 h at 4°C. The beads were washed in PBS, and then boiled in 1X loading sample buffer for Western blot analysis using 10% SDS-PAGE. The protein was transferred to a polyvinylidene difluoride membrane (GE Healthcare, Munich, Germany) using semidry transfer (BioRad, Munich, Germany). Membranes were incubated with first antibodies (dilution from 1:500 to 1:1000) overnight at 4°C. Proteins were visualized using a horseradish peroxidase (HRP)-conjugated secondary antibody (dilution 1:10,000) and ECL Detection Kit (GE Healthcare, Munich, Germany); the protein bands were detected by FujiFilm LAS-3000 (FujiFilm, Tokyo, Japan).

Immunocytochemistry

HEK293 cells were grown on glass cover slips and washed 3 times in phosphate-buffered saline (PBS). Cells were fixed with methanol at −20°C for 5 min and incubated with primary antibodies at 4°C overnight. Monoclonal rabbit anti-mouse TMEM16A antibody was used as first antibody. For immunofluorescence, cells were incubated with secondary AlexaFluro 488 goat anti-rabbit IgG for 1 h at room temperature and counterstained with Hoe33342 (Sigma-Aldrich, Taufkirchen, Germany). Immunofluorescence was detected using an Axiovert 200 microscope equipped with an ApoTome and Carl Zeiss AxioVision software (Axiovert 200M, Carl Zeiss, Jena, Germany).

Materials and statistical analysis

All compounds (ionomycin, 1EBIO; riluzole, cytochalasin D; BIM, dynasore, okadaic acid,

phalloidin, STO-609; KN93; KN62; KT5720; IBMX, forskolin, trifluoroperazine, Calmodulin, ATP, BAPTA-AM, U0126, apyrase, dasatinib) were from Sigma (Taufkirchen, Germany) or Merck (Darmstadt, Germany). Peptides were synthesized by Davids Biotechnologie (Regensburg Germany), the sequence of CAM-BD 1 is NH2- VRK YFG EKV GLY FA -COOH and CAM-BD 2 is NH2- LLS KRR KCG KYG ITS LLA –COOH. AO1 was generously provided by Sygnature Chemical Services Limited (Nottingham, UK). The anti-hTMEM16A was a generous gift from Prof. van de Rijn (Dept. of Pathology, Stanford University, USA). All cell culture reagents were from GIBCO/Invitrogen (Karlsruhe, Germany). Student's t-test (for paired or unpaired samples as appropriate) and analysis of variance (ANOVA) was used for statistical analysis. P<0.05 was accepted as significant.

Results

TMEM16A is strictly membrane localized and is regulated by cytoskeletal components
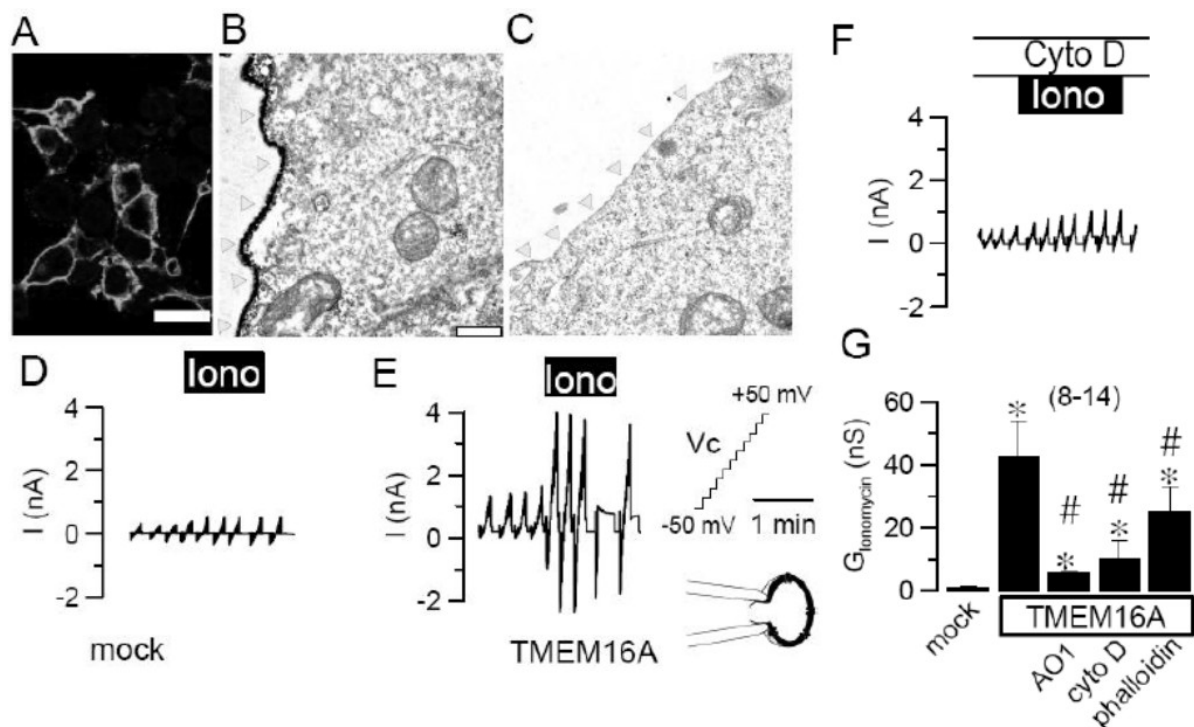
Fig. 1: TMEM16A is strictly membrane localized and is regulated by cytoskeletal components. (A) Immunofluorescence of TMEM16A expressed in HEK293 cells. (B) High-resolution electron microscopy showing tetracysteine-tagged TMEM16A in HEK293 cells using ReAsH technology (triangles). (C) Electron microscopy of mock transfected HEK293 control cells. (D-F) Original recordings of whole cell currents and effects of

ionomycin in mock transfected cells (D) or cells overexpressing mTMEM16A before (E) and after (F) treatment with cytochalasin D (10 µM/2h). (G) Summary of the effects of ionomycin in mock and mTMEM61A-expressing cells under control conditions and after incubation with a specific CaCC-inhibitor (AO1, 10 µM), cytochalasin D (cyto D; 10 µM), and phalloidin (1 µg/ml/2h). Cells were voltage clamped from -50 to +50 mV in steps of 10 mV. Means ± SE; n = 8- 14. Values in parentheses indicate n. Scale bars = 20µm (A); 500 nm (B). * P< 0.05 for activation of whole-cell conductance by ionomycin; paired t-test. # P<0.05 vs. control; ANOVA.

It is believed that Ca^{2+} dependent Cl^{-} currents are activated through increase in intracellular Ca^{2+} and binding to TMEM16A or an associated protein. However this has not been proven and alternatively the current may be activated by exocytosis of TMEM16A and insertion into the plasma membrane. This has been proposed for the exocrine pancreas (131). We examined localization of TMEM16A when overexpressed in HEK293 and Cos-7 cells, using immunocytochemistry and electron microscopy. TMEM16A appeared clearly membrane localized in immunohistochemistry of HEK293 cells (Fig. 1A). This was confirmed by high resolution electron microscopy using REASH labeling (c.f. Methods). The images clearly indicate a strict membrane localization of TMEM16A in overexpressing HEK293 cells (Fig. 1B). No REASH labeling was observed in mock transfected control cells (Fig. 1C). A similar staining was observed in Cos-7 cells after expression of TMEM16A (Supplemental Fig. S1).
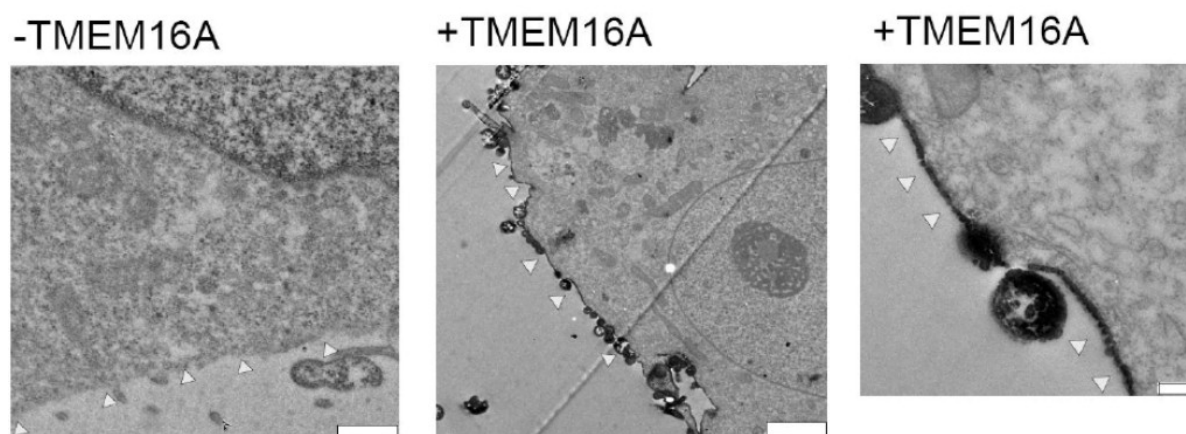
Supplemental Fig. S1: High resolution electron microscopy of mock transfected (-TMEM16A) and TMEM16A (+TMEM16A) expressing COS-7 cells at lower and higher magnification. Triangles indicate cell membrane. Bars indicate 500 and 200 nm, respectively.

Activation of TMEM16A in HEK293 cells was examined using whole cell patch clamp

recordings. We expressed both human and mouse TMEM16A, which produced similar whole cell Cl$^-$ conductances. While no currents were observed in HEK293 control cells, large whole cell Cl$^-$ currents were activated by the Ca^{2+} ionophore ionomycin (1 µM) in TMEM16A expressing cells (Fig. 1D, E). Notably in TMEM16A expressing cells whole cell baseline currents were enhanced, even in the absence of ionomycin, and both enhanced baseline conductance and ionomycin-activated conductance were inhibited by 10 µM AO1, a specific inhibitor of Ca^{2+} activated Cl$^-$ currents (31) (Fig. 1G). Interestingly activation of currents was suppressed by depolymerizing or stabilizing actin with cytochalasin D and phalloidin, respectively (Fig. 1F, G). Maneuvers that inhibit exocytosis or endocytosis (dynasore 10 µM; calmodulin dependent kinase kinase inhibitor STO-609, 10 µM; siRNA for synapsin 1) had no effects (data not shown). Thus membrane localized TMEM16A is activated by Ca^{2+} in an actin-dependent manner.

Phosphorylation is not a prerequisite for activation of TMEM16A

As reported earlier, intracellular N and C termini of TMEM6A carry a number of sites with consensus sequences for phosphorylation by protein kinases, such as PKA, PKC, CAMK, CK2 and Erk1,2 (92). Moreover the present results and a previous study suggest that cytosolic ATP is required for full activation of TMEM16A (3). Activation of TMEM16A by ionomycin (1 µM) or stimulation of P2Y receptors with ATP (100 µM) was unaffected in the presence of an ATP-free pipette filling solution (ΔG_{Iono} = 45 ± 5.2 nS; ΔG_{ATP} = 50 ± 5.7 nS) but was abolished with apyrase (2 U/ml) in the patch pipette (Fig.2A-E). This suggests that cytosolic ATP is required for complete activation of TMEM16A, and could be required for phosphorylation of the channel. We therefore applied ionomycin after inhibition of various kinases, for which potential phosphorylation sides have been detected in TMEM16A. Cells were stimulated in the presence of inhibitors of CAMKII (KN93, KN62), PKC (BIM), PKA (KT5720), or CK2 (TBB), or in the presence of IBMX and forskolin, which increase intracellular cAMP (Fig. 2B). None of these treatments changed activation of TMEM16A by ionomycin. In contrast the CAMKII inhibitor KN62 even augmented Ca^{2+}-activated Cl$^-$ currents, similar to what has been reported for smooth muscle cells (60; 185). Moreover the

broad non-specific kinase inhibitor staurosporine (5 µM, 2 h) or the phosphatase 2A inhibitor okadaic acid (10 nM, 2 h) had no effects on channel activation (data not shown). All inhibitors used in the present study have been demonstrated to exert their expected actions at the concentrations used in the present report: i) KN63 inhibited CaCC in CFPAC cells, ii) BIM prevented the epithelial Na^+ channel ENaC from inhibition by protein kinase C, iii) KT5720 and TBB inhibited activation of CFTR, and iv) U0126 attenuated $P2Y_2$- induced inhibition of ENaC. Finally neither siRNA knockdown of CAMKIIγ or CK2 inhibited TMEM16A (data not shown).

Expression of the double mutant S967A/S970A-TMEM16A (Erk1,2-mut) that lacks of two consensus sequences for extracellular regulated kinase (Erk1,2) in the C-terminus, did not change activation of TMEM16A by ionomycin but reduced receptor-mediated activation by ATP (10 µM) (Fig. 2C, F).
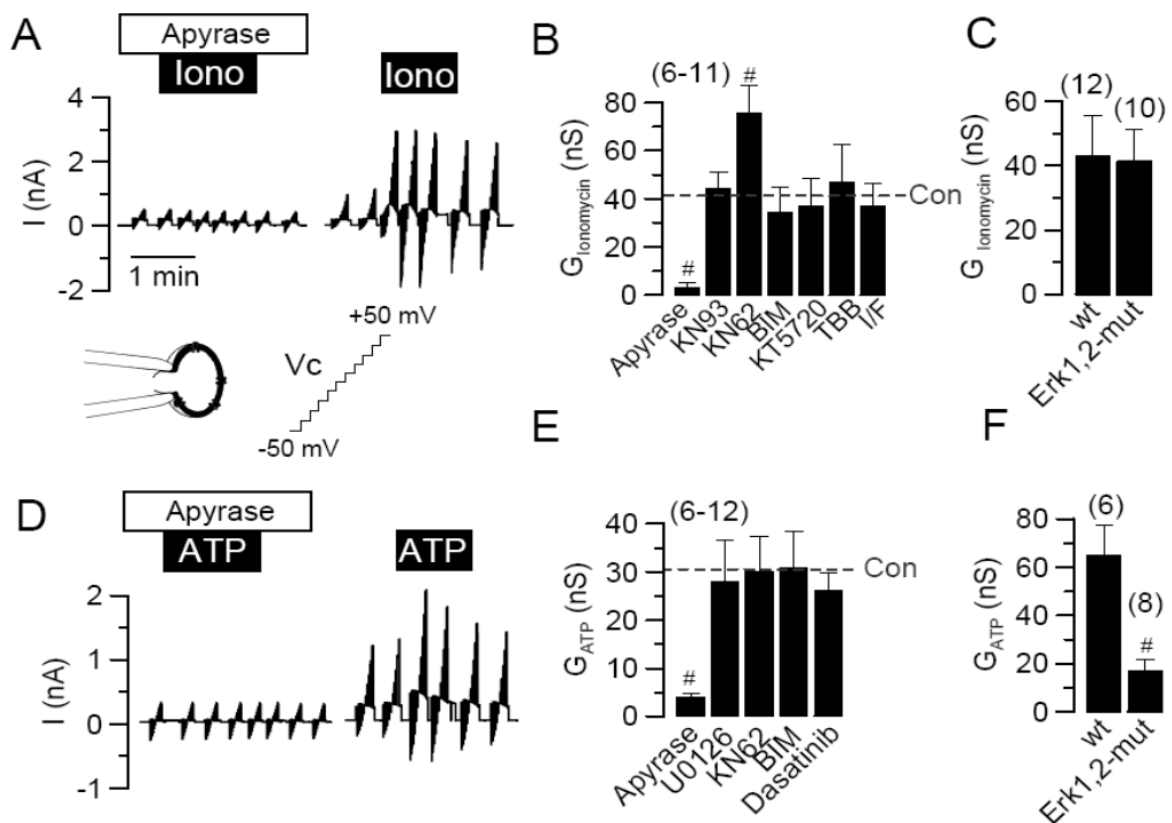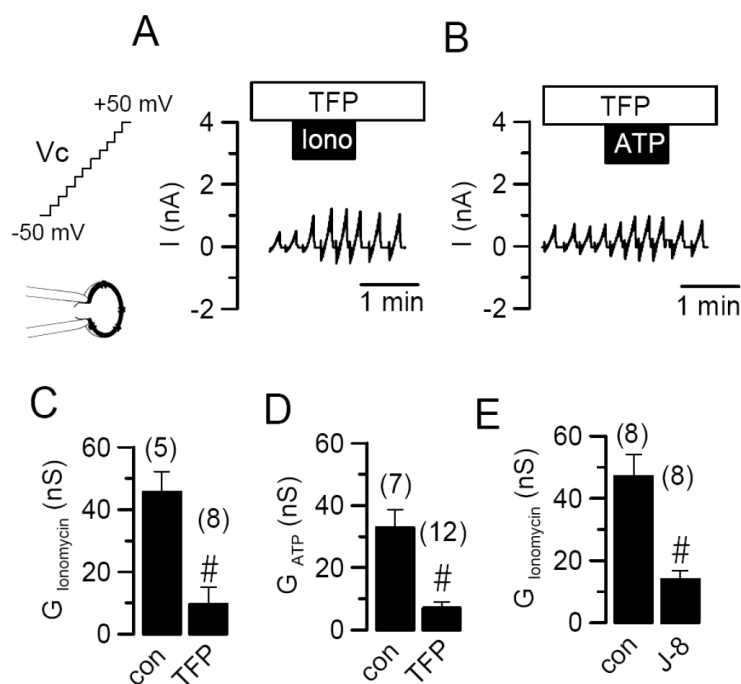

Fig. 2: Activation of mTMEM16A requires ATP but not phosphorylation by protein kinases. (A, D) Original recordings of whole cell currents activated by ionomycin (1 µM) or ATP (10 µM) in mTMEM16A expressing HEK293 cells, in the presence or absence of apyrase in the patch pipette. (B) Summary of whole cell conductances activated by ionomycin in the

presence of apyrase (1 U/ml), after inhibition of CAMKII by KN93 (10 µM) or KN62 (10 µM) or after incubation with BIM (1 µM; inhibition of PKC), KT5720 (10 µM; inhibition of PKA), TBB (10 µM; inhibition of CK2), and stimulation with IBMX/forskolin (I/F, 100 µM/2 µM; activation of PKA). Dashed line indicates activation by ionomycin under control conditions (absence of inhibitors). (C) Summary of the effects of ionomycin (1 µM) on cells expressing human wtTMEM16A or a mTMEM16A mutant in which two putative Erk1,2 phosphorylation sites have been eliminated. (E) Summary of whole cell conductances activated by ATP (10 µM) in the presence of apyrase in the patch pipette (1 U/ml), U0126 (10 µM; inhibition of Mek1,2), KN62 (10 µM; inhibition of CAMKII), and BIM (1 µM; inhibition of PKC). Dashed line indicates activation by ionomycin under control conditions. (F) Summary of the effects of ATP (100 µM) on cells expressing human wtTMEM16A or a hTMEM16A mutant in which two putative Erk1,2 phosphorylation sites have been eliminated. Cells were voltage clamped from -50 to +50 mV in steps of 10 mV. Means ± SE; n = 6 - 14. Values in parentheses indicate n. #$P< 0.05$ vs. control or wt; ANOVA.

Since the MEK-inhibitor U0126 did not inhibit receptor-dependent activation of TMEM16A, stimulation of P2Y$_2$ receptors may activate Erk1,2 and TMEM16A in a MEK-independent manner (3; 27). Nonetheless, Erk1,2 phosphorylation is not absolutely essential for channel activation, as high $[Ca^{2+}]_i$ levels (application of ionomycin) activates TMEM16a in an Erk1,2-independent fashion. Typically ion channels that are regulated by calmodulin and the cytoskeleton are often controlled by phosphatidylinositols such as PIP$_3$ and PIP$_2$ (8). However, we found that neither siRNA-knockdown of the phosphatase and tensin homologue (PTEN) which hydrolyzes PIP$_3$ to PIP$_2$, nor inhibition of the PI3-kinase by wortmannin (1 µM; n = 8) compromised activation of TMEM16A by ionomycin (data not shown). Thus it remains currently unclear how ATP is involved in regulation of TMEM16A.

Calmodulin is essential for activation of TMEM16A

A number of studies report activation of endogenous Ca^{2+}-dependent Cl^- currents by calmodulin dependent kinase II (23; 63; 67; 184). However, we did not find that CAMKII is essential for activation of TMEM16A overexpressed in HEK293 cells (Fig. 2). In contrast, when calmodulin (CAM) was inhibited by trifluoperazine (TFP, 10 µM) or the highly specific inhibitor J-8 (50 µM), activation of TMEM16A by both ionomycin and ATP was largely suppressed (Fig. 3). This calmodulin- and ATP-dependence of TMEM16A is reminiscent of Ca^{2+} dependent KCNN4 potassium channels, which also require both factors for complete

activation (128; 161; 164). Calmodulin binds to the intracellular C - terminus of KCNN4 channel and acts as a Ca^{2+} sensor to control channel assembly and surface expression of KCNN4 (88).

Using a Web-based prediction program (Calmodulin Target Database, Ikura Lab, Ontario, Cancer Institute), we identified two

Fig. 3: Calmodulin is essential for activation of mTMEM16A. (A, B) Original recordings of whole cell currents activated by ionomycin (Iono, 1 µM; A) or ATP (10 µM; B) in mTMEM16A expressing HEK293 cells in the presence of the CAM inhibitor trifluoperazine (TFP, 5 µM). (C-E) Summary of the whole cell conductances activated by ionomycin (C, E) or ATP (D) under control conditions and in the presence of TFP (C, D) or the specific calmodulin inhibitor J-8 (50 µM; E). Means ± SE; n = 5 - 12. Values in parentheses indicate n. #P< 0.05 vs. control; unpaired t test.

putative CAM-binding domains (CAM-BD1, CAM-BD2) located in the intracellular N-terminus of TMEM16A (Fig. 4A).

In fact, calmodulin could be coimmunoprecipitated using a TMEM16A antibody, while TMEM16A was coimmunoprecipitated by a CAM-antibody in lysates from TMEM16A-expressing cells (Fig. 4B). No coimmunoprecipitation was observed with protein A agarose beads only. TMEM16A is expressed in different splice forms, which are characterized by amino acid inserts (segments a-d) in the N-terminus and the 1. intracellular loop (Fig. 4A) (19). The putative CAM-BD1 overlaps with segment b of the splice form abc-TMEM16A. We expressed the different splice forms in HEK293 cells; however, coimmunoprecipitation and detection by Western blot was unsuccessful with ac-TMEM16 (data not shown), although ac-TMEM16A and abc-TMEM16A are comparably expressed at the plasma membrane (Supplemental Fig. S2B). To further examine the role of these putative

CAM-binding domains, we perfused the cytosol via the patch pipette with short peptides corresponding to the sequences of CAM-BD1 and CAM-BD2. In the presence of CAM-BP1 activation by ionomycin of human and mouse TMEM16A was inhibited, while CAM-BP2 had no effects (Fig. 4C-E). These results suggest that CAM-BP1 may bind to calmodulin thereby interfering with activation of TMEM16A.
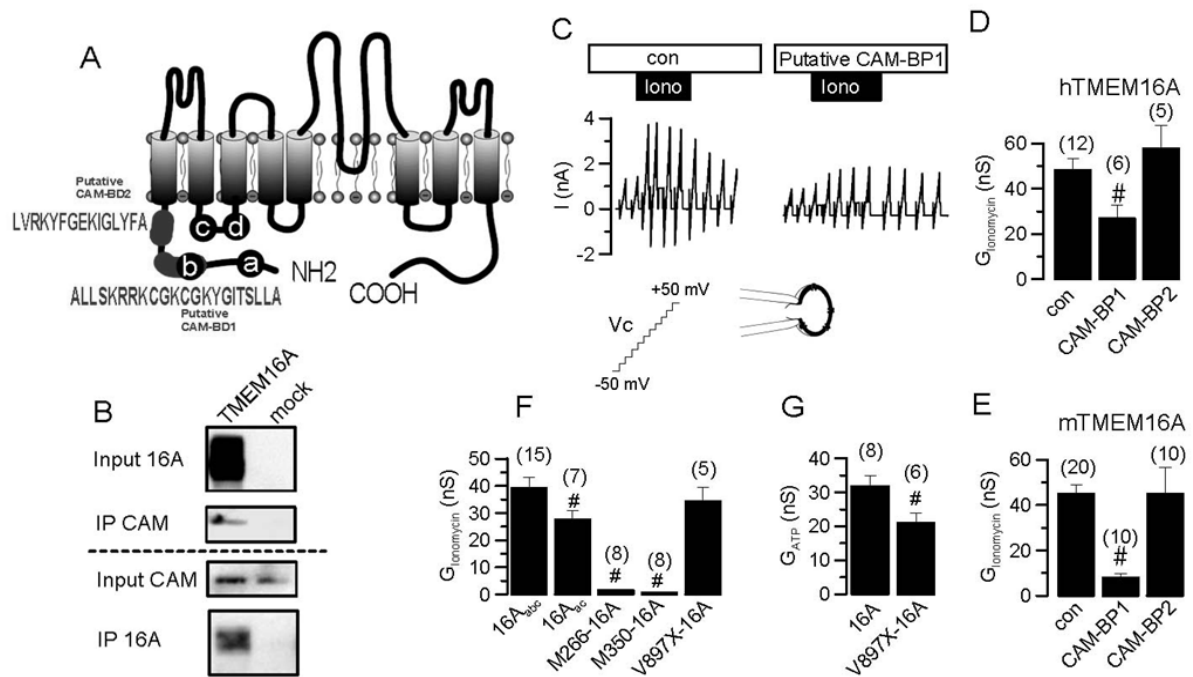
Fig. 4: Calmodulin physically interacts with mTMEM16A and controls channel activity. (A) N-terminal putative calmodulin binding domains CAM-BD1 and CAM-BD2 and location of the alternatively spliced sequences (a-d) are shown. (B) Coimmunoprecipitation of TMEM16A and calmodulin in hTMEM16A overexpressing HEK293 cells. Upper half shows overexpressed TMEM16A (Input 16A, 110 & 150 kDa; anti-hTMEM16A antibody) and coimmunoprecipitated calmodulin (IP CAM, 18 kDa; anti-hCAM antibody). Lower half shows endogenous calmodulin expressed in HEK293 cells (Input CAM; 18 kDa) and coimmunoprecipitated hTMEM16A (IP 16A; 110 & 150 kDa). (C) Activation of whole cell currents by ionomycin (1 μM) in hTMEM16A expressing HEK293 cells in the absence or presence of a peptide with the amino acid sequence of the putative calmodulin binding domain 1 (CAM-BP1) in the patch pipette filling solution. (D, E) Summary of the ionomycin activated whole cell conductances in human TMEM16A (D) or mouse TMEM16A (E) expressing HEK293 cells. CAM-BP1 but not CAM-BP2 inhibited activation of whole cell conductances by ionomycin. F) Summary of the ionomycin-activated whole cell conductances in cells expressing the splice forms abc-TMEM16A or ac-TMEM16A ($16A_{abc}$, $16A_{ac}$) or N- and C-terminal truncations of hTMEM16A (M266-16A, M350-16A, V897X-16A). G) Summary of ATP-activated whole cell conductances in cells expressing wtTMEM16A or C-terminally truncated V897X-TMEM16A. Cells were voltage clamped from -50 to +50 mV in steps of 10 mV. Mean ± SEM, (n = 5- 20). # significant inhibition (ANOVA).

Further attempts to confirm interaction of CAM with the N-terminus of TMEM16A were unsuccessful, since two N-terminal truncations of TMEM16A (M266-16A and M350-16A) annihilated membrane expression of the protein (Fig. 4F; Supplemental Fig2. A). Notably truncation of the C-terminus had no effect on channel activation by ionomycin, but attenuated receptor-mediated activation by ATP, probably due to elimination of the Erk1,2 sites (Fig. 4F, G). When we expressed the splice form ac-TMEM16A, we found that a Cl$^-$ current was still activated by ionomycin, albeit the whole cell conductance was slightly attenuated when compared to abc-TMEM16A. Thus the putative CAM-BD1 supports Ca^{2+}-dependent activation of the channel, but is not essential for the function of TMEM16A (Fig. 4F).
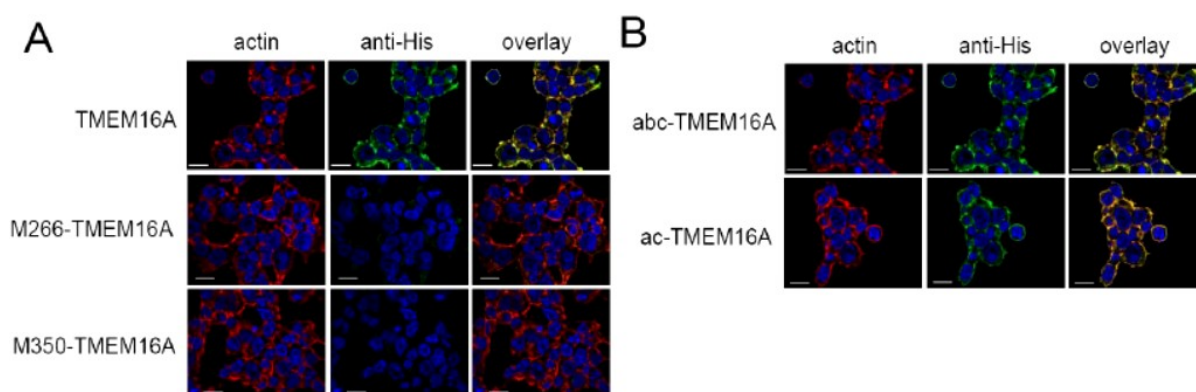
Supplemental Fig. S2: (A) Immunolabeling of His-tagged full length TMEM16A (green), and two N-terminal truncations (M266-TMEM16A and M350-TMEM16A), which are not expressed in HEK293 cells. Actin staining (red) indicates plasma membrane. (B) Comparison of membrane expression of abc-TMEM16A and ac-TMEM16A. Bar indicates 20μm.

TMEM16A requires Ca^{2+}, ATP and calmodulin for full activation

In cell-attached patches of TMEM16A-expressing HEK293 cells, we detected activation of a current noise after purinergic stimulation with ATP, which was not observed in control (mock) cells (Fig. 5A). However, we were unable to resolve single channel activity probably due to the very small single channel conductance. When membrane patches were excised inside/out after stimulation of TMEM16A-expressing cells, the channel noise disappeared within seconds, and removal of Ca^{2+} from the bath (cytosolic side) had no effects (Fig. 5B upper trace).
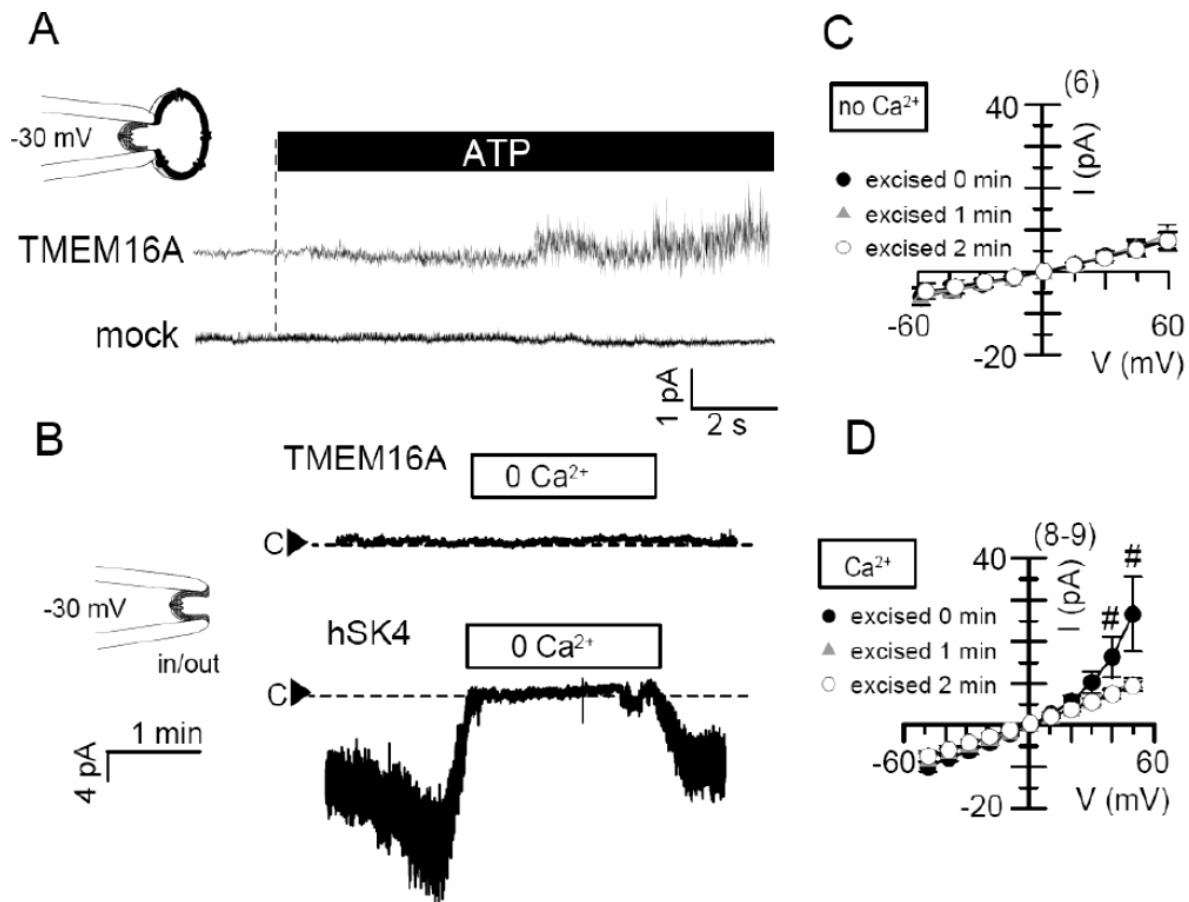
**Fig. 5:** Fast rundown of mTMEM16A currents. (A) Single channel noise was activated by purinergic stimulation with ATP in cell attached recordings from mTMEM16A expressing HEK293 cells, but not in mock transfected cells (Vc = -30 mV). (B) Lack of channel noise in excised inside/out membrane patches from cells expressing mTMEM16A (upper trace). Excised membrane patch from a SK4 expressing cell exhibits current noise that was inhibited by removal of Ca^{2+} from the bath solution (cytosolic side). (C, D) Current-voltage relationships obtained from membrane patches at different time points after excision into a Ca^{2+} free bath solution (C), or bath solution containing 1 mM Ca^{2+} (D). An outwardly rectifying current is observed immediately after excision into Ca^{2+} containing bath solution (D) that quickly inactivated. Cells were voltage clamped from -50 to +50 mV insteps of 10 mV. Means ± SE; n = 6 – 9. Values in parentheses indicate n. #P< 0.05; unpaired t-test.

In contrast to TMEM16A, Ca^{2+}-dependent K^+ channels (KCNN4, SK4) were readily detectable in excised inside/out patches and were inhibited by removal of cytosolic Ca^{2+} (Fig. 5B lower trace). We measured the conductance of excised membrane patches from ATP-stimulated and TMEM16A-expressing cells immediately after excision, and one or two minutes after removal from the whole cell. When excised into Ca^{2+} free Ringer solution, the membrane conductance of the patch was small right after excision (Fig. 5C). In contrast, when excised into a Ca^{2+} containing Ringer solution, an outwardly rectifying current was

detected that inactivated within a minute after excision, suggesting rapid run down of TMEM16A currents (Fig. 5D).

We speculated that cytosolic factors such as ATP or calmodulin might get lost during membrane excision and therefore added ATP (3 mM) to the bath solution (cytosolic side), which increased the current noise and slightly enhanced the conductance of patches from TMEM16A expressing cells, but not from mock transfected cells (Fig. 6).
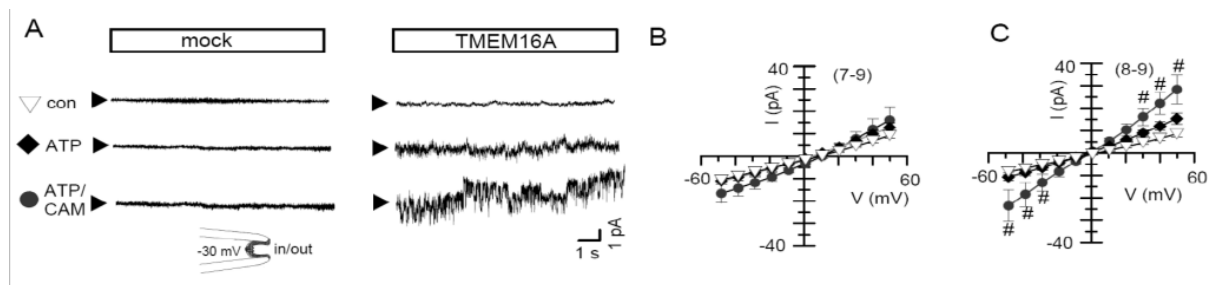

Fig. 6: Activation of mTMEM16A requires ATP and calmodulin. (A) Current recordings in inside /out excised membrane patches from TMEM16A and mock transfected HEK293 cells (Vc = +30 mV). Current noise was small after excision of the patch in a Ca^{2+} containing bath solution (con), but was activated in excised patches from mTMEM16A-expressing cells by adding ATP (3 mM) or calmodulin (1 μg/ml) together with ATP to the cytosolic side (right tracings). In contrast no current is activated in an excised membrane patch from a mock transfected cell (left tracings). (B, C) Current / voltage relationships measured in excised membrane patches obtained form mock transfected (B) and mTMEM16A expressing (C) cells, indicating current activation by ATP and calmodulin in mTMEM16A expressing cells. Cells were voltage clamped from -50 to +50 mV insteps of 10 mV. Means ± SE; n = 7-9. Values in parentheses indicate n. #P< 0.05; unpaired t-test.

Further addition of CAM (1 μg/ml) increased the channel noise and activated a membrane conductance in patches from TMEM16A expressing cells but not from control cells. Thus ATP and CAM may be required to keep TMEM16A channels active (Fig. 6).

TMEM16A and SK4 share pharmacological properties

Benzimidazolinones like 1-ethyl-2-benzimidazolinone (1-EBIO) are well known activators of Ca^{2+} dependent K^+ channels and enhance the affinity of K^+ channels for Ca^{2+}/calmodulin (35; 183). Since both SK4 and TMEM16A require CAM and ATP to be activated, we examined whether benzimidazolinone compounds are also able to activate TMEM16A. In excised

mouse tracheas, 1-EBIO (50 µM) activated a small and rather steady Cl⁻ secretion and augmented ATP activated short circuit currents, apparently by activating both luminal TMEM16A and basolateral SK4 channels (Fig. 7A, B). Notably, in the presence of the CFTR inhibitor $CFTR_{inh}172$ (5 µM) 1-EBIO still augmented ATP-induced Cl⁻ secretion (Fig. 7B). In whole cell patch clamp experiments with human airway epithelial (Calu-3) cells, 1-EBIO and the related compound S0011198 increased whole cell currents. However, in these cells SK4 channels were activated by the benzimidazolones and hyperpolarized the membrane voltage, since Calu-3 cells do not express TMEM16A and do not have CaCC (92) (Fig.7C, D, Supplemental Fig. S3C). When expressed in HEK293 cells, TMEM16A was activated by 1-EBIO (50 µM) and riluzole (50 µM), another known opener of SK4 channels (145). Moreover, the related compound DCEBIO (1 µM) also activated TMEM16A (ΔG = 23.1 ± 4.2 nS; n = 5). In summary, both luminal Ca^{2+} activated TMEM16A and basolateral SK4 K^+ channels are activated by the same compounds. Therefore benzimidazolinones may be ideal drugs for the treatment of the cystic fibrosis lung disease, which is characterized by defective CFTR-dependent Cl⁻ secretion and dehydration of the airways (16; 94; 133).
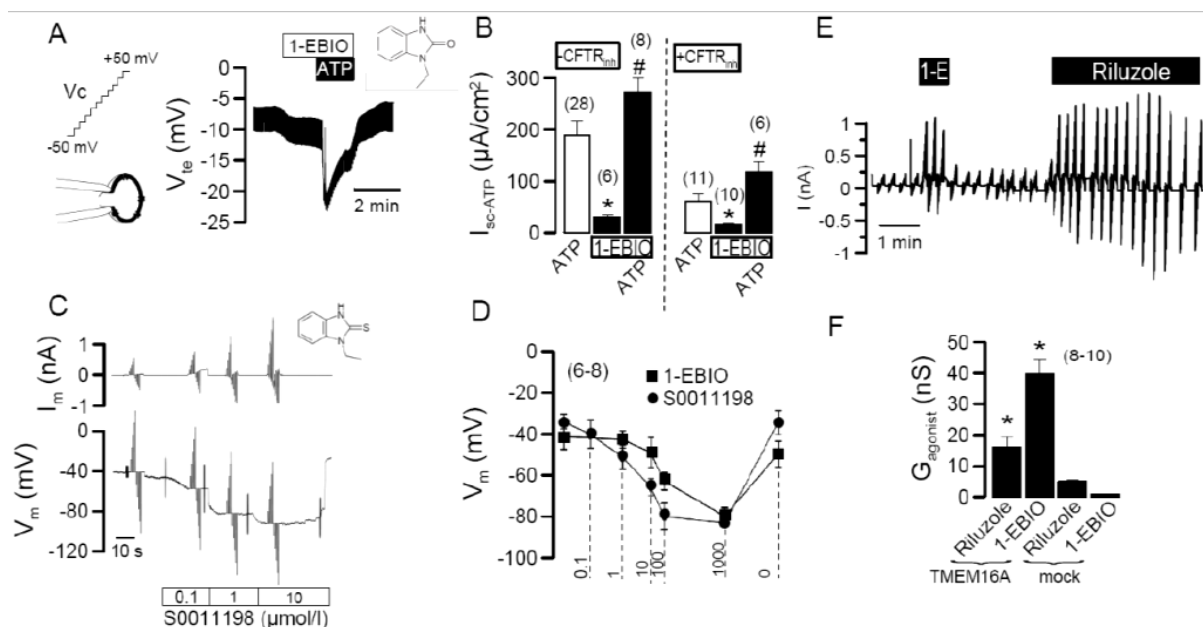
Fig. 7: Pharmacological activation of TMEM16A and SK4 channels. (A) Transepithelial voltage measured in Ussing chamber recordings from mouse trachea. 1-EBIO (1 mM) increases transepithelial voltage and augments subsequent negative voltage deflection induced by application of luminal ATP (100 µM). (B) Summary of the calculated equivalent short circuit currents activated by ATP, 1-EBIO or simultaneous application of both. ATP activated transport was significantly enhanced by 1-EBIO. Even after inhibition of CFTR Cl⁻ channels

by the compound $CFTR_{inh}172$ ($CFTR_{inh}$; 5 µM), 1-EBIO still augmented ATP-induced Cl^- secretion. (C) Activation of whole cell currents and hyperpolarization of the membrane voltage of Calu3 cells by different concentrations of the homologue of 1-EBIO, S0011198. (D) Comparison of the concentration-dependent hyperpolarizing effects of 1-EBIO and S0011198 in Calu-3 cells. E) Activation of whole cell currents by 1-EBIO (1 µM) and riluzole (50 µM) in mTMEM16A-expressing HEK293 cells. (F) Summary of the whole cell conductances activated by 1-EBIO and riluzole in mTMEM16A-expressing HEK293 cells. Cells were voltage clamped from -50 to +50 mV insteps of 10 mV. Means ± SE; n = 6-28. *P< 0.05 for augmentation of currents by 1-EBIO and riluzole; paired t-test. #P< 0.05 for augmentation of ATP effect by 1-EBIO; unpaired t test.

Discussion

Activation of membrane localized TMEM16A

In the present study we examined the mechanisms for activation of the novel Ca^{2+} activated Cl^- channel TMEM16A and identified pharmacological properties that allow interfering with the activity of this highly relevant channel. The data demonstrate that TMEM16A is membrane localized and is activated by Ca^{2+} in an actin dependent manner. Notably, a contribution of the actin cytoskeleton to activation of endogenous CaCC in epithelial cells has been suggested earlier (76). We found no evidence for a role of exocytosis in activating TMEM16A, and thus confirm earlier data from pancreatic acinar cells, showing exocytosis-independent activation of ion channels due to spatial distribution of cytosolic Ca^{2+} (111). Similar to other epithelial ion channels, anchoring of TMEM16A to the cytoskeleton and to membrane phosphatidylinositols (PIP_2) may be essential to maintain channel activity (112; 167). A regulatory link between endogenous CaCC, actin cytoskeleton and actin-bound annexin IV has been detected earlier in colonic carcinoma cells (23).

CAMKII, Calmodulin, and ATP

Initial studies demonstrated activation of TMEM16A by increase in cytosolic Ca^{2+}, but did not present evidence for a requirement of cytosolic ATP (149; 197). We found that the presence of the ATP-cleaving enzyme apyrase in the pipette solution largely reduced channel activity, suggesting a requirement of ATP for full activation of TMEM16A. Some properties of TMEM16A are clearly different to those found for endogenous CaCC in epithelial cells.

Firstly, TMEM16A expressed in HEK293 and FRT cells (148) is partially active at basal intracellular Ca^{2+} concentrations, while endogenous CaCC is closed under control conditions. Secondly, CAMKII inhibited TMEM16A currents expressed in HEK293 cells, but activates endogenous CaCC in colonic, airway and pancreatic epithelial cells (23; 63; 67; 184). Notably, regulation of CaCC by CAMKII is cell type dependent, and inhibition of CaCC by CAMKII has been described for smooth muscle cells (60; 185). Preliminary experiments also indicate that overexpressed TMEM16A is inhibited by CAMKII, while activation of endogenous CaCC in CFPAC-1 cells is CAMKII dependent (data not shown). However, CFPAC-1 cells express TMEM16A endogenously, and siRNA knockdown of TMEM16A inhibits CaCC, indicating that TMEM16A is a crucial component of the endogenous CaCC. It is therefore likely that the cellular environment and/or additional auxiliary proteins determine CAMKII-dependent regulation (92).

The present data demonstrate calmodulin as one of the auxiliary proteins necessary for activation of TMEM16A. According to the present data the putative site for calmodulin binding overlaps with segment b of the splice form abc of TMEM16A (Fig. 4A). We found a reduced activity of ac-TMEM16A, when compared with abc-TMEM16A, which is actually different to the results of a previous study (52). This discrepancy remains currently unexplained. However, in preliminary experiments we found that i) intracellular Ca^{2+} itself triggers inactivation of the channel and ii) inactivation of ac-TMEM16A occurs at lower $[Ca^{2+}]_i$ than for abc-TMEM16A (unpublished data). Also, it appears possible that Ca^{2+} and calmodulin have more than one binding site. In overexpressing cells additional accessory proteins may still be missing to produce a "complete" chloride channel complex. In preliminary experiments we performed two hybrid screening using the split ubiquitin system in order to identify additional interacting partners, and identified the Ca^{2+}-binding protein S100A11. However siRNA-knocked down of S100/A11 did not change TMEM16A currents.

Similar mechanisms for activation of SK4 and TMEM16A

Calmodulin regulation of TMEM16A is reminiscent of Ca^{2+}/CAM-dependent regulation of SK4 (KCNN4) potassium channels. The open probability of SK4/IK1 channels is tightly

regulated by cytosolic Ca^{2+} concentrations in the range between 100 and 1000 nM, although typical Ca^{2+} binding domains are not present in SK4. The pronounced Ca^{2+} sensitivity of SK4 is due to its high affinity for CAM (48; 81; 87; 128; 161; 164; 190). Activation of SK4/IK1 by the benzimidazolinone 1-EBIO is well established and is due to enhanced Ca^{2+} sensitivity of the CAM/SK4 channel complex (62; 127; 183; 186). 1-EBIO has also been shown to activate apical Cl^- channels of unknown molecular identity in rabbit conjunctival epithelium and intestinal epithelium (5; 61). However most studies claim that activation of Cl^- secretion by 1-EBIO is indirect, by increasing the driving force due to activation of basolateral SK4 channels (34; 62). In this regard a derivative of 1-EBIO, DCEBIO (5,6-dichloro-1-ethyl-1,3-dihydro-2*H*benzimidazol-2-one) was very potent in activating K^+ channels and on top activated an unknown apical membrane Cl^- conductance in monolayers of T_{84} colonic carcinoma cells (154).

We found that 1-EBIO, DCEBIO and riluzole activated TMEM16A. An exciting finding was that only low concentrations of these compounds were required to activate TMEM16A (Supplemental Fig. S3). While typically 0.1 – 1 mM of 1-EBIO is required to activate SK4, TMEM16A was activated at concentrations as low as 1 μM. Despite the complex Ca^{2+} dependent regulation of TMEM16A outlined above, activation by 1-EBIO, DCEBIO and riluzole was robust and was observed for overexpressed TMEM16A as well as endogenous CaCC in CFPAC-1 cells (Supplemental Fig. S3).
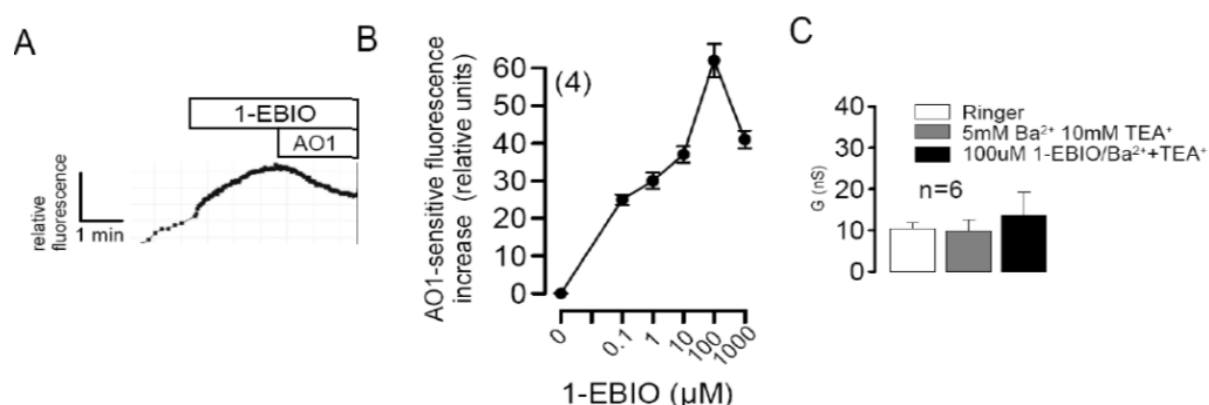
Supplemental Fig. S3: (A) Activation of endogenous Ca^{2+} dependent Cl^- currents (CaCC) in CFPAC cells by 1-EBIO, as detected by increase in FMP-fluorescence. Due to depolarization of the membrane voltage upon activation of Ca^{2+} dependent Cl^- channels FMP is taken up by the cell and fluorescence is increased. The CaCC-inhibitor AO1 (10μM) inhibited

1-EBIO-induced fluorescence increase. (B) Concentration-response of the effect of 1-EBIO on AO1-inhibitable currents. (C) No whole cell currents are activated by 1-EBIO in TMEM16A-expressing HEK293 cells in the presence of K^+ channel inhibitors Ba^{2+} and TEA^+. (number of experiments).

Since benzimidazolinones activate both basolateral SK4 and luminal TMEM16A channels, they could be ideal compounds for the treatment of CF lung disease. As cAMP-dependent Cl^- secretion is defective in CF, Ca^{2+}-dependent Cl^- secretion may compensate for the defect in CFTR-function. It will be exciting to search for more potent activators of both TMEM16A and SK4. Since pharmacological properties of Ca^{2+} activated Cl^- and K^+ channels appear to overlap considerably (144), it will also be interesting to learn whether pharmacological properties of TMEM16A are altered by factors such as CAMKII, ATP or histidine-phosphorylation, as described for SK4 channels (58; 188). As TMEM16A is broadly expressed in a number of tissues, it may become a highly relevant drug target in the future.

Acknowledgments

CHAPTER 5

Control of TMEM16A by INO-4995 and other inositolphosphates

Abstract

Background and Purpose: Ca^{2+}-dependent Cl^- secretion (CaCC) in airways and other tissues is due to activation of the Cl^- channel TMEM16A (anoctamin 1). Earlier studies suggested that Ca^{2+} activated Cl^- channels are regulated by membrane lipid inositol phosphates, and that 1-O-octyl-2-O-butyryl-myo-inositol 3,4,5,6-tetrakisphosphate octakis (propionoxymethyl) ester (INO-4995) augments CaCC. Here we examined whether TMEM16A is the target for INO-4995, and if the channel is regulated by inositol phosphates.

Experimental approach: The effects of INO-4995 on CaCC were examined in overexpressing HEK293, colonic and primary airway epithelial cells as well as *Xenopus* oocytes. We used patch clamping, double electrode voltage clamp and Ussing chamber techniques.

Key results: We found that INO-4995 directly activates a TMEM16A whole cell conductance of 6.1 ± 0.9 nS/pF in overexpressing cells. The tetrakisphosphates $Ins(3,4,5,6)P_4$ or $Ins(1,3,4,5)P_4$ and enzymes controlling levels of $InsP_4$ or PIP_2 and PIP_3 had no effects on the magnitude or kinetics of TMEM16A currents. In contrast in *Xenopus* oocytes, human airways and colonic cells, which all express TMEM16A endogenously, Cl^- currents were not acutely activated by INO-4995. However incubation with INO-4995 augmented $1.6 - 4$ fold TMEM16A-dependent Cl^- currents activated by ionomycin or ATP, while intracellular Ca^{2+} signals were not affected. The potentiating effect of INO-4995 on transient ATP-activated TMEM16A-currents in CF airways was twice of that observed in non-CF airways.

Conclusions and implications: These data indicate that TMEM16A is the target for INO-4995, although the mode of action appears different for overexpressed and endogenous channels. INO-4995 may be useful for the treatment of CF lung disease.

Key words: INO-4995, INO-4913, anoctamin 1, TMEM16A, inositol phosphates, $Ins(3,4,5,6)P_4$, inositol 3,4,5,6-tetrakisphosphate, $Ins(1,3,4,5)P_4$, inositol 1,3,4,5-tetrakisphosphate, Ca^{2+} activated Cl^- channels, CaCC

Introduction

Ca^{2+} activated Cl^{-} channels (CaCC) are highly relevant for secretion of electrolytes in epithelial tissues. Activation of CaCC in cystic fibrosis (CF) airways may ameliorate mucociliary clearance and compensate for defective cystic fibrosis transmembrane conductance regulator (CFTR) Cl^{-} channels (120). However, only recently the molecular counterpart of CaCC was identified as TMEM16A (anoctamin 1) (19; 149; 197). TMEM16A is the major component of Ca^{2+}-dependent Cl^{-} secretion in airways and other epithelial tissues (124; 137). In contrast to CFTR, activation of CaCC / TMEM16A is transient and does not strictly follow intracellular Ca^{2+} levels. Cl^{-} currents relax faster than intracellular Ca^{2+} levels decline upon stimulation of phospholipase C coupled receptors. However, local compartmentalized Ca^{2+} in close proximity of the channel may recover quicker than global $[Ca^{2+}]_i$ (118). Alternatively downstream products of $InsP_3$ such as the inositol tetrakisphosphate $Ins(3,4,5,6)P_4$ may inhibit CaCC, as shown for different types of epithelial cells (20; 32; 68; 82; 192). Thus long-term uncoupling of chloride secretion from intracellular calcium levels by $Ins(3,4,5,6)P_4$ has been proposed as a mechanism for the transient Ca^{2+} dependent Cl^{-} secretion (176). Following this, a novel therapeutic concept for treatment of CF lung disease had been develop, proposing cell permeant antagonists of endogenous $Ins(3,4,5,6)P_4$ to allow for continuing Ca^{2+} dependent chloride secretion (140; 141). The membrane permeable compound 1-O-octyl-2-O-butyryl-myo-inositol 3,4,5,6-tetrakisphosphate octakis (propionoxymethyl) ester (INO-4995; Inologic, Seattle,WA, USA) was demonstrated both to inhibit the epithelial Na^{+} channel ENaC and to activate Ca^{2+} dependent Cl^{-} secretion (141; 117; 173). Therefore the primary objective of the present study was to examine whether the novel Ca^{2+} dependent Cl^{-} channel TMEM16A is the target for INO4995.

Studies demonstrated that intracellular $Ins(3,4,5,6)P_4$ levels are a result of inositol 1,3,4-trisphosphate 5/6-kinase (ITPK1) dephosphorylation of $Ins(1,3,4,5,6)P_5$ and are regulated by $Ins(1,3,4)P_3$ levels (114; 143). Enzymes that generate inositolphosphate intermediates may therefore determine the magnitude and duration of CaCC (176; 173). In fact Yang et al. found that expression of ITPK1 is reduced in murine airway cells lacking

functional CFTR, thus causing enhanced Ca^{2+} activated secretion. ITPK1 was therefore suggested as a novel modifier gene in CF (152; 196). How $Ins(3,4,5,6)P_4$ inhibits Ca^{2+} activated Cl^- channels is unknown. Effects of $Ins(3,4,5,6)P_4$ on accessory proteins such as protein phosphatases have been proposed, although precise mechanisms remain elusive (67; 193). In order to guide future drug development programs, a more detailed understanding of the regulation by phosphatidylinositols ($PI(4,5)P_2$, $PI(3,4,5)P_3$) and $Ins(3,4,5,6)P_4$ is essential (152). The secondary objective of this study was therefore to examine whether TMEM16A is regulated by phosphoinositides and/or $Ins(3,4,5,6)P_4$ (117; 173). The results indicate that TMEM16A is activated by INO-4995 but otherwise not affected by phosphoinositides or $InsP_4$.

Materials and Methods

Cell culture, cDNAs, siRNAs and transfection

HEK293, HT_{29} and CFPAC cells were grown in DMEM and DMEM-F12 (GIBCO), respectively, supplemented with 10% fetal bovine serum at 37°C in a humidified atmosphere with 5% CO_2. Cells were plated on fibronectin- and collagen-coated 18 cm diameter cover slips and co-transfected with cDNA encoding either human TMEM16A (a,b,c-Ano1; NM_018043), or empty pcDNA3.1 vector (mock) along with $P2Y_2$ receptor (NM_176072) and CD8. Expression of TMEM16A, and PTEN was suppressed by RNAi and suppression of mRNA was monitored by real-time RT-PCR. For each type of siRNA-knockout, real-time RT-PCR was performed at least in triplicates. It showed siRNA-knockdown of Ano1-mRNA of 82 ± 4 % (HT_{29}), 68 ± 5 % (CFPAC), and 45 ± 6 % for PTEN (HEK293). Duplexes of 25-nucleotide of RNAi were designed and synthesized by Invitrogen (Paisley, UK) and Ambion (Darmstadt, Germany). RNAi was transfected using Lipofectamin (1 µg/µl). Cells were examined 48h or 72h after transfection. Transfections were carried out using lipofectamine 2000 (Invitrogen) according to the manufactures protocol.

Primary Human Bronchial Epithelial Cells Monolayers

Human lung tissues (non-CF and CF) were obtained from the Cardio-Thoracic Surgery Department (Hospital de Santa Marta; Lisbon, Portugal) after receiving patient's written consent and approval by the Ethics Committee. Primary HBE cells were isolated as described previously (55) and expanded on collagen I - fibronectin-coated plastic dishes before passage to the porous membrane inserts. The primary HBE monolayers (passage 1) were grown on collagen IV coated porous membranes (Snapwell, Corning-Costar®) in an air liquid interface for three weeks. Cells were incubated repetitively for 2 hrs in 5 µM INO-4995 on 4 subsequent days.

Patch clamping and double electrode voltage clamp

2-3 days after transfection, transfected HEK293, HT_{29} or CFPAC cells were identified by 1 - 2 min incubation with Dynabeads CD8 (Invitrogen), which permanently bind to transfected cells. Cover slips were mounted on the stage of an inverted microscope (IM35, Zeiss) and kept at 37 °C. The bath was perfused continuously with ringer solution (mmol/l: NaCl 145, KH_2PO_4 0.4, K_2HPO_4 1.6, d-glucose 6, $MgCl_2$ 1, Ca-gluconate 1.3, pH 7.4) at a rate of 5 ml/min. For fast whole cell and cell excised patch clamping pipettes were filled with intracellular like solution containing (mM) KCl 30, potassium gluconate 95, NaH_2PO_4 1.2, Na_2HPO_4 4.8, EGTA 1, calcium gluconate 0.758, $MgCl_2$ 1.034, D-glucose 5, ATP 3, pH was 7.2 and had an input resistance of 2 – 4 MΩ. The free Ca^{2+} concentration in the pipette solution was 0.1 µM. For measurement of excised membranes, patches were excised into a bath solution containing 0.1 µM $[Ca^{2+}]$. Experiments were conducted as described earlier (124). Typically the cells were kept in current clamp for most of the time and the membrane voltage was recorded. From time to time the cells were voltage clamped (± 50 mV in steps of 10 mV for 1 s). All data were recorded using an EPC7 and the program PULSE (HEKA, Lambrecht, Germany). All data were recorded continuously on a hard disc and analyzed using PULSE and Chart (ADInstruments GmbH, Spechbach, Germany).

Isolation and microinjection of oocytes have been described in details elsewhere (7). Oocytes were pre-incubated with 5 µM INO4995 for 2h or 24h. Oocytes were impaled with two electrodes (Clark Instruments Ltd, Salisbury, UK), which had a resistances of < 1 MΩ when

filled with 2.7 mol/l KCI. Using two bath electrodes and a virtual-ground head stage, the voltage drop across R_{serial} was effectively zero. Membrane currents were measured by voltage clamping (oocyte clamp amplifier, Warner Instruments LLC, Hamden CT) in intervals from -60 to +40 mV, in steps of 10 mV, each 1 s. Data were collected and analyzed using Powerlab and Chart (AD instruments, Berlin, Germany). The bath was continuously perfused at a rate of 5 ml/min. All experiments were conducted at room temperature (22 °C).

Measurement of intracellular Ca^{2+} concentration

For single cell fluorescence measurements HEK293 cells and HT_{29} cells were grown on glass covers slips, mounted in a cell chamber and perfused with ringer solution at 5 ml/min at 37˚C. Cell fluorescence measurements was measured continuously on an inverted microscope Axiovert S100 (Zeiss, Germany) using a Fluar20x/0.75 objective (Zeiss, Germany) and a high speed polychromator system (VisiChrome, Visitron Systems, Germany). Cells were loaded (1h at 37°C) with 2 μM Fura2-AM (Molecular Probes) in ringer solution or Opti-MEM containing 0.2% pluronic (Molecular Probes). Fura-2 was excited at 340/380 nm, and the emission was recorded between 470 and 550 nm using a CCD-camera (CoolSnap HQ, Visitron Systems, Germany). Acquisition and data analysis were done using Meta-Fluor (Universal imaging, USA) and Origin (OriginLab Corporation, USA). For calibration of intracellular Ca^{2+} concentration cells were perfused with ringer solution and Ca^{2+} free ringer with 1 μM ionomycin, 10 μM monensin and 5 μM nigericin.

Immunocytochemistry and Western blot

HT_{29} cells were fixed for 10 min with 4% (w/v) paraformaldehyde at room temperature and permeabilized after blocking with 2% (w/v, PBS) bovine serum albumin and 0.04% (v/v, PBS) Triton X-100. Cells were incubated for 1h with primary anti-ß-catenin antibody (1:1000, Qiagen, Hilden, Germany) at 37 °C. Binding of the primary antibody was visualized by an Alexa 568-labeled secondary antibody (1:1.000, Molecular Probes, Invitrogen). Nuclei were stained with Hoe33342. Cells were examined with an ApoTome Axiovert 200 M fluorescence microscope (Zeiss, Göttingen, Germany). For Western blotting cells were lysed with an

appropriate buffer (150 mM NaCl, 50 mM Tris–HCl, 1 mM EDTA, 1% NP-40, protease inhibitor, 100 mM DTT; pH 7.4) and DNA was sheared by sonication. Samples were quantified using a Bio-rad protein assay (Biorad) and the same amount of protein (50μg) was separated using PAGE (7,5%). Protein were transferred to PVDF membranes (Millipore), and probed overnight at 4°C with a rabbit monoclonal anti-ANO1 antibody (Novus Biologicals, Littleton, CO, USA). Blots were visualized using a secondary HRP-conjugated anti-rabbit antibody (Acris, Herford, Germany) and Super Signal® West Pico Chemiluminescent Substrate (Pierce, Rockford, IL, USA).

Micro-Ussing chamber recordings

Access to human tissues used in this study received approval from the local Ethics Committee of the Faculty of Medical Sciences and informed consent was obtained from all patients. HBE monolayers (resistance $\geq$ 600 Ωcm^2) were mounted in a modified micro-Ussing chamber. Apical and basolateral surfaces were perfused continuously at a rate of 5 - 10 ml/min (chamber volume 2 ml). The bath solution contained (mmol/l): NaCl, 145; KH_2PO_4, 0.4; K_2HPO_4, 1.6; D-glucose, 5; $MgCl_2$, 1; Hepes 5; and Ca-gluconate, 1.3. pH was adjusted to 7.4). Experiments were carried out under open circuit conditions at 37 °C. Transepithelial resistance (R_{te}) was determined by applying short (1 s) current pulses ($\Delta I = 0.5$ µA) and recording of the corresponding voltage deflections (ΔV_{te}). Values for transepithelial voltage (V_{te}) were referred to the luminal side of the monolayers and equivalent short-circuit currents (I_{sc}) were calculated according to Ohm's law.

Iodide Quenching

Quenching of the intracellular fluorescence generated by the iodide-sensitive enhanced yellow fluorescent protein (YFP) was used to measure anion conductance. YFP fluorescence was excited at 490 nm using a semi-automatic Novostar plate reader (BMG-Labtech, Offenburg, Germany). I^- influx was induced by replacing 20 mM extracellular Cl^- by I^-. Background fluorescence was subtracted and auto-fluorescence was negligible. Changes in fluorescence induced by I^- are expressed as initial rates of fluorescence decrease (arbitrary units/sec). For

the assays we used HT_{29} cells stably expressing YFP. Ca^{2+} stimulus and iodide were applied together because of the transient nature of the Ca^{2+} stimulation.

Materials

All compounds used (ionomycin, carbachol, ATP, DAG kinase inhibitor II, U73122) were of highest available grade of purity and were from Sigma (Taufkirchen, Germany) or Merck (Darmstadt, Germany). All cell culture reagents were from GIBCO/Invitrogen (Karlsruhe, Germany). The IPMK inhibitor chlorogenic acid (C3878) was from SIGMA (Taufkirchen, Germany). The inositol-1,4,5-trisphosphate 3-Kinase inhibitor N^2-(*m*-Trifluorobenzyl), N^6-(*p*-nitrobenzyl)purine and D-myo-Inositol 1,3,4,5-Tetrakisphosphate Octapotassium Salt were from Merck (Damstadt, Germany). D-myo-Inositol 3,4,5,6-tetrakisphosphate from Echelon (Salt Lake City, UT) was from Santa Cruz (Heidelberg, Germany). AO1 was from Sygnature Chemical (Nottingham, UK). INO-4995 and INO-4913 were from Inologic (Seattle, WA, USA).

Statistical analysis

Student's t test (for paired or unpaired samples as appropriate) and ANOVA were used for statistical analysis. Values of $p < 0.05$ were accepted as significant.

Results

INO-4995 and INO-4913 activate human TMEM16A

INO-4995 has been suggested to activate from the cytosolic side a non-CFTR Cl^- conductance that is Ca^{2+} dependent (CaCC) (173). Its non-esterified counterpart INO-4913 was shown to be less membrane permeable and thus less potent in activating CaCC. CaCC in airways and other epithelial and non-epithelial tissues is now known as TMEM16A (124; 137). It can be readily activated by increase in intracellular Ca^{2+} due to Ca^{2+} ionophores such as ionomycin (Fig. 1A, B). Notably, cells overexpressing TMEM16A have an increased baseline Cl^- conductance, indicating a considerable leakage activity of the overexpressed channel (97). We

examined if esterified membrane permeable. INO-4995 and the less membrane permeable, non-esterified INO-4913 (176) are able to activate TMEM16A. Stable baseline currents were measured under control whole cell conditions (Supplemental Fig. S1A). However, when patch pipettes were filled with 1 μM INO-4995 and INO-4913, respectively, whole cell currents were activated in HEK293 cells, expressing human TMEM16A (Fig. 1C-E) upon forming a whole cell recording (rupture of the cell attached membrane). Similar to the activation by ionomycin, INO-4995 and INO-4913 activated currents showed little time dependence (Fig. 1C, D; right panels) and were completely blocked by the TMEM16A-inhibitor CaCCinh-A01 (AO1; 20 μM) (3; 31). Activation of TMEM16A by INO-4995 was concentration dependent with a maximal activation at 5 μM (Fig. 1G). While 20 μM AO1 showed complete inhibition, 10 μM blocked 95 ± 6 % (n = 5) of the current. Moreover, INO-4995 induced conductances were inhibited significantly from 8 ± 1 to 2.7 ± 0.9 nS/pF. When measured under current clamp, the membrane voltages were depolarised by 11.4 ± 2 mV (n = 6) due to replacement of 115 mM extracellular Cl^- by impermeable gluconate (not shown). As HEK293 cells do not have endogenous Ca^{2+} activated (SK) K^+ channels there is no contribution of K^+ currents to Ca^{2+} activated whole cell currents. Thus no currents were activated in mock transfected cells. These experiments suggest that TMEM16A is the target for INO-4995 and INO-4913, and suggest that TMEM16A may be controlled by endogenous tetrakisphosphates.

TMEM16A is not controlled by IP$_4$ and phosphatidylinositols

We examined whether TMEM16A is inhibited by Ins(3,4,5,6)P$_4$, since uncoupling of CaCC from intracellular Ca^{2+} levels by Ins(3,4,5,6)P$_4$ had been observed earlier, leading to transient Cl^- currents (176). The baseline (con) and ionomycin-activated Cl^- conductance in TMEM16A-expressing cells were not affected by the presence of either 10 μM Ins(3,4,5,6)P$_4$ or Ins(1,3,4,5)P$_4$ in the patch pipette (Fig. 2A). Although baseline currents somewhat varied, ionomycin activated whole cell currents were quite similar in TMEM16A-overexpressing cells (Fig. 2A). We also examined whether the magnitude or time course of Ca^{2+} activated (1 μM ionomycin) TMEM16A-currents was affected by IP$_4$. However, we were unable to detect any significant effects of Ins(3,4,5,6)P$_4$ or Ins(1,3,4,5)P$_4$ on TMEM16A currents activate by

ionomycin (Fig. 2B).
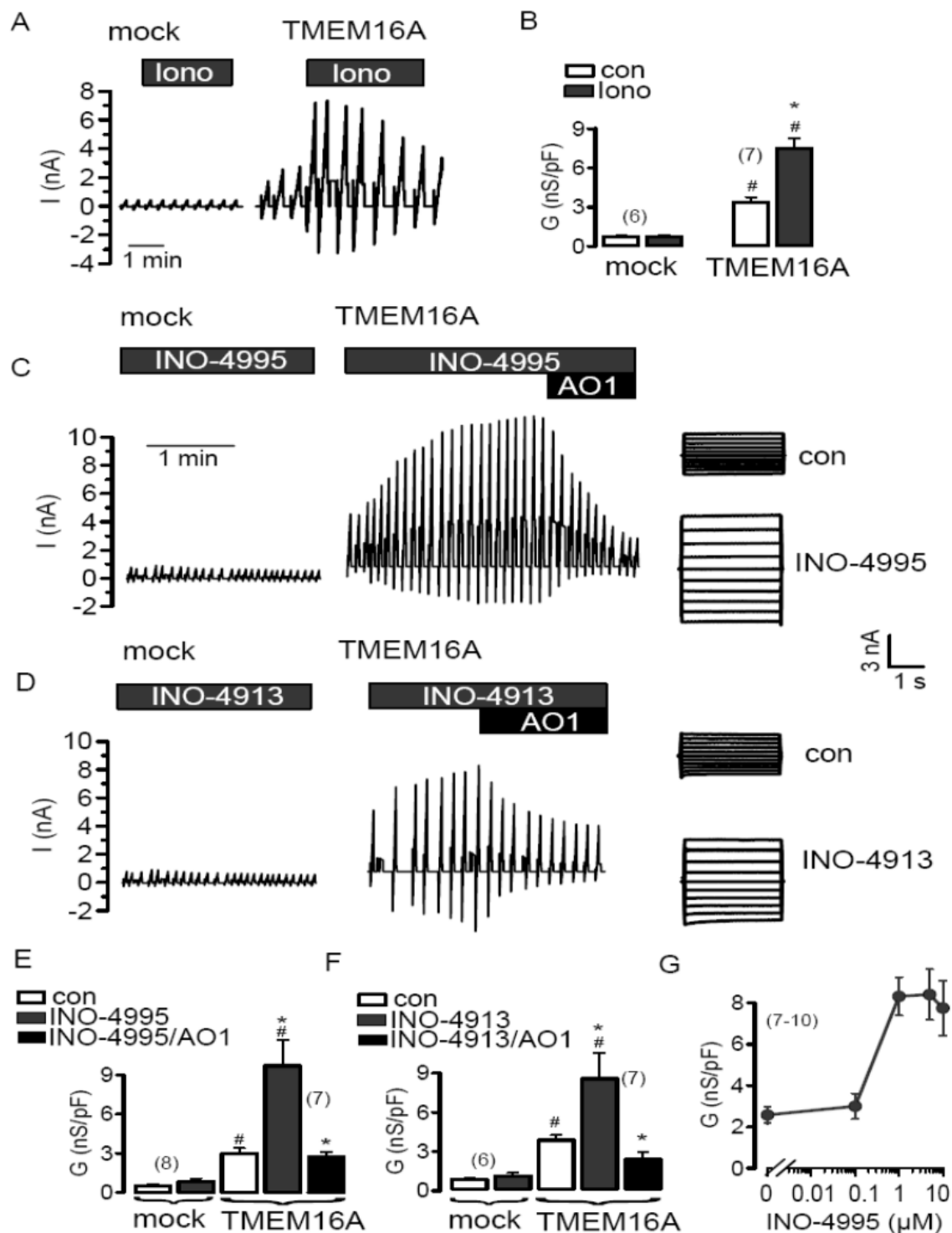
Fig. 1: INO-4995 and INO-4913 activate human TMEM16A. (A)   Original   recordings   of ionomycin (1 µM) activated whole cell currents measured in mock-transfected HEK293 cells or cells overexpressing TMEM16A. The cells were voltage clamped to +/- 50 mV. (B) Summary of the calculated whole cell conductances (related to the cell size; conductance density) before and after   stimulation   with   ionomycin. (C) Whole   cell   currents   in   mock   transfected   and TMEM16A-expressing HEK293 cells. Patch pipettes were filled with 1 µM INO-4995. Upon

forming a whole cell configuration, TMEM16A was activated by INO-4995 in TMEM16A-expressing cells. The CaCC-blocker AO1 (20 μM) inhibited TMEM16A currents activated by INO-4995. Right panels show overlay currents. (D) Whole cell currents in mock transfected and TMEM16A expressing HEK293 cells. Patch pipettes were filled with 1 μM INO-4913. The CaCC-blocker AO1 (20 μM) inhibited TMEM16A currents activated by INO-4913. Right panels show overlay currents. (E, F) Summary of the effects of INO-4995, INO-4913 and AO1 on whole cell conductances of mock transfected and TMEM16A expressing cells. (G) Concentration dependence for the effect of INO-4995 on whole cell conductance in TMEM16A-expressing cells. Means ± SE; n = 6-10. Values in parentheses indicate n. #P< 0.05, unpaired t-test; *P< 0.05, paired t-test.
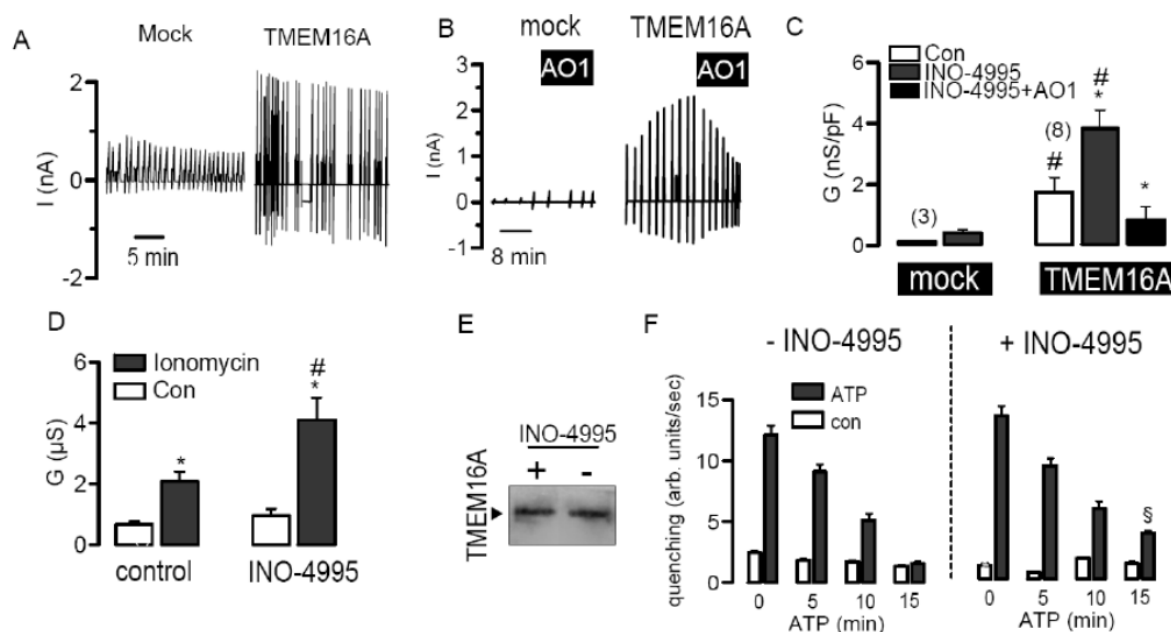
Supplemental Fig. S1: (A) Original recordings of stable resting whole cell currents in mock-transfected and TMEM16A-expressing HEK293 cells. The cells were voltage clamped to +/- 50 mV. (B) Activation of whole cell currents by 1 μM INO-4995 in the patch pipette filling solution and in the absence of cytosolic Ca^{2+} (Ca^{2+} free pipette solution containing 5 mM EGTA. (C) Summary of the effects of INO-4995 on whole cell conductances (conductance density) in mock transfected and TMEM16A expressing cells, in the absence of cytosolic Ca^{2+}. (D) Summary of the effects of 1 μM ionomycin on whole cell conductances measured in *Xenopus* oocytes 24 hrs after injection of water (control) or INO-4995 (5 μM). (E) Western blot analysis of TMEM16A-expression in CFBE airway epithelial cells, with and without treatment by INO-4995 (1 μM for 2 hrs at three consecutive days). (F) Summary from YFP-fluorescence quenching by I⁻ influx, indicating inactivation of Ca^{2+} activated Cl⁻ conductance in the continuous presence of 100 μM ATP. I⁻ was re-added every 5 min to measure remaining halide conductance. Treatment with INO-4995 (2hrs for three consecutive days) prolonged activation. Means ± SE (number of cells). #significant difference from control cells (unpaired t-test). *significant effects of INO-4995 and AO1 (paired t-test). §significant difference from non-treated cells (unpaired t-test).

Notably, ionomycin-induced TMEM16A Cl⁻ currents inactivated in the continuous presence of ionomycin, to even below the initial current level that was measured before stimulation

with ionomycin (dash line). In preliminary studies we found that this is likely due to Ca^{2+}/CAMKII-dependent phosphorylation of Ano1 (unpublished data). Activation of TMEM16A through stimulation of purinergic receptors with 100 μM ATP was also not affected by $Ins(3,4,5,6)P_4$ or $Ins(1,3,4,5)P_4$ (Fig. 2C). Moreover, although INO-4913 itself activated TMEM16A (Fig. 1D), it did not further augment TMEM16A currents activated by 100 μM ATP (Fig. 2D).
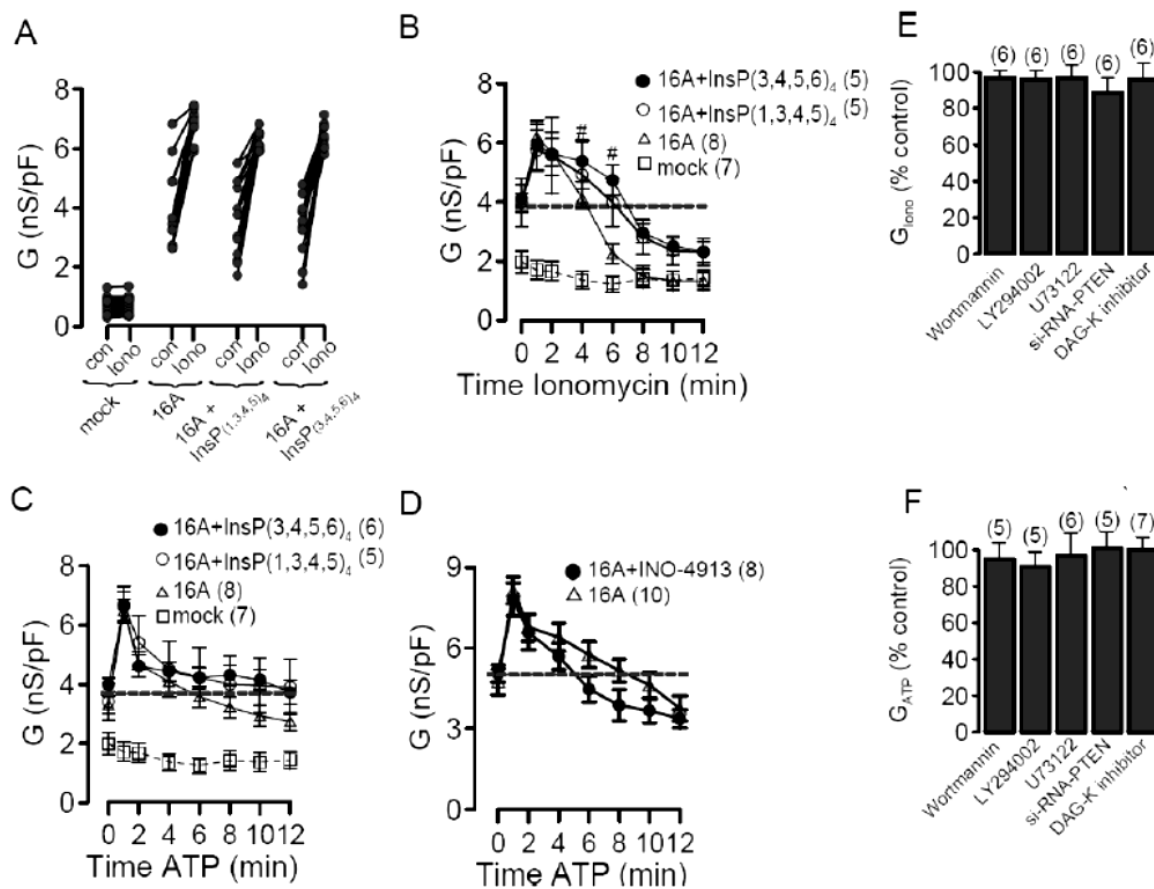
Fig. 2: TMEM16A is not controlled by IP_4 and phosphatidylinositols. (A) Individual whole cell baseline (no agonist) and ionomycin-activated conductances in mock transfected HEK293 cells and cells overexpressing TMEM16A (16A). Addition of $Ins(3,4,5,6)P_4$ or $Ins(1,3,4,5)P_4$ to the patch pipette filling solution did not change baseline or ionomycin-activated Cl^- conductance in TMEM16A expressing cells. (B) Time course of whole cell Cl^- conductances activated by 1 μM ionomycin in mock-transfected and TMEM16A-overexpressing HEK293 cells. $Ins(3,4,5,6)P_4$ or $Ins(1,3,4,5)P_4$ in the pipette filling solution did not change the time course for activation and spontaneous recovery in the presence of ionomycin. (C, D) Time course of whole cell Cl^- conductances activated by 100 μM ATP in mock-transfected and TMEM16A-overexpressing HEK293 cells. Neither $Ins(3,4,5,6)P_4$, $Ins(1,3,4,5)P_4$ nor INO-4913 changed ATP-dependent (100 μM) activation of overexpressed TMEM16A. (E, F) Summary of ionomycin- and ATP-induced whole cell Cl^- conductances measured in

TMEM16A-overexpressing HEK293 cells. Cells were treated with various compounds known to interfere with inositolphosphates and phosphatidylinositols. Activated conductances are shown relative to conductances in non-treated cells. Means ± SE; n = 5-10. Values in parentheses indicate n. #$P < 0.05$, unpaired t-test; *$P < 0.05$, paired t-test.

These data suggest that TMEM16A is not directly controlled by IP_4. A number of enzymes are crucial for the production of inositol tetrakisphosphates, such as inositol-1,4,5-trisphosphate *3-Kinase* (IP_3-3-K), Inositol polyphosphate multikinase (IMPK), and inositol 1,3,4-triphosphate 5/6 kinase (ITPK-1). We incubated TMEM16A expressing cells 2 - 20 hrs with inhibitors of IP_3-3-K (20 µM N²-(m-Trifluorobenzyl),N⁶-(p-nitrobenzyl)purine), IMPK (2 µM chlorogenic acid) or knocked down expression of ITPK-1 by siRNA (6; 12; 24). However, none of these treatments inhibited activation of TMEM16A by ionomycin (data not shown). Taken together these data suggest that INO-4913 (and INO-4995) activate overexpressed TMEM16A channels directly, which does not seem to involve endogenous tetrakisphosphates. Moreover, intracellular Ca^{2+} does not seem to be essential for activation of overexpressed TMEM16A channels: When we applied INO-4995 in a Ca^{2+} free pipette filling solution (containing 5 mM EGTA), we found a baseline Cl^- conductance that was reduced by about 50%. However, whole cell currents were still activated by INO-4995, but were reduced by about 40% when compared to currents activated in the presence of 0.1 µM $[Ca^{2+}]_i$ (Supplemental Fig. S1B, C). We performed additional experiments in excised inside out membrane patches of TMEM16A-expressing HEK293 cells. When we applied 1 µM INO-4913 to the cytosolic side, we observed an increase in channel noise and an increase in the conductance of cell excised membrane patches (Fig. 3A-C). In contrast no current was activated in membrane patches from mock transfected cells (Fig. 3D-F). These results suggest that INO-4913 is able to activate TMEM16A directly or by influencing regulatory proteins or the membrane lipid composition in close proximity of the channel.

Cytosolic inositolphosphates are closely linked to the membrane phosphatidy- linositols phosphatidylinositol 4,5-bisphos- phate (PIP_2) and phosphatidylinositol 3,4,5-trisphosphate (PIP_3). Other ion channels such as Ca^{2+} activated K^+ channels (KCNN4), epithelial Na^+ channels (ENaC) and renal K^+ channel (ROMK) are controlled by these membrane lipids (58; 71; 91; 157). We therefore examined the effects of the PI3 kinase inhibitors wortmannin (1

μM/4 hours) and LY294002 (100 nM/3hours), which are known to reduce PIP_3 levels in the plasma membrane. Moreover, we tested the effects of phospholipase C inhibitor U73122 (10 μM/5 hrs; increasing PIP_2 levels), siRNA knockdown of the enzyme PTEN (decreasing PIP_2 levels), as well as the diacylglycerol inhibitor 3-[2-[4-(bis(4- Fluorophenyl)methylene)-1 –piperi-dinyl]e- thyl]-2,3-dihydro-2-thioxo-4(1H)-quin- azolinone (25 μM/5 hrs; decreasing all phosphatidylinositols). However, we found no significant effects of any of these treatments on the activity of TMEM16A, activated directly by Ca^{2+} (1 μM ionomycin) or through stimulation of $P2Y_2$ receptors (100 μM ATP) (Fig. 2E, F). It is therefore unlikely that INO-4913 and INO-4995 act through any of these pathways. In contrast, these treatments strongly interfered with the activity of the epithelial Na^+ channel ENaC, which is known to be regulated by phospholipids (data not shown).
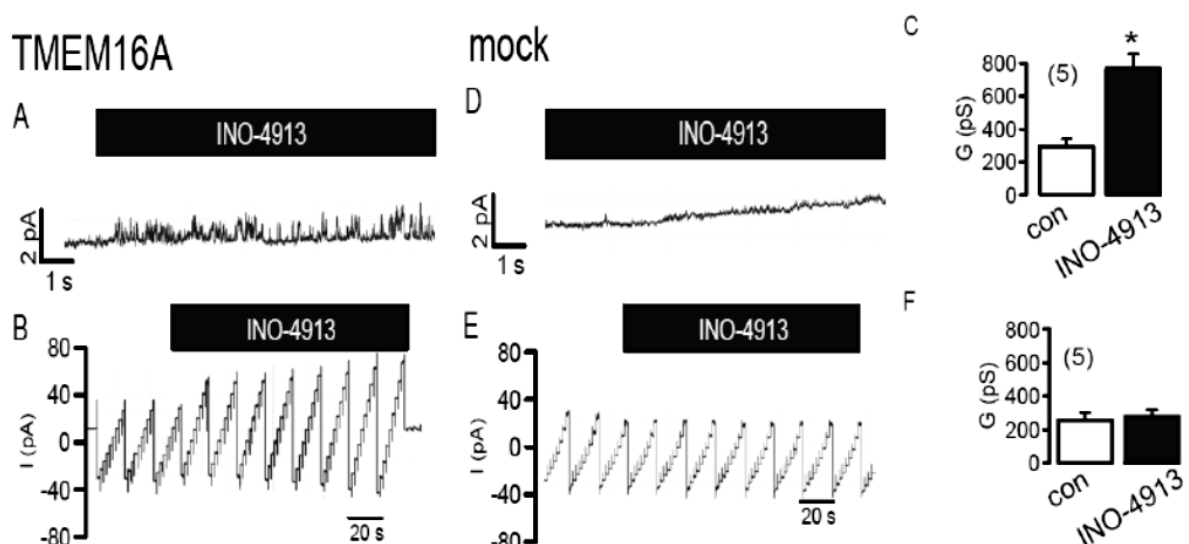
Fig. 3: TMEM16A may be directly activated by INO-4913. Current recordings from excised inside out membrane patches of HEK293 cells overexpressing TMEM16A. (A) Current noise was increased by application of 1 μM INO-4913 to the cytosolic site of the excised membrane patch. Clamp voltage was +80 mV. (B) Continuous recording of the patch current during voltage clamp between ± 50 mV. INO-4913 increased the patch current. (C) Summary of the conductance of the excised membrane patch and effect of INO-4913. (D-F) Comparable experiments obtained from mock transfected cells. Means ± SE; n = 5. Values in parentheses indicate n. *P< 0.05, paired t-test.

INO-4995 enhances endogenous Ca^{2+} activated chloride currents

We examined whether INO-4913 and INO-4995 are able to activate endogenous, i.e. non-overexpressed TMEM16A-currents. Oocytes from *Xenopus laevis* are known for their

pronounced endogenous Ca^{2+} activated Cl^- current, which is now known to be due to expression of TMEM16A (149). We found that acute application for up to 2 hrs, of 5 μM INO-4995 or INO-4913 did not augment baseline Cl^- conductance or TMEM16A currents activated by 1 μM ionomycin. In contrast, incubation for 24 hours with either INO-4995 or INO-4913 induced an enhanced baseline Cl^- current and augmented ionomycin-activated currents (Fig. 4).
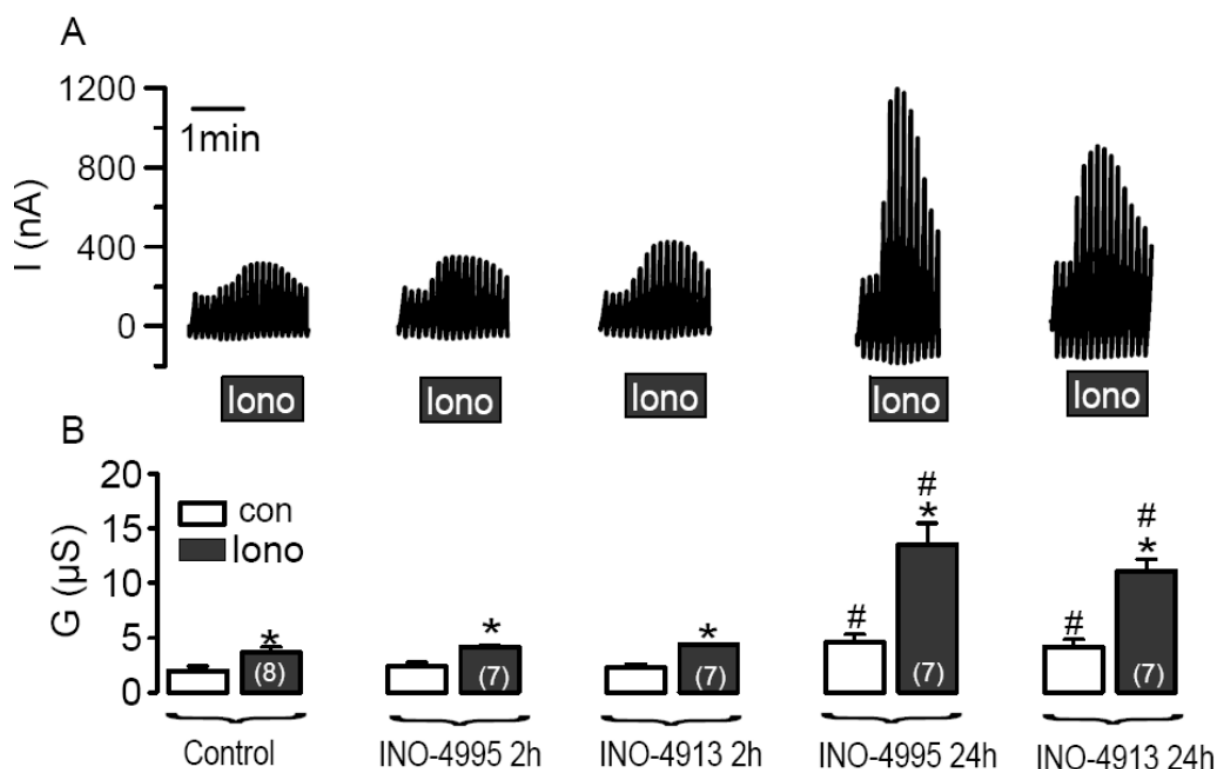
Fig. 4: Endogenous TMEM16A expressed in Xenopus oocytes is activated by INO-4995 and INO-4913. (A) Original recordings of whole cell currents measured in Xenopus oocytes. The cells were voltage clamped from -60 to + 40 mV. Ionomycin (1 μM) activated a whole cell Cl^- current, which was enhanced when cells were incubated for 24 hrs with 5 μM INO-4995 and INO-4913, respectively. (B) Summary of whole cell conductances measured under control conditions and after stimulation with 1 μM ionomycin. Means ± SE; n = 7-8. Values in parentheses indicate n. #P< 0.05, ANOVA; *P< 0.05, paired t-test.

Very similar results were obtained when INO-4995 was directly injected into the oocytes and when the oocytes were measured the following day (Supplemental Fig. S1D). Obviously longer incubation times are necessary to activate endogenous TMEM16A, as already suggested from previous results, obtained for INO-4995 dependent activation of endogenous TMEM16A in human CF airway epithelia and CF mouse airways (173).
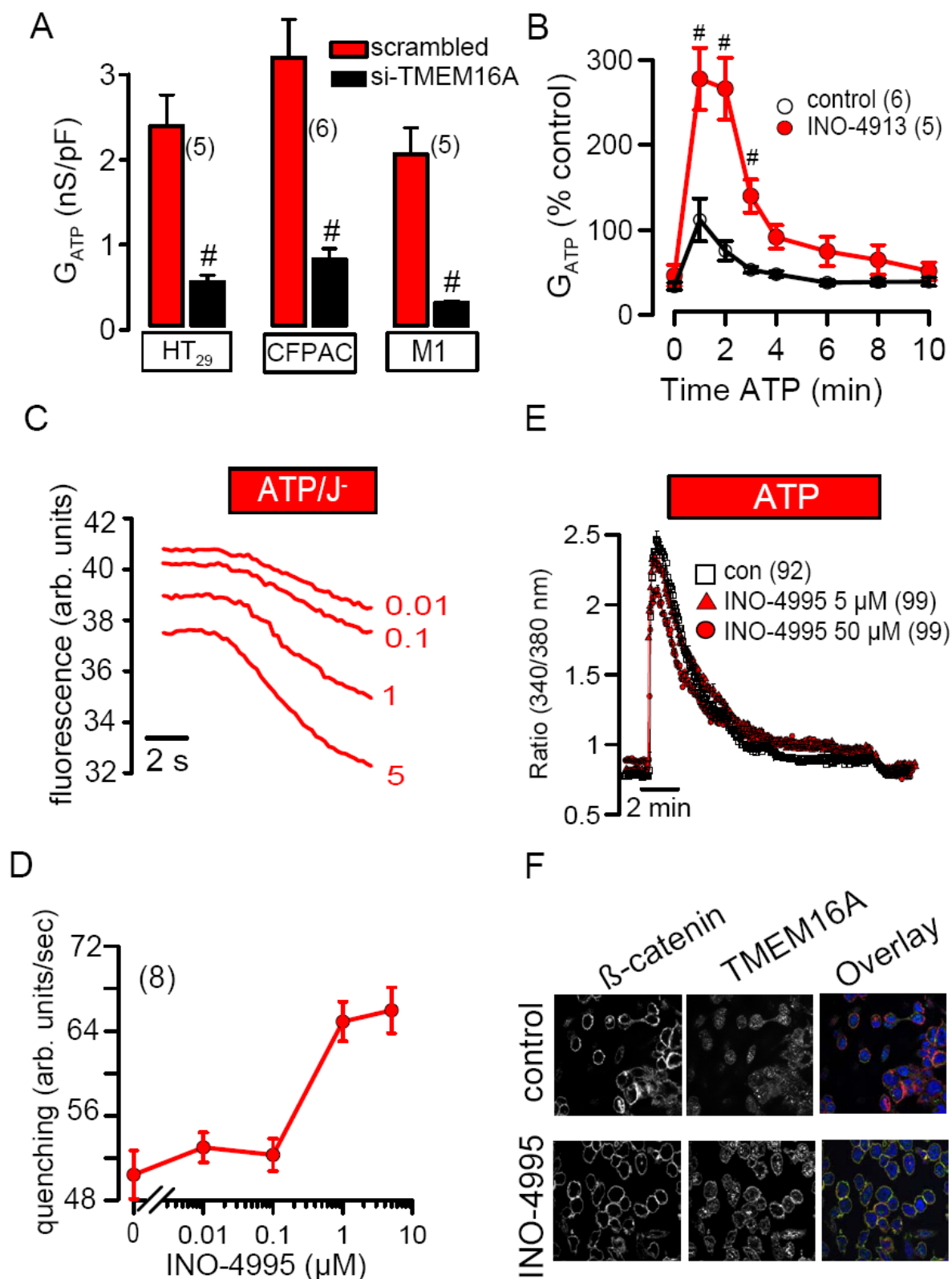
Fig. 5: INO-4995 and INO-4913 augment endogenous ATP-activated Cl⁻ currents in epithelial cells. (A) Summary of ATP (100 µM) induced whole cell Cl⁻ currents in HT$_{29}$, CFPAC and M1 cells. In all three cell lines, Cl⁻ currents were largely reduced after siRNA-knockdown of TMEM16A. (B) Time course of the whole cell conductances relative to control. ATP induced

a whole cell Cl⁻ conductance that was about 3 times larger when INO-4913 was present in the patch pipette solution. (C) Original tracings from I⁻ quenching of fluorescent YFP in HT_{29} cells after stimulation with 1 µM ATP. Cells were treated with different concentrations of INO-4995 (0.01 – 5 µM. (D) Concentration dependent effect of INO-4995 on I⁻ quenching of fluorescent YFP in HT_{29} cells, upon stimulation with 1 µM ATP. ATP was applied to cells which had been incubated for 2 hrs at three consecutive days, with different concentrations of INO-4995. (E) Effect of ATP on intracellular Ca^{2+} concentrations (measured as Fura-2 340/380 nm fluorescence ratio in HT_{29} cells). Ca^{2+} increase by ATP was essentially unaffected by 5 µM INO-4995. (F) Immunocytochemistry photo of endogenouse TMEM16A in HT_{29} cells, before (upper panel) and after (lower panel) treated with INO-4995 (2 hrs at three consecutive days). Means ± SE; n. Values in parentheses indicate n. #P< 0.05 vs. control, unpaired t-test.
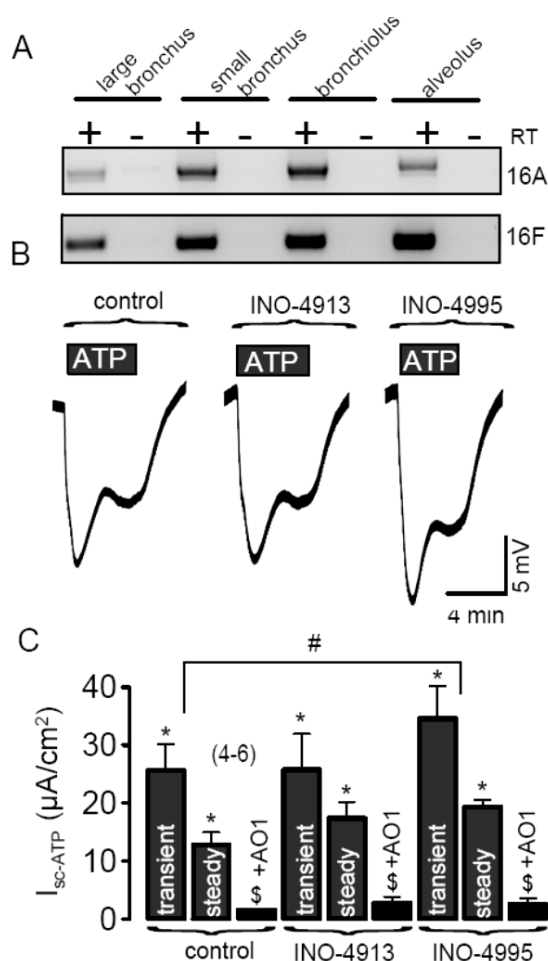
We further examined whether INO-4913 controls endogenous TMEM16A expressed in different types of epithelial cells. To that end we first examined whether TMEM16A is respo-nsible for endogen- ous Ca^{2+} activated Cl⁻ currents in epithelial cells of human colon (HT_{29}), human pancreas (CFPAC), and mouse collecting duct (M1). To that end we knocked down TMEM16A-expression using siRNA and stimulated Ca^{2+} activated Cl⁻ currents with 100 µM ATP (3; 92). In all three cell lines knockdown of TMEM16A largely reduced ATP-activated whole cell currents, suggesting that TMEM16A is the major component of endogenous CaCC (Fig. 5A).

Then we went on to examine activation of whole cell Cl⁻ currents by ATP in HT_{29} control cells, and cells that had been treated with 1µM INO-4913. We found that ATP-induced whole cell currents were augmented by treatment with INO-4913 (Fig. 5B). When cells were incubated with different concentrations of INO-4995 for 2 hours at three consecutive days (173), we found a concentrations-dependent increase of the ATP-activated anion permeability, as measured in iodide quenching assays (Fig. 5C, D). Similar results were found in (n = 5) whole cell patch clamp experiments (data not shown). Importantly, these positive effects of INO-4913 and INO-4995 on Ca^{2+} activated TMEM16A currents are not due to effects on $[Ca^{2+}]_i$, since ATP-induced rise in $[Ca^{2+}]_i$ in HT_{29} cells was basically unaffected by INO-4995 up to a concentration of 5 µM (Fig. 5E). These results indicate activation of TMEM16A by INO-4913 and INO-4995 in mammalian epithelial cells. We could not detecte a change of overall expression of TMEM16A by INO-4995 (Supplemental Fig. S1E), however,

immunocytochemistry suggested an increase in membrane expression of TMEM16A in HT_{29} cells, by treatment with INO-4995 (Fig. 5F).

INO-4995 activates TMEM16A in primary cultures of airways

The essential question is, whether INO-4995 is able to increase Ca^{2+} activated Cl^- currents in human airways.

Using RT-PCR we analyzed we found expression of TMEM16A in all parts of the human respiratory polarized human bronchial epithelial cell monolayers mounted in micro-Ussing chambers. Human airway cultures were treated repetitively (for 2 hrs in 4 subsequent days) with INO-4913 and INO-4995,

Fig. 6: INO-4995 activates endogenous TMEM16A in polarized human non-CF airway epithelial cells. (A) RT-PCR analysis indicates expression of TMEM16A throughout the native human respiratory tract. (B) Original Ussing chamber recordings (open circuit measurements) obtained from human primary airway epithelial cells grown on permeable supports with an air liquid interface. ATP (100 μM) induced transient and steady state voltage deflections of the transepithelial voltage, indicating activation of Cl^- secretion. ATP-induced voltage deflections were augmented after repetitive treatment (2 hrs at four consecutive days) with 5 μM INO-4995. (C) Summary of ATP-induced transient and steady state equivalent short circuit currents (calculated from voltage deflections) in control airway cells and cells treated with INO-4913 and INO-4995, respectively. The inhibitor AO1 (20 μM) completely blocked ATP-induced I_{sc}. Means ± SE (number of cells). Values in parentheses indicate n. #$P< 0.05$ vs. control; ANOVA; $^\$P< 0.05$, paired t-test indicates significant inhibition by AO1 or significant activation by ATP.

respectively, similar to a previous study (173). Luminal application of 100 μM ATP activated Ca^{2+} dependent Cl^- secretion, which had a transient and a steady state component (Fig. 6B). ATP is known to act primarily on luminal purinergic $P2Y_2$ receptors in human airways (124; 137). Both components were potently blocked by the CaCC inhibitors niflumic acid (10 μM)

(not shown) or CaCC$_{inh}$AO1 (20 µM)   (31) (Fig. 6C). After treatment with INO-4995 but not INO-4913, ATP- induced voltage deflections were augmented and calculated equivalent short circuit currents (I$_{sc}$-ATP) were enhanced (Fig. 6B, C). In some experiments with INO-4995 treated cells we applied ATP for up to 20 min and found that the steady state I$_{sc}$ was substantially larger than in control cells. In additional YFP-quenching experiments we exposed INO-4995-treated and non-treated HT$_{29}$ cells to 100 µM ATP for 15 min, and re-added iodide every 5 min. The results suggest a prolonged activation of Ca^{2+} dependent Cl$^-$ secretion after treatment with INO-4995 (Supplemental Fig. 1F).

   We also performed the same treatment by INO-4995 with primary cultures from CF-airways. As demonstrated in Fig. 7, ATP induces a voltage deflection that was clearly enhanced after treatment with INO-4995. Residual CFTR Cl$^-$ secretion by genistein in these CF-lung monolayers was not affected by INO-4995 (-INO: ΔI$_{sc}$ = 0.18 $\pm$ 0.5 µA/cm^2, n=3 vs. +INO: ΔI$_{sc}$ = 0.20 $\pm$ 0.4 µA/cm^2, n=3). We compared the effects of treatment with INO-4995 in normal and CF-airways and found a 50% enhanced effect of INO-4995 on the transient Ca^{2+} activated Cl$^-$ secretion in CF airways. Taken together, the present data indicate that INO-4995 augments Ca^{2+} activated Cl$^-$ secretion by activation of TMEM16A. The results suggest INO-4995 as a useful tool to augment a compensatory Ca^{2+} dependent Cl$^-$ secretion in dehydrated CF lungs.
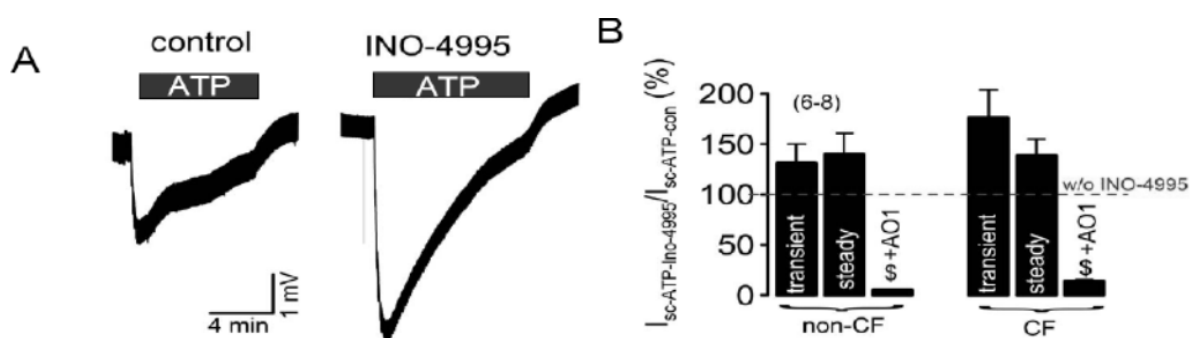
Fig. 7: INO-4995 activates endogenous TMEM16A in polarized human CF airway epithelial cells: (A) Original Ussing chamber recordings (open circuit) obtained from CF primary airway epithelial cells grown on permeable supports with an air liquid interface. ATP (100 µM) induced transient and steady state transepithelial voltage deflections, indicating activation of Ca^{2+} dependent Cl$^-$ secretion. Effect of treatment by INO-4995 (5 µM; 2 hrs at four consecutive days). (B) Summary showing activation of transient and steady state

equivalent short circuit currents (calculated from voltage deflections) by ATP after treatment with INO-4995 relative to non-treated cells. The data demonstrate a slightly enhanced effect of INO-4995 on CF-primary. Effect of ATP in non-treated tissues is set to 100% (dash line). The inhibitor AO1 (20 µM) completely blocked ATP-induced I_{sc}. Mean ± SEM (number of cells). [#]significant difference from control cells (unpaired t-test). [$]significant inhibition by 20 µM AO1 (paired t-test).

Discussion

Activation of TMEM16A by INO-4995

The aim of the present study was to examine whether the recently identified Ca^{2+} activated Cl^- channel TMEM16A is the target for two synthetic inositol tetrakisphosphates. INO-4995 and INO-4913 that have been demonstrated earlier to enhance Ca^{2+} activated Cl^- currents and therefore to improve electrolyte balance in airways of CF mice (140; 173). The present results clearly show that both INO-4995 and INO-4913 activate TMEM16A that was overexpressed in HEK293 cells. Interestingly activation of TMEM16A by INO-4995 and the less membrane permeable but active compound INO-4913 occurred even in the absence of cytosolic Ca^{2+} (Supplemental Fig. S1C). Moreover, the INO-compounds activated overexpressed TMEM16A without increasing intracellular Ca^{2+} (data not shown) and did not affect intracellular Ca^{2+} signalling (Fig. 5E). Notably TMEM16A channels, when overexpressed in HEK293 cells and other cell types, are partly active even at resting Ca^{2+} concentrations (97). The reasons for this is currently unclear, however, we speculate that additional proteins are required to regulate TMEM16A (170).

The effects of INO-4995 and INO-4913 were remarkably different on TMEM16A, expressed endogenously in *Xenopus* oocytes or mammalian cells from colon and airways. Inhibition of TMEM16A by siRNA indicated that TMEM16A is a main component of endogenous CaCC in these cells. Here we could not detect a direct and fast activation of CaCC, i.e. endogenous TMEM16A by INO-4995. However, INO-4995 increased TMEM16A-currents which were stimulated by agonists such as ATP. To see this effect, cells needed to be incubated repetitively with INO-4995, or for a longer duration. The results obtained in these experiments are remarkably similar to those obtained previously on airways of CF mice (173).

We have currently no explanation why the effect of INO-4995 is different on overexpressed and endogenous TMEM16A channels.

Notably, we obtained similar results with benzimidazolone compounds, which are known to activate Ca^{2+} activated (KCNN4) K^+ channels: Overexpressed TMEM16A but not endogenous CaCC was directly activated by these compounds (169; 170). From those and the present results we may speculate that endogenous TMEM16A are inhibited by unknown auxiliary proteins. INO-4995 and INO-4913 may augment endogenous TMEM16A, once released from inhibitory proteins due to increase in $[Ca^{2+}]_i$. Alternatively, prolonged and repetitive incubation with INO-4995 may up-regulate membrane expression of TMEM16A (Fig. 5F). Notwithstanding the data indicate that TMEM16A is the target of INO-4995.

Overexpressed TMEM16A is not controlled by IP$_4$ and phosphatidylinositols

Although the results suggest that INO-4995 and INO-4913 activate TMEM16A by interfering with endogenous inositolphosphates, we found no evidence for a regulation of TMEM16A by IP$_4$ or phosphatidylinositols. Ins(3,4,5,6)P$_4$ has been proposed earlier to control the time course of endogenous CaCC activity (67). Evidence has been provided that the Ca^{2+} peak induced by activation of PLC-coupled receptors switches on CaCC, while prolonged activation is due to CaMKII dependent phosphorylation, which is modulated by inositolphosphates (63). In CFPAC cells low concentrations of ATP (2 µM) were used to elicit rather small endogenous Cl$^-$ currents (68). It may be that at higher agonist concentrations of ATP, like those used in the present study, regulation by inositol phosphates is overrun. Alternatively, the endogenous CaCC of CFPAC cells that is inhibited by Ins(3,4,5,6)P$_4$ is not TMEM16A. This, however, is unlikely since endogenous CaCC in CFPAC cells was inhibited by siRNA for TMEM16A in this and in a previous study (3). Moreover, IP$_4$ protein phosphatases seem to have role for the inhibitory effect of IP$_4$ on CaCC (193). Taken together, Ins(3,4,5,6)P$_4$ dependent regulation of CaCC is poorly examined and could not be detected in any cases (20; 23; 83; 189; 192; 193). It is likely that Ca^{2+} activated Cl$^-$ channels are composed of several, still unknown proteins and that TMEM16A is only one, however, essential subunit of a channel complex (19). Data have been provided suggesting that

different TMEM16 paralogs can heterooligomerize (92; 148), and two recent papers show that TMEM16A exists as a homodimer (47; 153).

INO-4995 and INO-4913 activate endogenous TMEM16A in various cells types and in human airway cells

As mentioned above, the present results demonstrate that endogenous TMEM16A in *Xenopus* oocytes, colonic HT_{29} and human airway epithelial cells is activated by INO-4995. It appears that prolonged or repetitive incubation with INO-4995 increases CaCC, as described in (173). This is probably not due to an upregulation of TMEM16A-expression, as we could not detect enhanced TMEM16A protein after repetitive incubation INO-4995 (5 µM/ 2 hrs) for up to four days (Supplemental Fig. S1E). However, prolonged exposure to INO-4995 appears to increase membrane expression of TMEM16A, as demonstrated in HT_{29} cells (Fig. 5F). Taken together the present results suggest that INO-4995 and INO-4913 may be useful tools to augment Ca^{2+} dependent Cl^- secretion in the airways of CF patients.

Acknowledgments

CHAPTER 6

Discussion

Other anoctamins can also function as CaCCs

Anoctamins do not show any obvious homology to other ion channels. Ano2, the closest relative of Ano1, has been shown to function as CaCC in olfactory receptors and photoreceptor synaptic terminals (65; 160). Ano2, 3, and 4 are mostly expressed in neuronal tissues. mRNA of Ano3 and Ano4 are equally expressed in spinal cord, brain stem, cerebellum, and eye (115; 148). Ist2p, the anoctamin in *S. cerevisiae*, is translated locally at the peripheral endoplasmic reticulum (ER) and may be inserted into the plasma membrane by the fusion of peripheral ER with the plasma membrane. If these anion selective proteins in mammals are transported by a similar novel mechanism, they might have effects on protein synthesis in axons and dendrites (64). A new report on a genome-wide association study (GWAS) found that Ano3 is associated with Alzheimer's disease (17). Our data proved a function of Ano4 as CaCC. Thus Ano3, as the closest relative of Ano4, may also function as CaCC, which was confirmed in an unpublished study (Oh et al, personal communication).   It will be exciting to examine the role of Ano3 and its related single nucleotide polymorphisms (SNPs) in Alzheimer's disease.

An unpublished doctoral thesis written by Milana Chinenkova showed that Ano6 is expressed in the cytoplasm of osteoblast cells, and the phenotype of knockout mice demonstrated curved and shorter long bones, with delayed endochondral and intramembranous ossification. That means Ano6 is an important factor in bone mineralization. This result is reminiscent of the function of Ano5. Mutations in Ano5 lead to abnormal bone mineralization and bone fragility called gnathodiphyseal dysplasia (GDD) (175). It is known that Ano5 is expressed in chondrocytes and osteoblasts (116), indicating an important role in bone formation. These two anoctamins are closest relatives of the same branch of phylogenetic tree of the anoctamin family, and their similar localization makes it likely that they are functionally related. Perhaps

they may even compensate for each other. In our study, we have found that Ano5 and Ano6 require higher and maybe more sustained Ca^{2+} levels to be activated. The anion selectivity was similar for Ano1, 4, 6, and 10, and was $I^- > Br^- > Cl^- > HCO_3^-$, suggesting a low field strength anion selectivity.

Analysis of the cation permeability showed that Ano6 is permeable for K^+. Moreover, Ano6 is also permeable for Ca^{2+}, as reported earlier (195). Taken together these results suggest that anoctamins are either poorly selective for anions or they somehow induce parallel cation conductances. It is currently poorly understood why Ano6 is an essential component of outwardly rectifying Cl^- channels (ORCC) and, at the same time, operates as a membrane localized phospholipid scramblase (110; 163). This multi-function protein attracts more and more attention and needs to be investigated intensively.

Ano7, 8, 9 produce relatively small Cl^- currents, especially Ano8 activation was found to be extremely slow, with activation time far beyond that of Ano1. This property may be related to the predicted large extracellular loop between transmembrane domain 5 and 6. Ano7 and Ano9 are also related to cancer. Ano7 is expressed more specifically in the prostate and up regulated in prostate cancer (13), while Ano9 is expressed in human colorectal, lung and breast cancer (86). The relation to cancer may probably be similar to that described for Ano1, and could be due to the function of CaCC in cell volume regulation. Ano10 can be activated by both the purinergic receptor and directly by Ca^{2+} increase through ionophores. However, when we replaced the extracellular Na^+ with $NMDG^+$, the activation of the channel was dramatically suppressed, indicating that extracellular Na^+ is necessary for the channel to be fully open, or, alternatively, the channel has a pronounced permeability for cations. The Ano10 gene has been suggested to be the genetic basis of autosomal recessive cereballar ataxias. At the same time, we should note that the high Ano10 expression levels in brain areas important for cognitive performance, such as the cortex and hippocampus (182), which warrants future investigation of CaCC function in the brain.

Anoctamins are the molecular identities of CaCCs and contribute to RVD

Ubiquitous chloride channels with permeability to Cl⁻ and other anions may be housekeeping proteins present in all cells. They contribute to cell volume regulation, excitability, contraction, and transepithelial electrolyte transport (75). These specialized functions are typically carried out by different Cl⁻ channels whose molecular identities became known over the past 20 years. Most studies have made use of the patch-clamp technique which allows characterization of the biophysical properties, mechanism of regulation and pharmacology of these Cl⁻ channels. Among the various Cl⁻ channels, CaCCs have attracted the attention of many investigators, because they participate in many important physiological processes, including epithelial fluid secretion, smooth muscle contraction and olfactory transduction (97). The molecular identities of CaCC have emerged through discovery of Ano1 (19; 149; 197). Amoctamins are a family of transmembrane proteins with 10 members, which are evolutionarily well conserved. They have both intracellular C- and N- termini and eight transmembrane domains (97).

We have reported recently that all ten anoctamins are indeed a family of CaCCs (170). Among all other functions, we found that CaCCs also contribute to regulatory volume decrease (RVD) (3). When the extracellular osmolarity decreases, cells take up water and swell. Osmotic cell swelling increases intracellular free Ca^{2+} concentration in most cell types examined so far (113). Swelling-induced ATP release augments the Ca^{2+} response to a hypotonic challenge via stimulation of P2Y$_2$ receptor (36). Therefore RVD is facilitated by autocrine secretion of ATP and subsequent release of ER-Ca^{2+}. This process occurs via a G protein-coupled and PLC-linked P2Y$_2$ receptor. Through the increase in intracellular Ca^{2+}, CaCCs are activated which thereby contribute to RVD, as schematically depicted in Fig. 1 (122).

Through description of data outlined in chapter 3, it becomes clear that Ano1 and other members of the anoctamin family contribute to swelling-activated whole cell currents ($I_{Cl, swell}$) in different human cell types. After siRNA knockdown of each anoctamin, we observed a non-additive reduction in $I_{Cl, swell}$. This could indicate that anoctamins hetero-oligomerize to form CaCCs, which are then sensitive to osmotic cell swelling. This $I_{Cl, swell}$ is greatly dependent upon purinergic signaling, because when we removed ATP from our experimental bath solutions using ATP-hydrolyzing enzymes, or when we blocked the purinergic receptor,

$I_{Cl, swell}$ was reduced dramatically. The importance of Ano1 for cell volume regulation has also been shown in Ano1 knock out animals. Submandibular glands express high levels of Ano1 (124). We isolated acinar cells from submandibular glands and exposed these cells to hypotonic solutions. The whole cell current activated by cell swelling as detected in control mice was abolished in the Ano1 knockout mice.

Further support for our study was provided by a recent report which showed that alpha-Hemolysin from Escherichia coli (HlyA) triggers an acute erythrocyte shrinkage, which depends on Ca^{2+} activated Cl^- efflux via Ano1 (156). Taken together our data clearly indicate that anoctamins contribute to volume regulated Cl^- currents

Fig. 1: Schematic model of the molecular mechanism of RVD and its control mediated by G protein-coupled $P2Y_2$ receptors and Ca^{2+} release in intestinal 407 cells. Gq and Gs represent G proteins coupled to phospholipase C (PLC) and adenylate cyclase (AC); respectively. PMCA represents the plasmalemmal Ca^{2+} pump (120).

in both native mouse epithelial cells and different human cell lines. This house keeping function puts anoctamins in line with the true volume regulatory anion channel (VRAC), whose molecular identity still remains to be identified. It is important to note that the biophysical properties of CaCC are different from VRAC, particularly with respect to the typical time-dependent activation of CaCC. Despite these characteristic differences both currents support cellular RVD and are activated in parallel. Importantly, knockdown of Ano1 in HEK293 cells also reduced AVD (apoptosis volume decrease) an initial cell shrinkage during apoptosis, suggesting that anoctamins are important for both RVD and AVD.

How does Ca^{2+} regulate Ano1?

After Ano1 had been generally accepted as CaCC, its regulation was examined most extensively. The research team led by Galietta showed that alternate splicing, for example skipping of exon-6b, which encodes 22 amino acid localized in N-terminal, increases the Ca^{2+} sensitivity and skipping of exon-13 strongly reduces the characteristic time-dependent activation at positive membrane potentials (52). In contrast, the research team led by Hartzell reported that deleting amino acids $_{448}$EAVK in the first intracellular loop dramatically decreases the apparent Ca^{2+} affinity. In contrast, mutating the adjacent $_{444}$EEEE abolishes intrinsic voltage dependence without altering the apparent Ca^{2+} affinity (191). However, one year later, they revised their model of Ano1, and now suggest that the 4th extracellular loop should be intracellular, and that this fragment contains two negative amino acids, which are important for Ca^{2+} sensing (198). Clearly the data provided by these groups are contradictory, which leaves Ca^{2+} binding site still to be determined.

In Chapter 4, we elucidated the mechanisms for activation of Ano1 and found that calmodulin (CAM) is the auxiliary Ca^{2+} binding protein, which can bind to the putative CAM binding site localized in the N-terminal domain within the stretch of amino acids encoded by exon-6b. This putative CAM binding site is missing, after deletion of exon-6b through alternative splicing. It appears possible that Ca^{2+} and CAM have more than one binding site, while the Ano1 ac form without the CAM binding site can still be activated by Ca^{2+}, maybe through direct binding.

Interestingly, our data show that activation of Ano1 was suppressed by both depolymerizing and stabilizing actin, and thus demonstrates that Ano1 is activated by Ca^{2+} in an actin-dependent manner. Further support for this finding was provided by a recent report, which showed that Ano1 interacts with the signaling/scaffolding proteins ezrin, radixin, moesin, which link the channel to the actin cytoskeleton. This team also reported that knockdown of moesin reduced Ano1 currents, clearly showing that Ano1 activation depends on actin-binding regulatory proteins (130).

Similar to other epithelial ion channels, anchoring of Ano1 to the cytoskeleton and to membrane PIP_2 may be essential in maintaining channel activity (72; 138). We have also found in Ano1 overexpressing HEK293 cells and in the presence of 100 nM free Ca^{2+} concentration in the patch pipette that basal Cl^- currents are enhanced. These enhanced basal Cl^- currents were abolished after 30 min pre-incubation with the Ca^{2+} chelator BAPTA-AM. Surprisingly, when we coexpressed Ano1 together with Ano9, both the basal whole cell conductance and the currents activated by ATP were suppressed. This led us to the hypothesis that an inhibitory factor or additional protein might be missing in overexpressing cells that keeps overexpressed Ano1 closed under control conditions. It is possible that Ano9 is part of this inhibitory mechanism, which is under-represented in cells overexpressing Ano1 (148; 170).

We have also found for Ca^{2+}-dependent gating of Ano1 that an increase in intracellular Ca^{2+} initially activates the channel, but then triggers inactivation by a Ca^{2+} dependent process. This mechanism may be due to CAMKII, as we have shown that in the presence of the CAMKII inhibitor KN62, inactivation of the channel was significantly attenuated (170). This is similar to the inhibition of CaCC by CAMKII in smooth muscle cells (60). We tried to further localize the molecular site within Ano1 that is responsible for its transient activation by replacing the N-terminus of Ano1 with that of Ano6 (Ano1N6), since Ano6 produces more sustained Cl^- currents. Notably, whole cell currents generated by the chimerical Ano1N6 channel were no longer transient. This suggests that the N-terminus controls both activation and inactivation of anoctamins.

The CAM-dependent regulation of Ano1 is reminiscent of Ca^{2+}/CAM dependent regulation of SK4 (Kcnn4), a Ca^{2+}-dependent potassium channel. This channel is tightly regulated by intracellular Ca^{2+}, but also lacks of a typical Ca^{2+} binding domain (87). Surprisingly, the benzimidazolinone 1-EBIO, which is a well known SK4 channel activator (62), can also activate Ano1 with an even 1000 fold higher affinity. Since 1-EBIO activates both basolateral SK4 and luminal Ano1 channels in airway epithelial cells, it could be an ideal compound to induce Cl^- secretion in airways and may therefore be useful for the treatment of the lung

disease in cystic fibrosis (CF).

INO-4995 and other inositolphosphates activate Ano1 in a Ca^{2+} independent manner

Activation of CaCC in CF airways may ameliorate mucociliary clearance and compensate for defective CFTR. Since intracellular Ca^{2+} is a common second messenger in all living cells, it activates a large number of downstream molecules, depending on the cell type or cell compartment. To avoid the unwanted activation of downstream molecules, a compound which could activate CaCC directly without increasing cytosolic Ca^{2+} is the most preferential drug candidate. If CaCC could be activated without increasing cytosolic Ca^{2+}, it might be an ideal way to treat CF. The membrane permeable compound 1-O-octyl-2-O-but-yryl-myoinositol 3,4,5,6-tetrakis- phosphate octakis (propionoxymethyl) ester (INO-4995, Fig. 2) (172) was demonstrated both to inhibit the epithelial Na^+ channel ENaC and to activate Ca^{2+} dependent Cl^- secretion (117; 141; 172). In our study we showed that it can acutely activate Ano1 in overexpressing HEK293 cells, without enhancing cytosolic Ca^{2+}. More surprisingly, this activation can even happen in the absence of cytosolic Ca^{2+}.
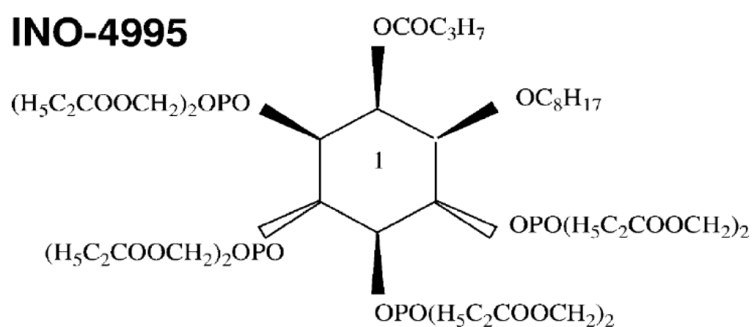
Fig. 2: Molecular structure of INO-4995.

However, we found no acute activation by INO-4995 of endogenous Ano1 expressed in *Xenopus* oocytes, human airways, and colonic cells. We have also tried prolonged and repetitive incubation with INO-4995. This treatment increases CaCC currents as described in (172). However, according to our Western blot analysis, there is no upregulation of Ano1 expression after repetitive incubation with INO-4995 for up to four days. The enhanced CaCC currents are probably due to increased membrane expression as demonstrated by immunostaining (171).

Another report described a cell-based functional screening of ~110,000 compounds, which

identified a group of N-aroylaminothiazole "activators" (E_{act}) of Ano1. These compounds activated Ano1 in the absence of intracellular and extracellular Ca^{2+}, whereas tetrazolylbenzamide "potentiators" (F_{act}) (Fig. 3) required intracellular Ca^{2+} but reduced the EC_{50} for Ca^{2+} dependent Ano1 activation (120). The team also generated an Ano1 inhibitor through minor structural modification of the activators. This strongly suggested direct binding of these small molecules to Ano1 channels. These molecules may be good candidate drugs for the treatment of CF patients.
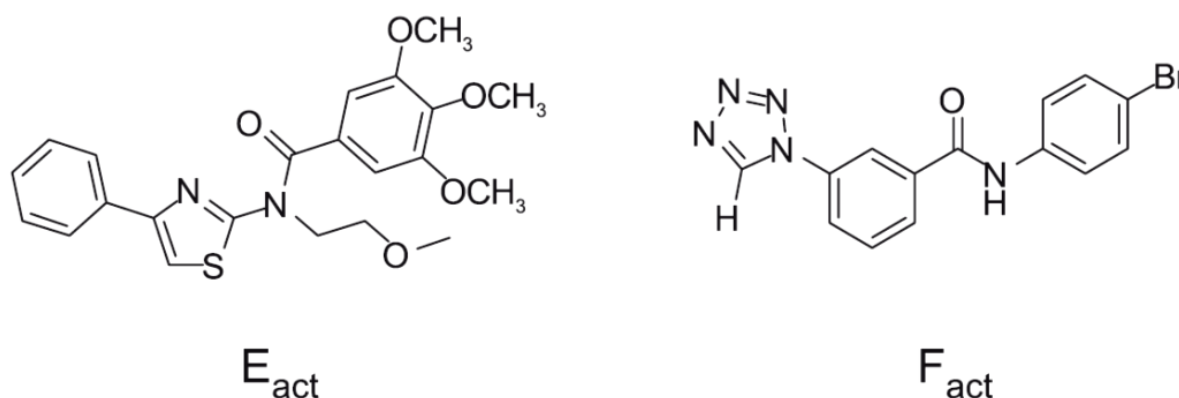
Fig. 3: Molecular structure of E_{act} and F_{act}.

Ano1 and cancer

Before Ano1 was identified as CaCC, it was actually known as cancer-associated protein in gastrointestinal stromal tumors (GISTs) and head and neck squamous cell carcinomas (21; 22; 187). Ano1 is embedded within the 11q13 amplicon, which is associated with a poor prognosis in squamous cell carcinoma of the head and neck (74). A new report shows that Ano1 is very little expressed in normal human tissues, such as gastrointestinal tract, esophagus, liver, pancreas, testis lung and kidney (106). The team found Ano1 overexpressed in human prostate cancer tissues, and knockdown of Ano1 with small hairpin RNAs (shRNAs) resulted in a significant reduction of proliferation, metastasis and invasion of PC-3 cells. Another recent report claimed that Ano1 induces MAPK and contributes directly to tumorigenesis and cancer progression. They found that Ano1 overexpression significantly promoted anchorage-independent cell growth *in vitro* and that loss of Ano1 resulted in inhibition of tumor growth both *in vitro and in vivo* (43). Taken together, overexpression of

Ano1 is highly linked to cancer, probably due to the volume regulatory function of CaCC. However, the precise mechanism behind its anti-apoptotic role is still not clear. The ability of cancer cells to metastasize is linked to their ability to migrate. Migration of cells depends on their intracellular ion concentration and their ability to increase their volume at the leading edge with extension of the lamellipodium and parallel shrinkage and retraction of the rear part of the cell (150; 159). This cell shrinkage process needs both K^+ and Cl^- channels to release both ions in order to maintain electro-neutrality (Fig. 4b).
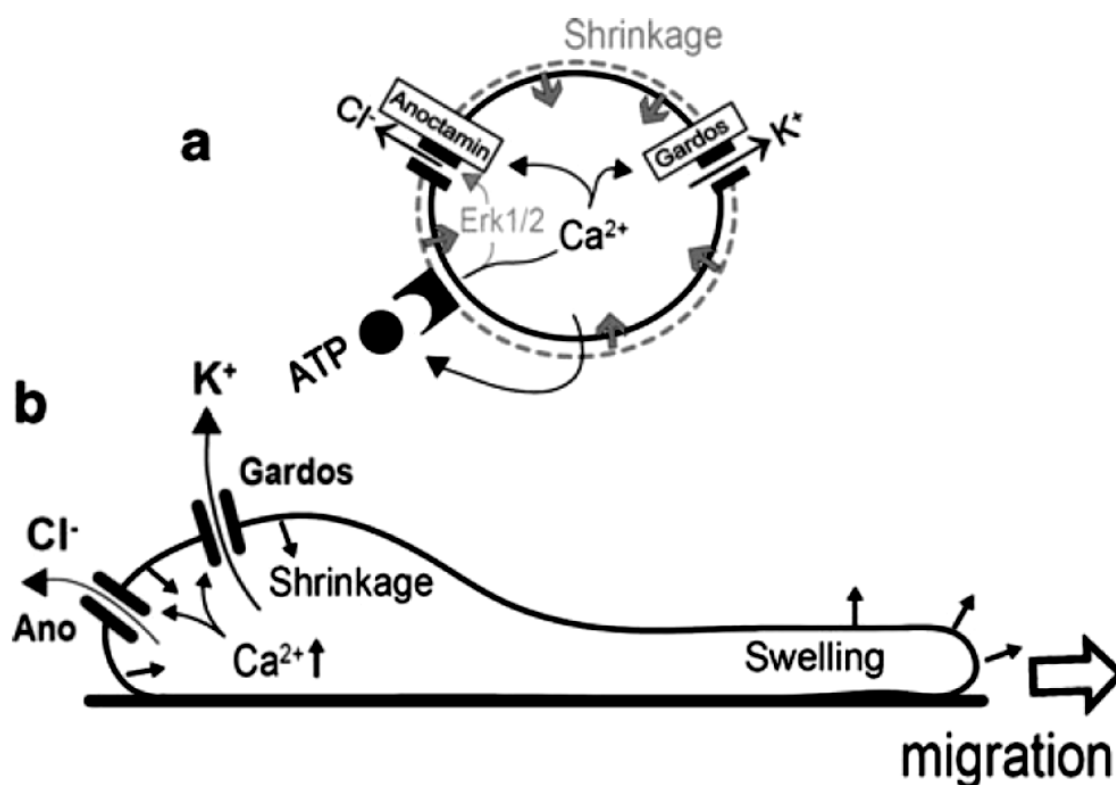
Fig. 4: Role of Ano1 in cancer: a Potential role of anoctamins and Gardos K^+ channels in volume regulation and cell shrinkage after hypotonic cell swelling or increase in intracellular Ca^{2+}. ATP release leads to activation of purinergic signaling along with activation of Erk1,2. b Anoctamin and Gardos-mediated cell shrinkage at the rear end of migrating cells.

Accordingly, anoctamins may serve as CaCC during cellular volume regulation (Fig. 4a) (97). These multiple effects of Ano1 on cell physiology call for attention when used for drug therapy in CF. Any compound which can enhance CaCC function or increase expression of CaCC may be helpful for airway secretion, but, on the other hand, may have undesired effects on cell proliferation and could be potentially tumorigenic.

Summary and outlook

To summarize, anoctamins as a newly identified family of CaCCs, play an essential role in embryonic development, sensation, neurobiology, epithelia secretion, muscle and bone formation, and gastrointestinal peristalsis (33; 77; 97; 134; 136). Overexpression of anoctamins is related to tumorigenesis, anoctamin mutations are related to various diseases (41; 97). For the most classic CaCC, Ano1, mutations in patients have not yet been reported, probably because loss-of-function mutations of Ano1 might be lethal in humans, just like Ano1 knockout mice, which can not survive after birth (124). Mutations in other anoctamins are extremely rare, such as those found for Ano6 and Ano5 (41). Also, defective function of anoctamin mutants may be compensated by other anoctamins.

It is almost sure that in the near future, anoctamins will attract more scientists to investigate this highly interesting family of proteins, as demonstrated by the ever increasing number of publications on anoctamins. It is known that the CaCCs are ubiquitously expressed and evolved conservatively. Their physiological role needs to be studied comprehensively. Among other methods, electrophysiology is a fundamental tool to study this family of chloride channels, and with the help of other novel techniques and institutions such as the world wide association study for single nucleotide polymorphisms, we will learn to understand this family of proteins.

REFERENCES

1. Adam,G., Ousingsawat J., Schreiber R. and Kunzelmann K. (2005) Increase in intracellular Cl$^-$ concentration by cAMP and Ca^{2+} dependent stimulation of M1 collecting duct cells. *Pflügers Arch* 449, 470-478.

2. Agre,P., Preston G.M., Smith B.L., Jung J.S., Raina S., Moon C., Guggino W.B. and Nielsen S. (1993) Aquaporin CHIP: the archetypal molecular water channel. *Am J Physiol* 265, F463-F476.

3. Almaca,J., Tian Y., AlDehni F., Ousingsawat J., Kongsuphol P., Rock J.R., Harfe B.D., Schreiber R. and Kunzelmann K. (2009) TMEM16 proteins produce volume regulated chloride currents that are reduced in mice lacking TMEM16A. *J Biol Chem* 284, 28571-28578.

4. Altamirano,J., Brodwick M.S. and Alvarez-Leefmans F.J. (1998) Regulatory volume decrease and intracellular Ca^{2+} in murine neuroblastoma cells studied with fluorescent probes. *J.Gen.Physiol.* 112, 145-160.

5. Alvarez,L.J., Zamudio A.C. and Candia O.A. (2005) Cl$^-$ secretory effects of EBIO in the rabbit conjunctival epithelium. *Am.J Physiol Cell Physiol.* 289, C138-C147.

6. Aruoma,O.I. (1999) Antioxidant actions of plant foods: use of oxidative DNA damage as a tool for studying antioxidant efficacy. *Free Radic.Res.* 30, 419-427.

7. Bachhuber,T., König J., Voelcker T., Mürle B., Schreiber R. and Kunzelmann K. (2005) Chloride interference with the epithelial Na$^+$ channel ENaC. *J Biol Chem* 280, 31587-31594.

8. Balla,T., Szentpetery Z. and Kim Y.J. (2009) Phosphoinositide signaling: new tools and insights. *Physiology.(Bethesda.).* 24, 231-244.

9. Bansal,D., Miyake K., Vogel S.S., Groh S., Chen C.C., Williamson R., McNeil P.L. and Campbell K.P. (2003) Defective membrane repair in dysferlin-deficient muscular dystrophy. *Nature* 423, 168-172.

10. Barro Soria,R., AlDehni F., Almaca J., Witzgall R., Schreiber R. and Kunzelmann K. (2009) ER localized bestrophin1 acts as a counter-ion channel to activate Ca^{2+}

dependent ion channels TMEM16A and SK4. *Pflügers Arch* 459, 485-497.

11. Barro Soria,R., Schreiber R. and Kunzelmann K. (2008) Bestrophin 1 and 2 are components of the Ca^{2+} activated Cl^- conductance in mouse airways. *BBA* 1783, 1993-2000.

12. Belkaid,A., Currie J.C., Desgagnes J. and Annabi B. (2006) The chemopreventive properties of chlorogenic acid reveal a potential new role for the microsomal glucose-6-phosphate translocase in brain tumor progression. *Cancer Cell Int.* 6, 7-19.

13. Bera,T.K., Das S., Maeda H., Beers R., Wolfgang C.D., Kumar V., Hahn Y., Lee B. and Pastan I. (2004) NGEP, a gene encoding a membrane protein detected only in prostate cancer and normal prostate. *Proc.Natl.Acad.Sci.U.S.A.* 101, 3059-3064.

14. Billig,G.M., Pál B., Fidzinski P. and Jentsch T.J. (2011) Ca^{2+}-activated Cl^- currents are dispensable for olfaction. *Nature neurosc.* 14, 763-769.

15. Bolduc,V., Marlow G., Boycott K.M., Saleki K., Inoue H., Kroon J., Itakura M., Robitaille Y., Parent L., Baas F., Mizuta K., Kamata N., Richard I., Linssen W.H., Mahjneh I., de Visser M., Bashir R. and Brais B. (2010) Recessive mutations in the putative calcium-activated chloride channel Anoctamin 5 cause proximal LGMD2L and distal MMD3 muscular dystrophies. *Am.J Hum.Genet.* 86, 213-221.

16. Boucher,R.C. (2007) Evidence for airway surface dehydration as the initiating event in CF airway disease. *J Intern.Med.* 261, 5-16.

17. Briones,N. and Dinu V. (2012) Data mining of high density genomic variant data for prediction of Alzheimer's disease risk. *BMC.Med.Genet.* 13, 7.

18. Bruce,J.I., Straub S.V. and Yule D.I. (2003) Crosstalk between cAMP and Ca^{2+} signaling in non-excitable cells. *Cell Calcium.* 34, 431-444.

19. Caputo,A., Caci E., Ferrera L., Pedemonte N., Barsanti C., Sondo E., Pfeffer U., Ravazzolo R., Zegarra-Moran O. and Galietta L.J. (2008) TMEM16A, A Membrane Protein Associated With Calcium-Dependent Chloride Channel Activity. *Science.* 322, 590-594.

20. Carew,M.A., Yang X., Schultz C. and Shears S.B. (2000) myo-inositol 3,4,5,6-tetrakisphosphate inhibits an apical calcium-activated chloride conductance in polarized monolayers of a cystic fibrosis cell line. *J Biol.Chem.* 275, 26906-26913.

21. Carles,A., Millon R., Cromer A., Ganguli G., Lemaire F., Young J., Wasylyk C., Muller D., Schultz I., Rabouel Y., Dembele D., Zhao C., Marchal P., Ducray C., Bracco L., Abecassis J., Poch O. and Wasylyk B. (2006) Head and neck squamous cell carcinoma transcriptome analysis by comprehensive validated differential display. *Oncogene.* 25, 1821-1831.

22. Carneiro,A., Isinger A., Karlsson A., Johansson J., Jonsson G., Bendahl P.O., Falkenback D., Halvarsson B. and Nilbert M. (2008) Prognostic impact of array-based genomic profiles in esophageal squamous cell cancer. *BMC.Cancer.* 8, 98.

23. Chan,H.C., Kaetzel M.A., Gotter A.L., Dedman J.R. and Nelson D.J. (1994) Annexin IV inhibits calmodulin-dependent protein kinase II-activated chloride conductance. A novel mechanism for ion channel regulation. *J Biol Chem.* 269, 32464-32468.

24. Chang,Y.T., Choi G., Bae Y.S., Burdett M., Moon H.S., Lee J.W., Gray N.S., Schultz P.G., Meijer L., Chung S.K., Choi K.Y., Suh P.G. and Ryu S.H. (2002) Purine-based inhibitors of inositol-1,4,5-trisphosphate-3-kinase. *Chembiochem.* 3, 897-901.

25. Chen,B., Nicol G. and Cho W.K. (2007) Role of calcium in volume-activated chloride currents in a mouse cholangiocyte cell line. *J Membr.Biol.* 215, 1-13.

26. Chen,Y., Shamu T., Chen H., Besmer P., Sawyers C.L. and Chi P. (2011) Visualization of the Interstitial Cells of Cajal (ICC) Network in Mice. *J Vis.Exp.* 2802, 10.3791.

27. Chorna,N.E., Chevres M., Santos-Berrios C., Orellano E.A., Erb L. and Gonzalez F.A. (2007) P2Y$_2$ receptors induced cell surface redistribution of alpha(v) integrin is required for activation of ERK 1/2 in U937 cells. *J.Cell Physiol.* 211, 410-422.

28. Collins,F.S. (1992) Cystic fibrosis: molecular biology and therapeutic implications. *Science* 256, 774-778.

29. Das,S., Hahn Y., Nagata S., Willingham M.C., Bera T.K., Lee B. and Pastan I. (2007) NGEP, a prostate-specific plasma membrane protein that promotes the association of LNCaP cells. *Cancer Res.* 67, 1594-1601.

30. Das,S., Hahn Y., Walker D.A., Nagata S., Willingham M.C., Peehl D.M., Bera T.K., Lee B. and Pastan I. (2008) Topology of NGEP, a prostate-specific cell:cell junction protein widely expressed in many cancers of different grade level. *Cancer Res.* 68, 6306-6312.

31. de la Fuente,R., Namkung W., Mills A. and Verkman A.S. (2007) Small molecule screen identifies inhibitors of a human intestinal calcium activated chloride channel. *Mol Pharmacol.* 73, 758-768.

32. DeLisle,S., Radenberg T., Wintermantel M.R., Tietz C., Parys J.B., Pittet D., Welsh M.J. and Mayr G.W. (1994) Second messenger specificity of the inositol trisphosphate receptor: reappraisal based on novel inositol phosphates. *Am.J.Physiol.* 266, C429-C436.

33. Deschauer,M., Joshi P.R., Glaser D., Hanisch F., Stoltenburg G. and Zierz S. (2011) [Muscular dystrophy due to mutations in anoctamin 5 : Clinical and molecular genetic findings]. *Nervenarzt.* 82, 1596-1603.

34. Devor,D.C., Singh A.K., Bridges R.J. and Frizzell R.A. (1996) Modulation of Cl$^-$ secretion by benzimidazolones. II. Coordinate regulation of apical G_{Cl} and basolateral G_K. *Am J Physiol* 271, L785-L795.

35. Devor,D.C., Singh A.K., Frizzell R.A. and Bridges R.J. (1996) Modulation of Cl$^-$ secretion by benzimidazolones. I. Direct activation of a Ca^{2+}- dependent K^+ channel. *Am.J.Physiol.* 271, L775-L784.

36. Dezaki,K., Tsumura T., Maeno E. and Okada Y. (2000) Receptor-mediated facilitation of cell volume regulation by swelling-induced ATP release in human epithelial cells [In Process Citation]. *Jpn.J Physiol* 50, 235-241.

37. Diener,M., Nobles M. and Rummel W. (1992) Activation of basolateral Cl$^-$ channels in the rat colonic epithelium during regulatory volume decrease. *Pflügers Arch* 421, 530-538.

38. Dizier,M.H., Margaritte-Jeannin P., Madore A.M., Esparza-Gordillo J., Moffatt M., Corda E., Monier F., Guilloud-Bataille M., Franke A., Weidinger S., Annesi-Maesano I., Just J., Pin I., Kauffmann F., Cookson W., Lee Y.A., Laprise C., Lathrop M., Bouzigon E. and Demenais F. (2012) The ANO3/MUC15 locus is associated with eczema in families ascertained through asthma. *J.Allergy Clin.Immunol.* 129, 1547-1553.

39. Duan,D. (2009) Phenomics of cardiac chloride channels: the systematic study of chloride channel function in the heart. *J Physiol.* 587, 2163-2177.

40. Duan,D.Y., Fermini B. and Nattel S. (1992) Sustained outward current observed after I(to1) inactivation in rabbit atrial myocytes is a novel Cl⁻ current. *Am.J.Physiol* 263, H1967-H1971.

41. Duran,C. and Hartzell H.C. (2011) Physiological roles and diseases of Tmem16/Anoctamin proteins: are they all chloride channels? *Acta Pharmacol.Sin.* 32, 685-692.

42. Duran,C., Qu Z., Osunkoya A.O., Cui Y. and Hartzell H.C. (2012) ANOs 3-7 in the anoctamin/tmem16 Cl⁻ channel family are intracellular proteins. *Am J Physiol Cell Physiol.* 302, 482-493.

43. Duvvuri,U., Shiwarski D.J., Xiao D., Bertrand C., Huang X., Edinger R.S., Rock J., Harfe B.D., Henson B.J., Kunzelmann K., Schreiber R., Seethala R.R., Egloff A.M., Chen X., Lui V.W., Grandis J.R. and Gollin S.M. (2012) TMEM16A, induces MAPK and contributes directly to tumorigenesis and cancer progression. *Cancer Res.* 72, 3270-3281.

44. Eggermont,J. (2004) Calcium-activated chloride channels: (un)known, (un)loved? *Proc.Am.Thorac.Soc.* 1, 22-27.

45. Eggermont,J., Trouet D., Carton I. and Nilius B. (2001) Cellular function and control of volume-regulated anion channels. *Cell Biochem Biophys.* 35, 263-274.

46. Espinosa,I., Lee C.H., Kim M.K., Rouse B.T., Subramanian S., Montgomery K., Varma S., Corless C.L., Heinrich M.C., Smith K.S., Wang Z., Rubin B., Nielsen T.O., Seitz R.S., Ross D.T., West R.B., Cleary M.L. and van de R.M. (2008) A novel monoclonal antibody against DOG1 is a sensitive and specific marker for gastrointestinal stromal tumors. *Am J Surg.Pathol.* 32, 210-218.

47. Fallah,G., Roemer T., Detro-Dassen S., Braam U., Markwardt F. and Schmalzing G. (2010) TMEM16A(a)/anoctamin-1 Shares a Homodimeric Architecture with CLC Chloride Channels. *Mol.Cell Proteomics.* 79, 649-661.

48. Fanger,C.M., Ghanshani S., Logsdon N.J., Rauer H., Kalman K., Zhou J., Beckingham K., Chandy K.G., Cahalan M.D. and Aiyar J. (1999) Calmodulin mediates calcium-dependent activation of the intermediate conductance KCa channel, IKCa1. *J Biol Chem.* 274, 5746-5754.

49. Faria,D., Schreiber R. and Kunzelmann K. (2009) CFTR is activated through stimulation of purinergic P2Y$_2$ receptors. *Pflügers Arch* 457, 1373-1380.

50. Fein,A. and Terasaki M. (2005) Rapid increase in plasma membrane chloride permeability during wound resealing in starfish oocytes. *J.Gen.Physiol* 126, 151-159.

51. Ferrera,L., Caputo A. and Galietta L.J. (2010) TMEM16A protein: a new identity for Ca(2+)-dependent Cl channels. *Physiology.(Bethesda.).* 25, 357-363.

52. Ferrera,L., Caputo A., Ubby I., Bussani E., Zegarra-Moran O., Ravazzolo R., Pagani F. and Galietta L.J. (2009) Regulation of TMEM16A chloride channel properties by alternative splicing. *J.Biol.Chem.* 284, 33360-33368.

53. Ferrera,L., Scudieri P., Sondo E., Pedemonte N., Caci E., Ubby I., Pagani F. and Galietta L.J. (2011) Native calcium activated chloride channels and their association with TMEM16A protein expressoin. *8th ECFS Basic Science Conference, 30.March.2.April, Tirennia, Italy* (Abstract).

54. Franco,R., Panayiotidis M.I. and de la Paz L.D. (2008) Autocrine signaling involved in cell volume regulation: the role of released transmitters and plasma membrane receptors. *J Cell Physiol.* 216, 14-28.

55. Fulcher,M.L., Gabriel S., Burns K.A., Yankaskas J.R. and Randell S.H. (2005) Well-differentiated human airway epithelial cell cultures. *Methods Mol.Med.* 107, 183-206.

56. Furst,J., Gschwentner M., Ritter M., Botta G., Jakab M., Mayer M., Garavaglia L., Bazzini C., Rodighiero S., Meyer G., Eichmuller S., Woll E. and Paulmichl M. (2002) Molecular and functional aspects of anionic channels activated during regulatory volume decrease in mammalian cells. *Pflugers Arch.2002.May.;444.(1.-2.):1.-25.* 444, 1-25.

57. Galietta,L.J. (2009) The TMEM16 protein family: a new class of chloride channels? *Biophys.J.* 97, 3047-3053.

58. Gerlach,A.C., Syme C.A., Giltinan L., Adelman J.P. and Devors D.C. (2001) ATP-dependent activation of the intermediate conductance, Ca^{2+}-activated K$^+$ channel, hIK1, is conferred by a C-terminal domain. *J Biol Chem.* 276, 10963-10970.

59. Gomez-Pinilla,P.J., Gibbons S.J., Bardsley M.R., Lorincz A., Pozo M.J., Pasricha P.J.,

van de R.M., West R.B., Sarr M.G., Kendrick M.L., Cima R.R., Dozois E.J., Larson D.W., Ordog T. and Farrugia G. (2009) Ano1 is a selective marker of interstitial cells of Cajal in the human and mouse gastrointestinal tract. *Am J Physiol Gastrointest.Liver Physiol.* 296, G1370-G1381.

60. Greenwood,I.A., Ledoux J. and Leblanc N. (2001) Differential regulation of Ca(2+)-activated Cl(-) currents in rabbit arterial and portal vein smooth muscle cells by Ca(2+)-calmodulin-dependent kinase. *J Physiol.* 534, 395-408.

61. Hamilton,K.L. and Kiessling M. (2006) DCEBIO stimulates Cl$^-$ secretion in the mouse jejunum. *Am.J Physiol Cell Physiol.* 290, C152-C164.

62. Hamilton,K.L., Meads L. and Butt A.G. (1999) 1-EBIO stimulates Cl$^-$ secretion by activating a basolateral K$^+$ channel in the mouse jejunum. *Pflugers Arch.* 439, 158-166.

63. Hartzell,H.C., Putzier I. and Arreola J. (2005) Calcium-Activated Chloride Channels. *Annu.Rev.Physiol* 67, 719-758.

64. Hartzell,H.C., Yu K., Xiao Q., Chien L.T. and Qu Z. (2008) Anoctamin / TMEM16 family members are Ca^{2+}-activated Cl$^-$ channels. *J Physiol.* 587, 2127-2139.

65. Hengl,T., Kaneko H., Dauner K., Vocke K., Frings S. and Mohrlen F. (2010) Molecular components of signal amplification in olfactory sensory cilia. *Proc.Natl.Acad.Sci.U.S.A.* 107, 6052-6057.

66. Hicks,D., Sarkozy A., Muelas N., Koehler K., Huebner A., Hudson G., Chinnery P.F., Barresi R., Eagle M., Polvikoski T., Bailey G., Miller J., Radunovic A., Hughes P.J., Roberts R., Krause S., Walter M.C., Laval S.H., Straub V., Lochmuller H. and Bushby K. (2011) A founder mutation in Anoctamin 5 is a major cause of limb-girdle muscular dystrophy. *Brain.* 134, 171-182.

67. Ho,M.W., Kaetzel M.A., Armstrong D.L. and Shears S.B. (2001) Regulation of a human chloride channel. a paradigm for integrating input from calcium, type ii calmodulin-dependent protein kinase, and inositol 3,4,5,6-tetrakisphosphate. *J Biol Chem.* 276, 18673-18680.

68. Ho,M.W., Shears S.B., Bruzik K.S., Duszyk M. and French A.S. (1997) Ins(3,4,5,6)P$_4$ specifically inhibits a receptor-mediated Ca^{2+}-dependent Cl$^-$ current in CFPAC-1 cells.

Am.J.Physiol. 272, C1160-C1168.

69. Hoffmann,E.K. (2000) Intracellular signalling involved in volume regulatory decrease. *Cell Physiol Biochem.* 10, 273-288.

70. Hoffmann,E.K., Simonsen L.O. and Lambert I.H. (1984) Volume-induced increase of K^+ and Cl^- permeabilities in Ehrlich ascites tumor cells. Role of internal Ca^{2+}. *J Membr.Biol.* 78, 211-222.

71. Huang,C.L., Feng S. and Hilgemann D.W. (1998) Direct activation of inward rectifier potassium channels by PIP2 and its stabilization by Gbetagamma. *Nature* 391, 803-806.

72. Huang,F., Rock J.R., Harfe B.D., Cheng T., Huang X., Jan Y.N. and Jan L.Y. (2009) Studies on expression and function of the TMEM16A calcium-activated chloride channel. *Proc.Natl.Acad.Sci.U.S.A.* 106, 21413-21418.

73. Huang,P., Liu J., Di A., Robinson N.C., Musch M.W., Kaetzel M.A. and Nelson D.J. (2001) Regulation of human CLC-3 channels by multifunctional Ca^{2+}/calmodulin-dependent protein kinase. *J Biol Chem.* 276, 20093-20100.

74. Huang,X., Godfrey T.E., Gooding W.E., McCarty K.S., Jr. and Gollin S.M. (2006) Comprehensive genome and transcriptome analysis of the 11q13 amplicon in human oral cancer and synteny to the 7F5 amplicon in murine oral carcinoma. *Genes Chromosomes.Cancer.* 45, 1058-1069.

75. Hubner,C.A. and Jentsch T.J. (2002) Ion channel diseases. *Hum.Mol.Genet.* 11, 2435-2445.

76. Hug,T., Koslowsky T., Ecke D., Greger R. and Kunzelmann K. (1995) Actin-dependent activation of ion conductances in bronchial epithelial cells. *Pflügers Arch* 429, 682-690.

77. Hwang,S.J., Blair P.J., Britton F.C., O'Driscoll K.E., Hennig G., Bayguinov Y.R., Rock J.R., Harfe B.D., Sanders K.M. and Ward S.M. (2009) Expression of anoctamin 1/TMEM16A by interstitial cells of Cajal is fundamental for slow wave activity in gastrointestinal muscles. *J Physiol.* 587, 4887-4904.

78. Jensen,B.S., Strobaek D., Olesen S.P. and Christophersen P. (2001) The Ca^{2+}-activated K^+ channel of intermediate conductance: a molecular target for novel treatments?

Curr.Drug Targets. 2, 401-422.

79. Jentsch,T.J., Günther W., Pusch M. and Schwappach B. (1995) Properties of voltage-gated chloride channels of the ClC gene family. *J.Physiol.* 482, 19S-25S.

80. Jentsch,T.J., Stein V., Weinreich F. and Zdebik A.A. (2001) Molecular structure and physiological function of chloride channels. *Physiol Rev.* 82, 503-568.

81. Joiner,W.J., Khanna R., Schlichter L.C. and Kaczmarek L.K. (2001) Calmodulin regulates assembly and trafficking of SK4/IK1 Ca^{2+}-activated K^+ channels. *J Biol Chem.* 276, 37980-37985.

82. Kachintorn,U., Vajanaphanich M., Traynor-Kaplan A.E., Dharmsathaphorn K. and Barrett K.E. (1993) Activation by calcium alone of chloride secretion in T84 epithelial cells. *Br.J Pharmacol* 109, 510-517.

83. Kaetzel,M.A., Chan H.C., Dubinsky W.P., Dedman J.R. and Nelson D.J. (1994) A role for annexin IV in epithelial cell function. Inhibition of calcium-activated chloride conductance. *J Biol Chem.* 269, 5297-5302.

84. Katoh,M. and Katoh M. (2003) FLJ10261 gene, located within the CCND1-EMS1 locus on human chromosome 11q13, encodes the eight-transmembrane protein homologous to C12orf3, C11orf25 and FLJ34272 gene products. *Int.J Oncol.* 22, 1375-1381.

85. Katoh,M. and Katoh M. (2004) Characterization of human TMEM16G gene in silico. *Int.J Mol Med.* 14, 759-764.

86. Katoh,M. and Katoh M. (2004) Identification and characterization of human TP53I5 and mouse Tp53i5 genes in silico. *Int.J Oncol.* 25, 225-230.

87. Khanna,R., Chang M.C., Joiner W.J., Kaczmarek L.K. and Schlichter L.C. (1999) hSK4/hIK1, a calmodulin-binding KCa channel in human T lymphocytes. Roles in proliferation and volume regulation. *J Biol Chem.* 274, 14838-14849.

88. Kolb,H.-A. (1990) Potassium channels in excitable and non-excitable cells. *Rev.Physiol.Biochem.Pharmacol.* 115, 51-91.

89. Kongsuphol,P., Schreiber R., Kraidith K. and Kunzelmann K. (2011) CFTR induces extracellular acid sensing in Xenopus oocytes which activates endogenous Ca(2+)-activated Cl (-) conductance. *Pflugers Arch.* 462, 479-487.

90. Kunzelmann,K., Allert N., Kubitz R., Breuer W.V., Cabantchik Z.I., Normann C., Schumann S., Leipziger J. and Greger R. (1994) Forskolin- and PMA-pretreatment alter the acute electrical response of HT_{29} cells to cAMP, ATP, neurotensin, ionomycin and hypotonic cell swelling. *Pflügers Arch* 428, 76-83.

91. Kunzelmann,K., Bachhuber T., Regeer R.R., Markovich D., Sun J. and Schreiber R. (2005) Purinergic inhibition of the epithelial Na^+ channel ENaC via hydrolysis of PIP_2. *FASEB J* 18, 142-163.

92. Kunzelmann,K., Kongsuphol P., AlDehni F., Tian Y., Ousingsawat J., Warth R. and Schreiber R. (2009) Bestrophin and TMEM16 - Ca^{2+} activated Cl^- channels with different functions. *Cell Calcium* 46, 233-241.

93. Kunzelmann,K., Kongsuphol P., Chootip K., Toledo C., Martins J.R., Almaca J., Tian Y., Witzgall R., Ousingsawat J. and Schreiber R. (2011) Role of the Ca(2+)-activated Cl(-) channels bestrophin and anoctamin in epithelial cells. *Biol Chem.* 392, 125-134.

94. Kunzelmann,K. and Mall M. (2003) Pharmacotherapy of the ion transport defect in cystic fibrosis: role of purinergic receptor agonists and other potential therapeutics. *American Journal of Respiratory Medicine* 2, 299-309.

95. Kunzelmann,K., Milenkovic V.M., Spitzner M., Barro Soria R. and Schreiber R. (2007) Calcium dependent chloride conductance in epithelia: Is there a contribution by Bestrophin? *Pflügers Arch* 454, 879-889.

96. Kunzelmann,K., Schreiber R., Kmit A., Jantarajit W., Martins J.R., Faria D., Kongsuphol P., Ousingsawat J. and Tian Y. (2012) Expression and function of epithelial anoctamins. *Exp.Physiol.* 97, 184-192.

97. Kunzelmann,K., Tian Y., Martins J.R., Faria D., Kongsuphol P., Ousingsawat J., Thevenod F., Roussa E., Rock J.R. and Schreiber R. (2011) Anoctamins. *Pflugers Arch.* 462, 195-208.

98. Kunzelmann,K., Tian Y., Martins J.R., Faria D., Kongsuphol P., Ousingsawat J., Wolf L. and Schreiber R. (2012) Airway epithelial cells-Functional links between CFTR and anoctamin dependent Cl(-) secretion. *Int.J.Biochem.Cell Biol.* 44, 1897-1900.

99. Lan,W.Z., Abbas H., Lam H.D., Lemay A.M. and Hill C.E. (2005) Contribution of a time-dependent and hyperpolarization-activated chloride conductance to currents of

resting and hypotonically shocked rat hepatocytes. *Am J Physiol Gastrointest.Liver Physiol.* 288, G221-G229.

100. Lang,F., Busch G.L., Ritter M., Volkl H., Waldegger S., Gulbins E. and Haussinger D. (1998) Functional significance of cell volume regulatory mechanisms. *Physiol Rev* 78, 247-306.

101. Lang,F., Madlung J., Bock J., Lukewille U., Kaltenbach S., Lang K.S., Belka C., Wagner C.A., Lang H.J., Gulbins E. and Lepple-Wienhues A. (2000) Inhibition of Jurkat-T-lymphocyte Na^+/H^+-exchanger by CD95(Fas/Apo-1)-receptor stimulation. *Pflugers Arch.* 440, 902-907.

102. Lang,F., Ritter M., Gamper N., Huber S.M., Fillon S., Tanneur V., Lepple-Wienhues A., Szabo I. and Gulbins E. (2000) Cell volume in the regulation of cell proliferation and apoptotic cell death. *Cell Physiol Biochem* 10, 417-428.

103. Large,W.A. and Wang Q. (1996) Characteristics and physiological role of the $Ca(2+)$-activated Cl^- conductance in smooth muscle. *Am.J.Physiol* 271, C435-C454.

104. Lee,R.J. and Foskett J.K. (2009) Mechanisms of Ca^{2+}-stimulated fluid secretion by porcine bronchial submucosal gland serous acinar cells. *Am.J.Physiol Lung Cell Mol.Physiol.* 298, L210-L231.

105. Liu,B., Linley J.E., Du X., Zhang X., Ooi L., Zhang H. and Gamper N. (2010) The acute nociceptive signals induced by bradykinin in rat sensory neurons are mediated by inhibition of M-type K^+ channels and activation of Ca^{2+}-activated Cl^- channels. *J.Clin.Invest.* 120, 1240-1252.

106. Liu,W., Lu M., Liu B., Huang Y. and Wang K. (2012) Inhibition of $Ca(2+)$-activated $Cl(-)$ channel ANO1/TMEM16A expression suppresses tumor growth and invasiveness in human prostate carcinoma. *Cancer Lett.* (in press)

107. Loewen,M.E. and Forsyth G.W. (2005) Structure and function of CLCA proteins. *Physiol Rev.* 85, 1061-1092.

108. Mahjneh,I., Jaiswal J., Lamminen A., Somer M., Marlow G., Kiuru-Enari S. and Bashir R. (2010) A new distal myopathy with mutation in anoctamin 5. *Neuromuscul.Disord.* 20, 791-795.

109. Manoury,B., Tamuleviciute A. and Tammaro P. (2010) TMEM16A/Anoctamin1

protein mediates calcium-activated chloride currents in pulmonary arterial smooth muscle cells. *J Physiol.* 588, 2305-2314.

110. Martins,J.R., Faria D., Kongsuphol P., Reisch B., Schreiber R. and Kunzelmann K. (2011) Anoctamin 6 is an essential component of the outwardly rectifying chloride channel. *Proc.Natl.Acad.Sci.U.S.A.* 108, 18168-18172.

111. Maruyama,Y. (1996) Selective activation of exocytosis by low concentrations of ACh in rat pancreatic acinar cells. *J Physiol.* 492, 807-814.

112. Mazzochi,C., Benos D.J. and Smith P.R. (2006) Interaction of epithelial ion channels with the actin-based cytoskeleton. *Am J Physiol Renal Physiol.* 291, F1113-F1122.

113. McCarty,N.A. and O'Neil R.G. (1992) Calcium signalling in volume regulation. *Physiol.Rev.* 72, 1037-1061.

114. Menniti,F.S., Oliver K.G., Nogimori K., Obie J.F., Shears S.B. and Putney J.W., Jr. (1990) Origins of myo-inositol tetrakisphosphates in agonist-stimulated rat pancreatoma cells. Stimulation by bombesin of myo-inositol 1,3,4,5,6-pentakisphosphate breakdown to myo-inositol 3,4,5,6-tetrakisphosphate. *J.Biol.Chem.* 265, 11167-11176.

115. Milenkovic,V.M., Brockmann M., Stohr H., Weber B.H. and Strauss O. (2010) Evolution and functional divergence of the anoctamin family of membrane proteins. *BMC Evolutionary Biology* 10, 319-324.

116. Mizuta,K., Tsutsumi S., Inoue H., Sakamoto Y., Miyatake K., Miyawaki K., Noji S., Kamata N. and Itakura M. (2007) Molecular characterization of GDD1/TMEM16E, the gene product responsible for autosomal dominant gnathodiaphyseal dysplasia. *Biochem Biophys Res Commun.* 357, 126-132.

117. Moody,M., Pennington C., Schultz C., Caldwell R., Dinkel C., Rossi M.W., McNamara S., Widdicombe J.H., Gabriel S.E. and Traynor-Kaplan A.E. (2005) Inositol polyphosphate derivative inhibits Na^+ transport and improves fluid dynamics in cystic fibrosis airway epithelia. *Am.J.Physiol Cell Physiol.* 289, C512-C520.

118. Morris,A.P., Kirk K.L. and Frizzell R.A. (1990) Simultaneous analysis of cell Ca^{2+} and Ca2(+)-stimulated chloride conductance in colonic epithelial cells (HT-29). *Cell Regul.* 1, 951-963.

119. Namkung,W., Finkbeiner W.E. and Verkman A.S. (2010) CFTR-Adenylyl Cyclase I Association Is Responsible for UTP Activation of CFTR in Well-Differentiated Primary Human Bronchial Cell Cultures. *Mol.Biol.Cell.* 21, 2639-2648.

120. Namkung,W., Yao Z., Finkbeiner W.E. and Verkman A.S. (2011) Small-molecule activators of TMEM16A, a calcium-activated chloride channel, stimulate epithelial chloride secretion and intestinal contraction. *FASEB J.* 25, 4048-4062.

121. Nilius,B. and Droogmans G. (2003) Amazing chloride channels: an overview. *Acta Physiol Scand.* 177, 119-147.

122. Okada,Y., Maeno E., Shimizu T., Dezaki K., Wang J. and Morishima S. (2001) Receptor-mediated control of regulatory volume decrease (RVD) and apoptotic volume decrease (AVD). *J Physiol.* 532, 3-16.

123. Okada,Y., Maeno E., Shimizu T., Manabe K., Mori S. and Nabekura T. (2004) Dual roles of plasmalemmal chloride channels in induction of cell death. *Pflugers Arch* 448, 287-295.

124. Ousingsawat,J., Martins J.R., Schreiber R., Rock J.R., Harfe B.D. and Kunzelmann K. (2009) Loss of TMEM16A causes a defect in epithelial Ca^{2+} dependent chloride transport. *J Biol Chem* 284, 28698-28703.

125. Pafundo,D.E., Mut P., Perez R.M., Gonzalez-Lebrero R.M., Fachino V., Krumschnabel G. and Schwarzbaum P.J. (2004) Effects of extracellular nucleotides and their hydrolysis products on regulatory volume decrease of trout hepatocytes. *Am.J.Physiol Regul.Integr.Comp Physiol.* 287, R833-R843.

126. Pawlowski,K., Lepisto M., Meinander N., Sivars U., Varga M. and Wieslander E. (2006) Novel conserved hydrolase domain in the CLCA family of alleged calcium-activated chloride channels. *Proteins* 63, 424-439.

127. Pedarzani,P., Mosbacher J., Rivard A., Cingolani L.A., Oliver D., Stocker M., Adelman J.P. and Fakler B. (2001) Control of electrical activity in central neurons by modulating the gating of small conductance Ca^{2+}-activated K^+ channels. *J.Biol.Chem.* 276, 9762-9769.

128. Pedersen,K.A., Schroder R.L., Skaaning-Jensen B., Strobaek D., Olesen S.P. and Christophersen P. (1999) Activation of the human intermediate-conductance

Ca(2+)-activated K(+) channel by 1-ethyl-2-benzimidazolinone is strongly Ca(2+)-dependent. *Biochim.Biophys.Acta* 1420, 231-240.

129. Pedersen,S.F., Prenen J., Droogmans G., Hoffmann E.K. and Nilius B. (1998) Separate swelling- and Ca^{2+}-activated anion currents in Ehrlich ascites tumor cells. *J Membr.Biol.* 163, 97-110.

130. Perez-Cornejo,P., Gokhale A., Duran C., Cui Y., Xiao Q., Hartzell H.C. and Faundez V. (2012) Anoctamin 1 (Tmem16A) Ca^{2+}-activated chloride channel stoichiometrically interacts with an ezrin-radixin-moesin network. *Proc.Natl.Acad.Sci.U.S.A.* 109, 10376-10381.

131. Petersen,O.H. and Tepikin A.V. (2008) Polarized calcium signaling in exocrine gland cells. *Annu.Rev.Physiol.* 70, 273-299.

132. Pifferi,S., Dibattista M. and Menini A. (2009) TMEM16B induces chloride currents activated by calcium in mammalian cells. *Pflugers Arch.* 458, 1023-1038.

133. Preston,P., Wartosch L., Gunzel D., Fromm M., Kongsuphol P., Ousingsawat J., Kunzelmann K., Barhanin J., Warth R. and Jentsch T.J. (2010) Disruption of the K^+ channel beta-subunit KCNE3 reveals an important role in intestinal and tracheal Cl^- transport. *J.Biol.Chem.* 285, 7165-7175.

134. Rasche,S., Toetter B., Adler J., Tschapek A., Doerner J.F., Kurtenbach S., Hatt H., Meyer H., Warscheid B. and Neuhaus E.M. (2010) Tmem16b is Specifically Expressed in the Cilia of Olfactory Sensory Neurons. *Chem.Senses.* 35, 239-245.

135. Rock,J.R., Futtner C.R. and Harfe B.D. (2008) The transmembrane protein TMEM16A is required for normal development of the murine trachea. *Dev.Biol.* 321, 141-149.

136. Rock,J.R. and Harfe B.D. (2008) Expression of TMEM16 paralogs during murine embryogenesis. *Dev.Dyn.* 237, 2566-2574.

137. Rock,J.R., O'Neal W.K., Gabriel S.E., Randell S.H., Harfe B.D., Boucher R.C. and Grubb B.R. (2009) Transmembrane protein 16A (TMEM16A) is a Ca^{2+} regulated Cl^- -secretory channel in mouse airways. *J Biol Chem.* 284, 14875-14880.

138. Romanenko,V.G., Catalan M.A., Brown D.A., Putzier I., Hartzell H.C., Marmorstein A.D., Gonzalez-Begne M., Rock J.R., Harfe B.D. and Melvin J.E. (2010) Tmem16A

encodes the Ca^{2+}-activated Cl^- channel in mouse submandibular salivary gland acinar cells. *J Biol.Chem* 285, 12990-3001.

139. Ruan,Y.C., Guo J.H., Liu X., Zhang R., Tsang L.L., Dong J.D., Chen H., Yu M.K., Jiang X., Zhang X.H., Fok K.L., Chung Y.W., Huang H., Zhou W.L. and Chan H.C. (2012) Activation of the epithelial Na(+) channel triggers prostaglandin E(2) release and production required for embryo implantation. *Nat.Med.* (in press)

140. Rudolf,M.T., Dinkel C., Traynor-Kaplan A.E. and Schultz C. (2003) Antagonists of myo-inositol 3,4,5,6-tetrakisphosphate allow repeated epithelial chloride secretion. *Bioorg.Med.Chem.* 11, 3315-3329.

141. Rudolf,M.T., Li W.H., Wolfson N., Traynor-Kaplan A.E. and Schultz C. (1998) 2-Deoxy derivative is a partial agonist of the intracellular messenger inositol 3,4,5,6-tetrakisphosphate in the epithelial cell line T84. *J Med.Chem.* 41, 3635-3644.

142. Sagheddu,C., Boccaccio A., Dibattista M., Montani G., Tirindelli R. and Menini A. (2010) Calcium concentration jumps reveal dynamic ion selectivity of calcium-activated chloride currents in mouse olfactory sensory neurons and TMEM16b-transfected HEK 293T cells. *J Physiol.* 588, 4189-4204.

143. Saiardi,A. and Cockcroft S. (2008) Human ITPK1: a reversible inositol phosphate kinase/phosphatase that links receptor-dependent phospholipase C to Ca^{2+}-activated chloride channels. *Sci.Signal.* 1, e5.

144. Saleh,S.N., Angermann J.E., Sones W.R., Leblanc N. and Greenwood I.A. (2007) Stimulation of Ca^{2+}-gated Cl^- currents by the calcium-dependent K^+ channel modulators NS1619 [1,3-dihydro-1-[2-hydroxy-5-(trifluoromethyl)phenyl]-5-(trifluoro-o-methyl)-2H-benzi midazol-2-one] and isopimaric acid. *J Pharmacol.Exp.Ther.* 321, 1075-1084.

145. Sankaranarayanan,A., Raman G., Busch C., Schultz T., Zimin P.I., Hoyer J., Kohler R. and Wulff H. (2009) Naphtho[1,2-d]thiazol-2-ylamine (SKA-31), a new activator of KCa2 and KCa3.1 potassium channels, potentiates the endothelium-derived hyperpolarizing factor response and lowers blood pressure. *Mol.Pharmacol.* 75, 281-295.

146. Sardini,A., Amey J.S., Weylandt K.H., Nobles M., Valverde M.A. and Higgins C.F.

(2003) Cell volume regulation and swelling-activated chloride channels. *Biochim.Biophys Acta.* 1618, 153-162.

147. Scheuring,S., Ringler P., Borgnia M., Stahlberg H., Muller D.J., Agre P. and Engel A. (1999) High resolution AFM topographs of the escherichia coli water channel aquaporin Z [In Process Citation]. *EMBO J* 18, 4981-4987.

148. Schreiber,R., Uliyakina I., Kongsuphol P., Warth R., Mirza M., Martins J.R. and Kunzelmann K. (2010) Expression and Function of Epithelial Anoctamins. *J.Biol.Chem.* 285, 7838-7845.

149. Schroeder,B.C., Cheng T., Jan Y.N. and Jan L.Y. (2008) Expression cloning of TMEM16A as a calcium-activated chloride channel subunit. *Cell.* 134, 1019-1029.

150. Schwab,A. (2001) Ion channels and transporters on the move. *News Physiol Sci.* 16, 29-33.

151. Schwiebert,E.M., Egan M.E., Hwang T.-H., Fulmer S.B., Allen S.S., Cutting G.R. and Guggino W.B. (1995) CFTR regulates outwardly rectifying chloride channels through an autocrine mechanism involving ATP. *Cell* 81, 1063-1073.

152. Shears,S.B. (2005) Can intervention in inositol phosphate signalling pathways improve therapy for cystic fibrosis? *Expert.Opin.Ther.Targets.* 9, 1307-1317.

153. Sheridan,J.T., Worthington E.N., Yu K., Gabriel S.E., Hartzell H.C. and Tarran R. (2010) Characterization of the oligomeric structure of the Ca^{2+}-activated Cl^- channel Ano1/TMEM16A. *J Biol.Chem.* 286, 1381-1388.

154. Singh,S., Syme C.A., Singh A.K., Devor D.C. and Bridges R.J. (2001) Benzimidazolone activators of chloride secretion: potential therapeutics for cystic fibrosis and chronic obstructive pulmonary disease. *J Pharmacol Exp Ther.* 296, 600-611.

155. Skals,M., Jensen U.B., Ousingsawat J., Kunzelmann K., Leipziger J. and Praetorius H.A. (2010) E. coli alpha-hemolysin triggers shrinkage of erythrocytes via KCa3.1 and TMEM16A channels with subsequent phosphatidyl serine exposure. *J.Biol.Chem* 285, 15557-15565.

156. Skals,M., Jorgensen N.R., Leipziger J. and Praetorius H.A. (2009) Alpha-hemolysin from Escherichia coli uses endogenous amplification through P2X receptor activation

to induce hemolysis. *Proc.Natl.Acad.Sci.U.S.A.* 106, 4030-4035.

157. Srivastava,S., Choudhury P., Li Z., Liu G., Nadkarni V., Ko K., Coetzee W.A. and Skolnik E.Y. (2006) Phosphatidylinositol 3-phosphate indirectly activates KCa3.1 via 14 amino acids in the carboxy terminus of KCa3.1. *Mol.Biol Cell.* 17, 146-154.

158. Stephan,A.B., Shum E.Y., Hirsh S., Cygnar K.D., Reisert J. and Zhao H. (2009) ANO2 is the cilial calcium-activated chloride channel that may mediate olfactory amplification. *Proc.Natl.Acad.Sci.U.S.A.* 106, 11776-11781.

159. Stock,C. and Schwab A. (2009) Protons make tumor cells move like clockwork. *Pflugers Arch.* 458, 981-992.

160. Stohr,H., Heisig J.B., Benz P.M., Schoberl S., Milenkovic V.M., Strauss O., Aartsen W.M., Wijnholds J., Weber B.H. and Schulz H.L. (2009) TMEM16B, A Novel Protein with Calcium-Dependent Chloride Channel Activity, Associates with a Presynaptic Protein Complex in Photoreceptor Terminals. *J Neurosci.* 29, 6809-6818.

161. Strobaek,D., Teuber L., Jorgensen T.D., Ahring P.K., Kjaer K., Hansen R.S., Olesen S.P., Christophersen P. and Skaaning-Jensen B. (2004) Activation of human IK and SK Ca^{2+}-activated K^+ channels by NS309 (6,7-dichloro-1H-indole-2,3-dione 3-oxime). *Biochim.Biophys.Acta.* 1665, 1-5.

162. Stutzin,A. and Hoffmann E.K. (2006) Swelling-activated ion channels: functional regulation in cell-swelling, proliferation and apoptosis. *Acta Physiol (Oxf).* 187, 27-42.

163. Suzuki,J., Umeda M., Sims P.J. and Nagata S. (2010) Calcium-dependent phospholipid scrambling by TMEM16F. *Nature* 468, 834-838.

164. Syme,C.A., Gerlach A.C., Singh A.K. and Devor D.C. (2000) Pharmacological activation of cloned intermediate- and small-conductance Ca^{2+}-activated K^+ channels. *Am J Physiol* 278, C570-C581.

165. Takizawa,P.A., DeRisi J.L., Wilhelm J.E. and Vale R.D. (2000) Plasma membrane compartmentalization in yeast by messenger RNA transport and a septin diffusion barrier. *Science.* 290, 341-344.

166. Tarran,R., Loewen M.E., Paradiso A.M., Olsen J.C., Gray M.A., Argent B.E., Boucher R.C. and Gabriel S.E. (2002) Regulation of murine airway surface liquid volume by CFTR and Ca^{2+}-activated Cl^- conductances. *J Gen.Physiol..* 120, 407-418.

167. Thelin,W.R., Chen Y., Gentzsch M., Kreda S.M., Sallee J.L., Scarlett C.O., Borchers C.H., Jacobson K., Stutts M.J. and Milgram S.L. (2007) Direct interaction with filamins modulates the stability and plasma membrane expression of CFTR. *J Clin.Invest.* 117, 364-374.

168. Thomas-Gatewood,C., Neeb Z.P., Bulley S., Adebiyi A., Bannister J.P., Leo M.D. and Jaggar J.H. (2011) TMEM16A channels generate Ca^{2+}-activated Cl^- currents in cerebral artery smooth muscle cells. *Am J Physiol Heart Circ.Physiol.* 301, 1819-1827.

169. Tian,Y., Kongsuphol P., Hug M.J., Ousingsawat J., Witzgall R., Schreiber R. and Kunzelmann K. (2011) Calmodulin-dependent activation of the epithelial calcium-dependent chloride channel TMEM16A. *FASEB J* 25, 1058-1068.

170. Tian,Y., Schreiber R. and Kunzelmann K. (2012) Anoctamins are a family of Ca^{2+} activated Cl^- channels. *J Biol Chem.* (in press).

171. Tian,Y., Schreiber R., Wanitchakool P., Kongsuphol P., Sousa M., Uliyakina I., Palma M., Faria D., Traynor-Kaplan A.E., Fragata J.I., Amaral M.D. and Kunzelmann K. (2012) Control of TMEM16A by INO-4995 and other inositolphosphates. *Br.J Pharmacol.* (in press).

172. Traynor-Kaplan,A.E., Moody M., Nur M., Gabriel S., Majerus P.W., Drumm M.L. and Langton-Webster B. (2010) INO-4995 therapeutic efficacy is enhanced with repeat dosing in cystic fibrosis knockout mice and human epithelia. *Am.J.Respir.Cell Mol.Biol.* 42, 105-112.

173. Traynor-Kaplan,A.E., Moody M., Nur M., Gabriel S.E., Majerus P.W., Drumm M.L. and Langton-Webster B. (2010) INO-4995 Therapeutic Efficacy is Enhanced with Repeat Dosing in CF KO Mice and Human Epithelia. *Am.J.Respir.Cell Mol.Biol.* 42, 105-112.

174. Tsutsumi,S., Inoue H., Sakamoto Y., Mizuta K., Kamata N. and Itakura M. (2005) Molecular cloning and characterization of the murine gnathodiaphyseal dysplasia gene GDD1. *Biochem.Biophys.Res.Commun.* 331, 1099-1106.

175. Tsutsumi,S., Kamata N., Vokes T.J., Maruoka Y., Nakakuki K., Enomoto S., Omura K., Amagasa T., Nagayama M., Saito-Ohara F., Inazawa J., Moritani M., Yamaoka T.,

Inoue H. and Itakura M. (2004) The novel gene encoding a putative transmembrane protein is mutated in gnathodiaphyseal dysplasia (GDD). *Am.J.Hum.Genet.* 74, 1255-1261.

176. Vajanaphanich,M., Schultz C., Rudolf M.T., Wasserman M., Enyedi P., Craxton A., Shears S.B., Tsien R.Y., Barrett K.E. and Traynor-Kaplan A.E. (1994) Long-term uncoupling of chloride secretion from intracellular calcium levels by Ins(3,4,5,6)P$_4$. *Nature* 371, 711-714.

177. Valverde,M.A., O'Brien J.A., Sepulveda F.V., Ratcliff R., Evans M.J. and Colledge W.H. (1993) Inactivation of the murine cftr gene abolishes cAMP-mediated but not Ca^{2+}-mediated secretagogue-induced volume decrease in small-intestinal crypts. *Pflügers Arch* 425, 434-438.

178. Valverde,M.A., O`Briens J.A., Sepulveda F.V., Ratcliff R.A., Evans M.J. and Colledge W.H. (1995) Impaired cell volume regulation in intestinal crypt epithelia of cystic fibrosis. *Proc.Natl.Acad.Sci.* 92, 9038-9041.

179. Van der,W.T., De Jonge H.R. and Tilly B.C. (1999) Osmotic cell swelling-induced ATP release mediates the activation of extracellular signal-regulated protein kinase (Erk)-1/2 but not the activation of osmo-sensitive anion channels. *Biochem J.* 343 Pt 3, 579-586.

180. Vennekens,R., Trouet D., Vankeerberghen A., Voets T., Cuppens H., Eggermont J., Cassiman J.J., Droogmans G. and Nilius B. (1999) Inhibition of volume-regulated anion channels by expression of the cystic fibrosis transmembrane conductance regulator. *J Physiol (Lond.)* 515, 75-85.

181. Verkman,A.S. and Galietta L.J. (2009) Chloride channels as drug targets. *Nat.Rev.Drug Discov.* 8, 153-171.

182. Vermeer,S., Hoischen A., Meijer R.P., Gilissen C., Neveling K., Wieskamp N., de Brouwer A., Koenig M., Anheim M., Assoum M., Drouot N., Todorovic S., Milic-Rasic V., Lochmuller H., Stevanin G., Goizet C., David A., Durr A., Brice A., Kremer B., van de Warrenburg B.P., Schijvenaars M.M., Heister A., Kwint M., Arts P., van der W.J., Veltman J., Kamsteeg E.J., Scheffer H. and Knoers N. (2010) Targeted next-generation sequencing of a 12.5 Mb homozygous region reveals ANO10

mutations in patients with autosomal-recessive cerebellar ataxia. *Am J Hum.Genet.* 87, 813-819.

183. von Hahn,T., Thiele I., Zingaro L., Hamm K., Garcia-Alzamora M., Köttgen M., Bleich M. and Warth R. (2001) Characterisation of the rat SK4/IK1 K(+) channel. *Cell Physiol Biochem* 11, 219-230.

184. Wagner,J.A., Cozens A.L., Schulman H., Gruenert D.C., Stryer L. and Gardner P. (1991) Activation of chloride chanels in normal and cystic fibrosis airway epithelial cells by multifunctional calcium/calmodulin- dependent protein kinase. *Nature* 349, 793-796.

185. Wang,Y.X. and Kotlikoff M.I. (1997) Inactivation of calcium-activated chloride channels in smooth muscle by calcium/calmodulin-dependent protein kinase. *Proc.Natl.Acad.Sci.U.S.A.* 94, 14918-14923.

186. Warth,R., Hamm K., Bleich M., Kunzelmann K., vonHahn T., Schreiber R., Ullrich E., Mengel M., Trautmann N., Kindle P., Schwab A. and Greger R. (1999) Molecular and functional characterization of the small Ca^{2+}-regulated K^+ channel (rSK4) of colonic crypts. *Pflügers Arch* 438, 437-444.

187. West,R.B., Corless C.L., Chen X., Rubin B.P., Subramanian S., Montgomery K., Zhu S., Ball C.A., Nielsen T.O., Patel R., Goldblum J.R., Brown P.O., Heinrich M.C. and van de R.M. (2004) The novel marker, DOG1, is expressed ubiquitously in gastrointestinal stromal tumors irrespective of KIT or PDGFRA mutation status. *Am J Pathol.* 165, 107-113.

188. Wiwchar,M., Ayon R., Greenwood I.A. and Leblanc N. (2009) Phosphorylation alters the pharmacology of Ca(2+)-activated Cl channels in rabbit pulmonary arterial smooth muscle cells. *Br.J Pharmacol.* 158, 1356-1365.

189. Worrell,R.T. and Frizzell R.A. (1991) CaMKII mediates stimulation of chloride conductance by calcium in T_{84}. *Am.J.Physiol.* 260, C877-C882.

190. Xia,X.M., Fakler B., Rivard A., Wayman G., Johnson-Pais T., Keen J.E., Ishii T., Hirschberg B., Bond C.T., Lutsenko S., Maylie J. and Adelman J.P. (1998) Mechanism of calcium gating in small-conductance calcium-activated potassium channels. *Nature.* 395, 503-507.

191. Xiao,Q., Yu K., Perez-Cornejo P., Cui Y., Arreola J. and Hartzell H.C. (2011) Voltage- and calcium-dependent gating of TMEM16A/Ano1 chloride channels are physically coupled by the first intracellular loop. *Proc.Natl.Acad.Sci.U.S.A.* 108, 8891-8896.

192. Xie,W., Kaetzel M.A., Bruzik K.S., Dedman J.R., Shears S.B. and Nelson D.J. (1996) Inositol 3,4,5,6-tetrakisphosphate inhibits the calmodulin-dependent protein kinase II-activated chloride conductance in T84 colonic epithelial cells. *J.Biol.Chem.* 271, 14092-14097.

193. Xie,W., Solomons K.R., Freeman S., Kaetzel M.A., Bruzik K.S., Nelson D.J. and Shears S.B. (1998) Regulation of Ca^{2+}-dependent Cl^- conductance in a human colonic epithelial cell line (T84): cross-talk between $Ins(3,4,5,6)P_4$ and protein phosphatases. *J Physiol.* 510, 661-673.

194. Yang,D., Shcheynikov N., Zeng W., Ohana E., So I., Ando H., Mizutani A., Mikoshiba K. and Muallem S. (2009) IRBIT coordinates epithelial fluid and HCO_3-secretion by stimulating the transporters pNBC1 and CFTR in the murine pancreatic duct. *J Clin.Invest* 119, 193-202.

195. Yang,H., Jin T., Cheng T., Jan Y.N., and Jan L.Y. (2011) Scan: A Novel Small-Conductance Ca^{2+}-Activated Non-Selective Cation Channel Encoded by TMEM16F. *Biophysical Journal.* 100, 259a.

196. Yang,L., Reece J., Gabriel S.E. and Shears S.B. (2006) Apical localization of ITPK1 enhances its ability to be a modifier gene product in a murine tracheal cell model of cystic fibrosis. *J.Cell Sci.* 119, 1320-1328.

197. Yang,Y.D., Cho H., Koo J.Y., Tak M.H., Cho Y., Shim W.S., Park S.P., Lee J., Lee B., Kim B.M., Raouf R., Shin Y.K. and Oh U. (2008) TMEM16A confers receptor-activated calcium-dependent chloride conductance. *Nature.* 455, 1210-1215.

198. Yu,K., Duran C., Qu Z., Cui Y.Y. and Hartzell H.C. (2012) Explaining calcium-dependent gating of anoctamin-1 chloride channels requires a revised topology. *Circ.Res.* 110, 990-999.

199. Yu,K., Lujan R., Marmorstein A., Gabriel S.E. and Hartzell H.C. (2010) Bestrophin-2 mediates bicarbonate transport by goblet cells in mouse colon. *J Clin.Invest.* 120, 1722-1735.

ACKNOWLEDGEMENTS

Yuemin Tian

ERKLÄRUNGEN

Hiermit erkläre ich, gem. § 6 Abs. 2, Nr. 6 der Promotionsordnung der Math.-Nat.-

Fachbereiche zur Erlangung des Dr. rer. nat., dass ich die vorliegende Dissertation

selbständig verfasst und mich keiner anderen als der angegebenen Hilfsmittel

bedient habe.

Regensburg, den 01.09.2012

Yuemin Tian

CURRICULUM VITAE

Personal information

Date of Birth: April 4th, 1981

Sex: Female

Place of birth: Hebei province, P. R. China

Nationality: P. R. China

Address: Karl-Stieler-Street 86, Room 1203, 93051 Regensburg, Germany

Tel: 941-20051255 (home) 17663345990 (mobile)

Email: opopiuywo@yahoo.com.cn

Education

2008-2012   Ph.D., (Physiology) Faculty of Natural Scienes III: Biology and
                        Preclinical medicine, University of Regensburg, Germany

2004-2007   M.Sc., (Physiology) School of Basic Medical Sciences, Capital
                        Medical University, China

1999-2003   B.Sc., (Water and Soil Protection) Dept. of Water and Soil Protection
                        Beijing Forest University, China

Research experience

2007-2008   Research assistant, Epithelia Cell Biology Research Center, Dept. of
                        Physiology, Chinese University of Hong Kong, China

Publications

1.   **Tian Y**, Schreiber R, and Kunzelmann K. (2012) Anoctamins are a family of Ca^{2+} activated Cl^- channels. *J Cell Sci*. (in press).

2.   **Tian Y**, Schreiber R, Wanitchakool P, Kongsuphol P, Sousa M, Uliyakina I, Palma M, Faria D, Traynor-Kaplen E. A, Fragata I. J, Amaral D. M, and Kunzelmann K. (2012) Control of TMEM16A by INO-4995 and other inositolphosphates. *Br J Pharmacol*. (in press).

3.   Oeggerli M, **Tian Y**, Ruiz C, Wijker B, Sauter G, Obermann E, Güth U, Zlobec I, Sausbier M, Kunzelmann K, and Bubendorf L. (2012) Role of KCNMA1 in Breast Cancer. *PLoS One*. 7, e41664.

4.   Kunzelmann K, **Tian Y**, Martins JR, Faria D, Kongsuphol P, Ousingsawat J, Wolf L, and Schreiber R. (2012) Airway epithelial cells-Functinal links between CFTR and anoctamin dependent Cl(-)secretion. *Int J Biochem Cell Biol*. 44, 1897-1900.

5.   Faria D, Lentze N, Almaça J, Luz S, Alessio L, **Tian Y**, Martins JP, Cruz P, Schreiber R, Rezwan M, Farinha CM, Auerbach D, Amaral MD, and Kunzelmann K. (2012) Regulation of ENaC biogenesis by the stress response protein SERP1. *Pflugers Arch*. 463, 819-827.

6.   Liu Y, Jiang X, Zhang X, Chen R, Sun T, Fok KL, Dong J, Tsang LL, Yi S, Ruan Y, Guo J, Yu MK, **Tian Y**, Chung YW, Yang M, Xu W, Chung CM, Li T, and Chan HC. (2011) Dedifferentiation-reprogrammed mesenchymal stem cells with improved therapeutic potential. *Stem Cells*. 29, 2077-2089.

7.   Kunzelmann K, Schreiber R, Kmit A, Jantarajit W, Martins JR, Faria D, Kongsuphol P, Ousingsawat J, and **Tian Y**. (2012) Expression and function of epithelial anoctamins. *Exp Physiol*. 97, 184-192.

8.   Kunzelmann K, **Tian Y**, Martins JR, Faria D, Kongsuphol P, Ousingsawat J, Thevenod F, Roussa E, Rock J, and Schreiber R. (2011) Anoctamins. *Pflugers Arch*. 462, 195-208.

9.   Ousingsawat J, Mirza M, **Tian Y**, Roussa E, Schreiber R, Cook DI, and Kunzelmann K. (2011) Rotavirus toxin NSP4 induces diarrhea by activation of TMEM16A and inhibition of Na(+) absorption *Pflugers Arch*. 461, 579-589.

10.   Kunzelmann K, Kong esuphol P, Chootip K, Toledo C, Martins JR, Almaca J, **Tian Y**, Witzgall R, Ousingsawat J, and Schreiber R. (2011) Role of the Ca^{2+} activated Cl^{-} channels bestrophin and anoctamin in epithelial cells. *Biol Chem*. 392, 125-134.

11.   **Tian Y**, Kongsuphol P, Hug M, Ousingsawat J, Witzgall R, Schreiber R, and Kunzelmann K. (2011) Calmodulin-dependent activation of the epithelial calcium-dependent chloride channel TMEM16A. *FASEB J*. 25, 1058-1068.

12.   Duning K, Rosenbusch D, Schlüter MA, **Tian Y**, Kunzelmann K, Meyer N, Schulze U, Markoff A, Pavenstädt H, and Weide T. (2010) Polycystin-2 activity is controlled by transcriptional coactivator with PDZ binding motif and PALS1-associated tight junction protein. *J Biol Chem*. 285, 33584-33588.

13.   Kunzelmann K, Kongsuphol P, Aldehni F, **Tian Y**, Ousingsawat J, Warth R, and Schreiber R. (2009) Bestrophin and TMEM16-Ca(2+) activated Cl(-) channels with different functions. *Cell Calcium*. 46, 233-241.

14.   Almaça J, **Tian Y**, Aldehni F, Ousingsawat J, Kongsuphol P, Rock JR, Harfe BD, Schreiber R, and Kunzelmann K. (2009) TMEM16 proteins produce volume-regulated chloride currents that are reduced in mice lacking TMEM16A. *J Biol Chem*. 284, 28571-28578.

15.   Zhang XH, Zhang XF, Zhang JQ, **Tian YM**, Xue H, Yang N, and Zhu JX. (2008) Beta-adrenoceptors, but not dopamine receptors, mediate dopamine-induced ion transport in late distal colon of rats. *Cell Tissue Res*. 334, 25-35.

16.   **Tian YM**, Chen X, Luo DZ, Zhang XH, Xue H, Zheng LF, Yang N, Wang XM, and Zhu JX. (2008) Alteration of dopaminergic markers in gastrointestinal tract of different rodent models of Parkinson's disease. *Neuroscience*. 153, 634-644.

17.   Yang N, **Tian YM**, Zhang XH, Zheng LF, Xue H, Chen X, Zhu L, and Zhu JX. (2008) A dual role of 5-hydroxytryptamine receptor 3 in serotonin induced ion transport in rat distal colon. *Eur J Pharmacol*. 584, 137-143.

18.   Xue H, **Tian YM**, Yan M, Yang N, Chen X, Xing Y, and Zhu JX. (2007) Appearance of segmental discrepancy of anion transport in rat distal colon. *Biol Pharm Bull*. 30, 1407-1411.